Microbial analysis by microencapsulation and its application to study proliferation heterogeneity

October 2016

Doctoral supervisors:

Director,	Co-director,	Doctoral candidate,
		
Sebastián Chávez de Diego	María de la Cruz Muñoz Centeno	Lidia Delgado Ramos

INDEX

1. Introduction

1.1 Heterogeneity of cell populations

It is widely known that single cells in a population display variable behaviour (Elsasser 1984; Pelkmans 2012). Although heterogeneity between single cells is evident in tissues, organs and different organisms, it can also be observed in populations of monoclonal cells that have been cultured under the same conditions. This phenomenon is known as cell-to-cell variability and is the responsible for population heterogeneity (Altschuler and Wu 2010; Pelkmans 2012) (Figure 1A). Thus, heterogeneity is a common characteristic in all populations, from tumor cells, where heterogeneity plays a role in cancer treatment resistance and tumor recurrence, to clonal microbial cultures (Sanchez-Romero and Casadesus 2014; Lipinski, Barber et al. 2016) (Figure1B). When cell-to-cell variability is ignored and populations are studied from an average perspective, some parts of them are at the risk of being masked (Figure 1C).

A

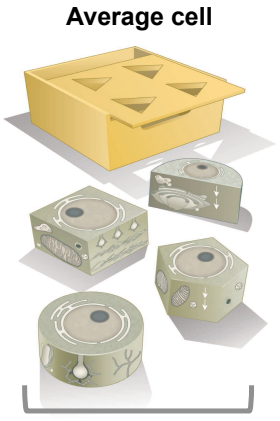

Adapted from Pelkmans. Science, 2012

B

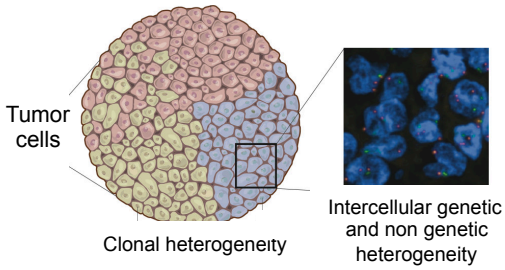

Adapted from Burrell. Nature, 2013

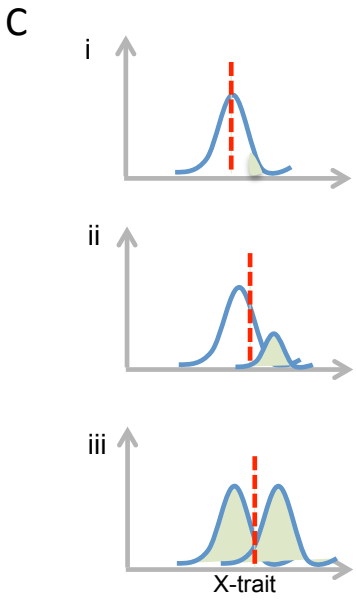

Figure 1. heterogeneity of clonal populations. A. Cell to cell variability in monoclonal population of cells. Genetically identical cells (circle, half circle, pentagon, and square) are not the same as the average cell (yellow box, triangle). Individual cells may display many cell-to-cell differences in some machineries or processes making each individual cell clearly different. Adapted from Pelkmans, 2012**. B.** Some parts of the population are masked when averages are studied. Behaviours of cells in (i) the tail of a distribution (shaded area) or (ii) a small subpopulation (at right) may differ from the remainder of the population or from the mean behaviour (dashed line). (iii) For bimodal cellular behaviours, a population mean may poorly represent the majority of cells. **C.** Cancer cells is the most clear example of cell to cell variability in clonal populations.

In cancer cells, variable protein expression results in different responses to anticancer agents so only a part of the population is killed. This is beneficial to the tumour but harmful to the patient (Cohen, Geva-Zatorsky et al. 2008). (Figure 3C). For example, it has been demonstrated that in the case of apoptosis mediated by TRAIL (tumour necrosis factor (TNF)- related apoptosis-inducing ligand), there is a divergence in cell fate: some cells in a clonal population die while others survive. Among cells that die, the time between TRAIL exposure and caspase activation is highly variable. They imaged sister

cells expressing reporters of caspase activation and mitochondrial outer membrane permeabilization after exposure to TRAIL. They concluded that differences in the levels or states of proteins regulating receptor-mediated apoptosis are the main causes of cell-to-cell variability in the probability and timing of death in human cell lines (Spencer, Gaudet et al. 2009).

Cell to cell variability in cancer cells has also been observed at chromatin level. Some cells maintain an altered chromatin state that requires a histone demethylase what makes them drug- tolerant (Sharma, Lee et al. 2010).

The protection of cyclin B1 from degradation has also been proposed as a mechanism that produce cell to cell variability is response to cancer drugs (Gascoigne and Taylor 2008).

Altogether these findings suggest that cancer population employ a survival strategy in which individual cells assume a reversibly drug-tolerant state to protect the population from eradication by lethal exposures to anticancer agents (Sharma, Lee et al. 2010).

The stochastic transition among multiple phenotypes to enhance fitness has also been described in yeast, Murat Acar et al experimentally demonstrated in *Saccharomyces cerevisiae* how switching affects population growth by using the galactose pathway. They used an isogenic population that randomly transitions between two phenotypes at different switching rates as a result of stochastic gene expression in two different environments. Each phenotype was designed to confer a growth advantage over the other phenotype in a specific environment. When the growth of the two populations was compared, they found that fast switching populations outgrow slow switchers when the environment changes rapidly, whereas slow-switching phenotypes outgrow fast switchers when the environment changes hardly ever. These results suggest that isogenic cells may fit the phenotype switching rates to the frequency of environmental changes (Acar, Mettetal et al. 2008)

1.1.1 A historical perspective of cell-to-cell variability

Heterogeneity in cell populations is not a new concept (Yuan, Wulf et al. 2011). It has been historically observed and supposed to be a fundamental property of

cellular systems (Elsasser 1984; Rubin 1990; Altschuler and Wu 2010). The concept of cell-to-cell variability emerged in the pre-molecular biology era from studies on *E. coli*. Delbrück realized in 1940 that, inside living cells, stochasticity of chemical interactions may affect the outcome of cellular decisions (Delbruck 1940). He proposed that this might partly explain the wide distribution of burst sizes in the growth of bacteriophages in *E.Coli* (Delbruck 1945). However, he also suggested that such variability could be predetermined by influencing factors, such as cell size (Snijder and Pelkmans 2011). In fact, nowadays it is known that bacteriophage lambda infection of *E. coli* can result in distinct cell fate outcomes. For example, some cells lyse whereas others survive as lysogens. This hypothesis is supported by some models about phage lambda infection where it is proposed that the spontaneous differences in the timing of individual molecular events during lambda infection leads to variation in the cell fates. This is an example of how intrinsic molecular noise can influence cellular behaviour, drive developmental processes, and produce population heterogeneity (Delbruck 1945; St-Pierre and Endy 2008).

Some years later, in 1957, Novick and Weiner suggested that, in bacteria, the decision to switch from glucose to lactose metabolism could be made by random fluctuations in the levels of some regulatory components involved. They showed that the production of beta-galactosidase, necessary for the utilization of this sugar in individual cells was highly variable and random. They found that the induction increase the proportion of cells expressing the enzyme rather than increasing every cell's expression level equally (Novick and Weiner 1957). However such early studies were hindered by the lack of accurate single-cell assays of gene expression (Raj and van Oudenaarden 2008).

Much later, Arkin and collaborators came back to the studies of phage lambda infection in bacteria. They applied stochastic mathematical modelling to the regulatory mechanism that decides between the lytic versus lysogenic switch. The stochastic model predictions adjusted with experimental population averaged data, suggesting that this switch is stochastically determined (Arkin, Ross et al. 1998). However, in the 1970s Herskowitz and others had suggested that this switch could be predisposed by the nutrient status in *E. coli* cells (Herskowitz and Hagen 1980).

In 1976, it was demonstrated the existence of a different behaviour at single cell levels during the studies of migration in bacterial chemotaxis although the cells were genetically identical and grew in homogeneous conditions. It was showed that the irregular partitioning of molecular regulators during cell division, and not cell size or cell cycle effects was the cause of this variability (Spudich and Koshland 1976).

At the same time, different works with mammalian tissue culture cells showed a big variability between individual cells at the level of cell migration, growth rate and cell shape. Those differences were a consequence of cellular crowding and cell–cell contacts (Eagle and Levine 1967).

However the fact that stochasticity in biochemical interactions can largely influences cell decisions became stronger by the experiments of Michael B.Elowitz et al. They demonstrated that the expression of a gene inside a single living *E.Coli* cell could show a significant amount of intrinsic noise by measuring the correlation in expression of two different fluorescent protein reporter genes under control of the same promoters. They conclude that both intrinsic noise (stochastic fluctuations in the expression of each reporter protein) and extrinsic noise (differences in the levels of cellular components that are necessary for the expression of both reporters) could generate long term heterogeneity in a clonal population (Elowitz, Levine et al. 2002).

All these studies are examples of non-genetic variations that difficult the attribution of these phenomenons to environmental inhomogeneities or genetic causes.

Moreover, in 2005, during studies of the mating pheromone response pathway in yeast it was shown that only a small proportion of total cell-to-cell variation is caused by random fluctuations in gene transcription and translation during the response. Contrary, they found that this variation was dominated at 99% by two predetermined factors: the capacity of individual cells to transmit signals through the pathway and to express proteins from genes. In fact, they identified specific mechanisms that regulate this cell-to-cell variability (auto-regulatory negative feedback involving MAP kinases protein). This experiments showed that, despite intrinsic noise, deterministic and robust responses are achieved (Colman-Lerner, Gordon et al. 2005).

In the past few years, new findings of deterministic process that were thought to

be stochastic have been described. One of them is referred to the lambda lysis-lysogenic decision. It has been demonstrated that cell volume at the time of infection determine the cell fate: while larger cells are lysed after phage lambda infection, the smaller cells undergo lysogenic (St-Pierre and Endy 2008).
Similarly, it has been shown that the lactose operon switch in *E. Coli*, which can create two different subpopulations, is not totally stochastic at the single-cell level. The analysis of genealogy and cell history revealed the existence of pre-disposing factors for switching, such as the cell's physiology and growth rate that are epigenetically inherited (Robert, Paul et al. 2010).

In spite of this long list of observations, this interesting phenomenon has been historically ignored by molecular and cell biologists, in part because of technical limitations, but also because research has focused on mechanisms and processes shared between cells. However, the mechanisms that make cells different are probably equally important (Pelkmans 2012).

1.1.2 Genetic and non-genetic variability

Population heterogeneity can be the result of genetic and non-genetic variability (Huang 2009) (Figure 3D).
Historically any variation in phenotype has been explained by a genetic variation, this is, changes in the DNA sequence. The findings of Watson and Crick strongly promoted this genetic determinism (Strohman 1997). However, the vast diversity in nature can be poorly explained only by genetic variability (Strohman 1995) (Condit 2002). In spite of that, the attention to non-genetic variability has been scarce because we usually assume uniformity of the cell populations that serve as starting material for experimental analysis (Huang 2009).
For example, in cancer biology, genetic variability supposes a strong source of heterogeneity. In this way, heterogeneity among tumour cells is commonly explained by genetic mutations. In fact, genomic instability is a feature of pre-cancerous and cancerous cells (Gaillard, Garcia-Muse et al. 2015) (Figure 3C).
Otherwise, non-genetic sources of heterogeneity are not fixed in the population

by heritable transmission. These sources can be stochastic in nature, such as random fluctuations in transcription or translation, or they can be regulated, such as through feedback mechanisms, so that variability is deliberately maintained (Yuan, Wulf et al. 2011).

Non-genetic heterogeneity in clonal cell populations helps to explain how the same set of genes can generate so different, stable, and often inherited gene expression profiles and, thereby, distinct phenotypes. In fact, in the theory of evolutionary dynamics, the variations that do not necessarily imply differences in the DNA sequence are becoming increasingly appreciated (Huang 2009).

Several examples of non genetic memory has been demonstrated in human cells (Sigal, Milo et al. 2006) (Spencer, Gaudet et al. 2009).

To avoid confusions in further discussion, it is necessary to distinguish the general term “non-genetic” from the more specific term “epigenetic” (Huang 2009). The classic definition of epigenetics is the study of heritable phenotype changes that do not involve alterations in DNA sequence (DNA methylation and histone modifications). A number of cellular phenotypes are transmitted in this way, including imprinting, X chromosome inactivation, aging, heterochromatin formation, reprogramming, and gene silencing (Kouzarides 2007). So an ‘epigenetic mark’ can be considered the conceptual cousin of a ‘genetic mutation’ because both of them are used to explain phenotypic changes as a result of a molecular event (Huang 2009).

1.1.3 Intrinsic and extrinsic variability

Recent experimental results in single cells of *S.Cerevisiae* show that the same mean protein levels can be achieved with very different variability and highlight the role of mRNA turnover in the control of noise in protein expression (Newman, Ghaemmaghami et al. 2006)

This cell-to-cell variability in protein levels is generated by two fundamentally different sources: intrinsic and extrinsic variability. The former, emerge from the stochastic nature of the biochemical processes involved in transcription regulation, translation, and degradation, and affects the expression of a specific protein encoded by a particular gene.

The latter, comes from differences at the level of cell size, stage of cell cycle, and the concentration of the molecular machines involved in transcription and translation such as ribosomes, RNA polymerases, and RNA/protein degradation pathways. The extrinsic variability affects to some degree the expression of all proteins in the cell. The distinction between these so different sources of variability is essential for analysing and interpreting the observed variability and to understand the mechanistic behind such observations. However, unravelling the sources of variation is not trivial (Rinott, Jaimovich et al. 2011). Both sources are sometimes referred as “noise” (Figure 2) and (Table 1).

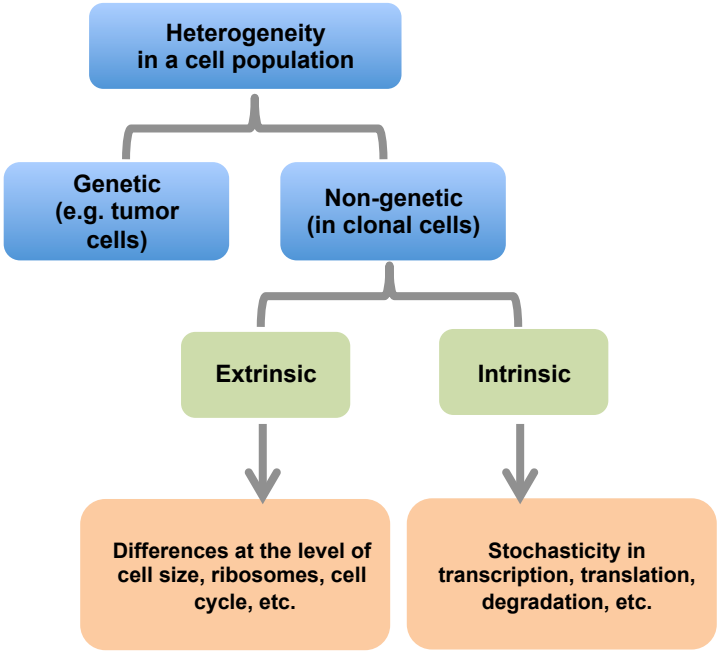

Figure 2. Terminologies in cell population heterogeneity field. A schematic representation of terminologies and concepts used in the study of cell population heterogeneity, organized into a hierarchy of dichotomies.

Studies of intrinsic noise over the past 10 years have revealed that it has been adjusted during the functional evolution of signalling pathways helping to buffering the level of uncertainty in the outcome of regulatory systems. Such regulatory systems or decisions, in which the fate of a cellular event is at least partially the result of intrinsic noise, are said to be stochastic. Several examples of stochastic regulatory systems have been reviewed previously in this thesis

(Eldar and Elowitz 2010) (Raj and van Oudenaarden 2008) (McAdams and Arkin 1997).

However, new genome-wide studies of cell-to-cell variability in mRNA or protein levels in *E. coli* and *S. cerevisiae* have indeed revealed a huge variation in the molecular components of genetically identical cells (Newman, Ghaemmaghami et al. 2006; Taniguchi, Choi et al. 2010) indicating that the main source of variability in protein levels grow out from upstream sources of variability, this is, from the extrinsic noise. This term could in turn reflect either stochastic or deterministic influences. However, the existence of upstream stochastic influences does not mean that the system under study is itself stochastic. In the other hand, the term determinism does not necessary imply regulation, however the presence of upstream deterministic influences is likely to reflect complex regulatory systems that control the cell's physiology (Snijder and Pelkmans 2011). To avoid confusion during this thesis, we are going to use the term cellular noise only when randomness has been explicitly shown and there are not any deterministic influences that could explain the cell-to-cell variability (Table1).

1.1.4 Determinism and stochasticity

A stochastic process is described like a process with randomness in transcription and translation leading to cell-to-cell variations in mRNA and protein levels. Gene expression is a fundamentally stochastic process. This has important consequences for cells: is beneficial in some contexts while damaging in others. The main situations that trigger changes in gene expression are the stress response, metabolism, development, the cell cycle, circadian rhythms, and aging (Raj and van Oudenaarden 2008).

Contrary, a deterministic process is that in which there is a specific regulation and coordination like cell differentiation, senescence or development.

Often the decision of a process to be stochastic or deterministic has been made by appealing to the statistics of large numbers, thus diminishing the importance of any one molecule in particular. However, more and more, researchers have

found that one of the most notable sources of variability in genetically identical individuals are random fluctuations in the expression of individual genes (Raj and van Oudenaarden 2008).

In spite of the stochasticity in gene expression, single-cell and lineage-tracing experiments have demonstrated that phenotypic cell-to-cell variability is often the result of deterministic processes, despite the existence of intrinsic noise in molecular networks. This has made possible the characterization of molecular regulatory mechanisms unknown until now. Some of them has been previously described in this thesis and place the study of cell-to-cell variability in a key position of molecular cell biology (St-Pierre and Endy 2008; Robert, Paul et al. 2010).

Sometimes is difficult to distinguish stochasticity from determinism at the level of cellular phenotypes and activities. We can only affirm that an important fraction of observed cell-to-cell variability is deterministic while the remaining is explained by stochastic processes (Paulsson 2004) (Table 1).

Table 1. The semantic of cell-to-cell variability.

TERM	DEFINITION
Cell to cell variability	Cell to cell variability refers to differences in the properties of individual cells in an otherwise similar population.
Heterogeneity	It is a property of a cell population, not of individual cells. Heterogeneity of a population implies the presence of cell-to-cell variability with respect to one (or more than one) measurable trait *X*, where *X* can be the cellular level of a given molecule, such as a protein, or any quantifiable morphological or functional parameter.
Cellular noise	Random or irregular fluctuations which are not a part of a signal or which interfere with a signal.
Clone or a clonal group of cells	A group of cells that are derived from a single ancestor cell within the same uniform and constant micro-environment and hence are assumed to be genetically identical.
Extrinsic heterogeneity	Cell-to-cell variability in a population caused by non-uniform environmental factors that differentially affect individual cells.
Intrinsic heterogeneity	Cell-to-cell variability in the absence of inhomogeneities in the microenvironment. Most commonly explained by 'gene expression noise'
Genetic heterogeneity	A property of a population of cells in which the genomes of the individual cells are not identical. Frequently considered in tumour biology, where the genome sequence differences between the tumour cells could explain trait differences due to somatic mutations.
Non-genetic heterogeneity	A property of a population (that refers to the phenotypic variability between its members, which share the same genome. Hence, the trait differences are not due to genetic differences between the cells.
Stochastic process	A process with randomness in transcription and translation leading to cell-to-cell variations in mRNA and protein levels.
Deterministic process	A process with an specific regulation and coordination.

1.2 Processes that influence cell-to-cell variability

Non genetic differences in populations of genetically identical cells are likely heritable between successive generations and can also be influenced by processes such as proliferation rate, cell size and morphology (Aldridge, Fernandez-Suarez et al. 2012), cell cycle (Ricicova, Hamidi et al. 2013) (Overton, Spencer et al. 2014), age (Passos, Saretzki et al. 2007), or interplay between microenvironment and phenotypic state of the cell (Figure 4).

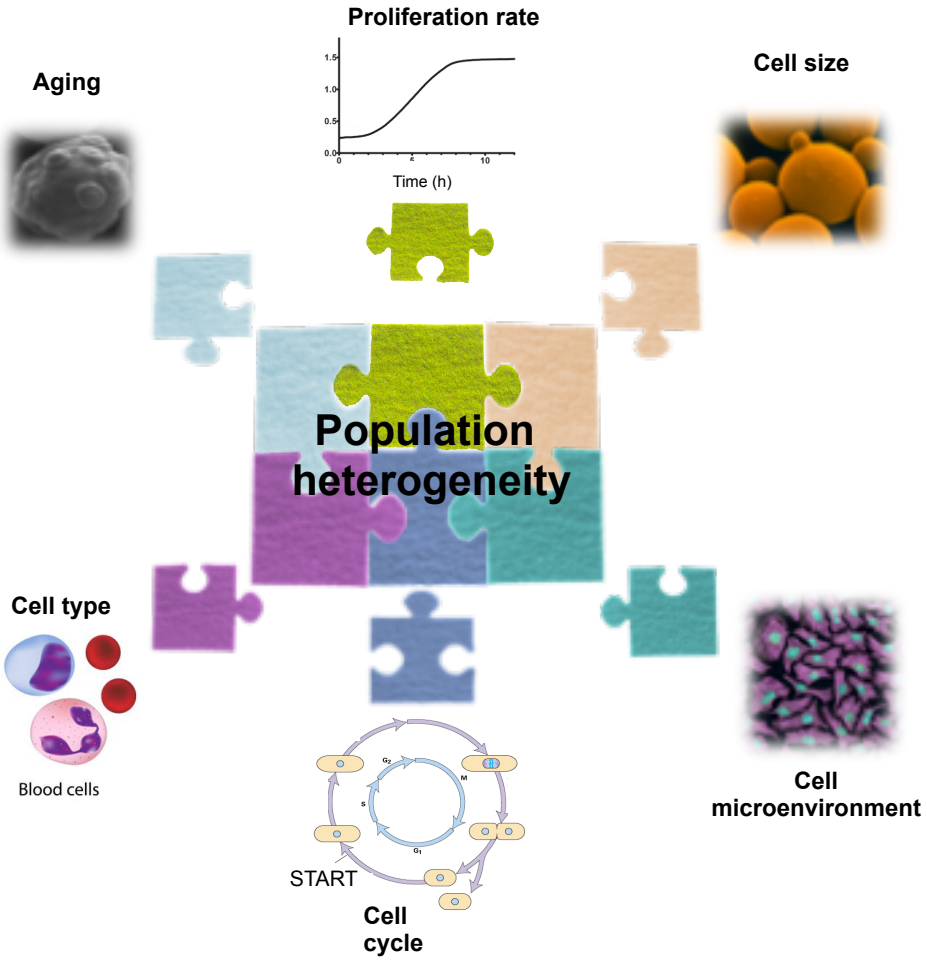

Figure 3. processes that regulates cell to cell variability. Non genetic differences in populations of genetically identical cells are likely heritable between successive generations and can also be influenced by processes such as proliferation rate, cell size and morphology , cell cycle , age , or interplay between microenvironment and phenotypic state of the cell.

1.2.1 Growth rate

In budding yeast, heterogeneity takes many shapes, including proliferation rate. This proliferation rate depends on the growth rate and the rate of cell division, and it is determined by the abundance of an environmental carbon source, such as glucose.

So free-living organisms need to regulate growth rate (GR) to maintain fitness and to compete with other genotypes during the natural selection process (Garcia-Martinez, Delgado-Ramos et al. 2016). Somatic cells of complex organisms also regulate GR in order to fit their developmental program. It is commonly assumed that free-living microorganisms have evolved to grow as fast as possible because this is the simplest behaviour that fits Darwinian natural selection for single cells (Bosdriesz et al. 2015). As fitness is the net growth of a genotype over time, one of the most important variables for single cell organisms during the course of adaptation is the GR of a population composed only of one genotype in relation to the growth rate of other isogenic populations. In these scenarios one of the most important issues is adjusting the cellular GR with gene expression. In the last few years, transcriptomic works in budding yeast have shown that a large fraction of its genes is coordinately regulated with growth rate. However, the mRNA level is determined by the balance between transcription and mRNA decay (Chavez, Garcia-Martinez et al. 2016) (Figure 4A and 4B).

In terms of population heterogeneity, the fact that mRNA levels do not correlate at global levels with their corresponding protein levels complicates the extrapolation of such changes in the transcription of single genes to variability in cellular activity and also makes more difficult to differentiate between gene expression noise or determinist changes (Snijder and Pelkmans 2011). One relevant question that remains unanswered at this point is which side of the mRNA expression balance (synthesis or decay) is regulated in those genes whose mRNA levels change with the GR (Garcia-Martinez, Delgado-Ramos et al. 2016).

1.2.1.1 Gene expression as a function of growth rate

It is often assumed that higher population growth rates in microorganisms require higher protein synthesis rates (Furusawa and Kaneko 2008; Molenaar, van Berlo et al. 2009; Scott, Gunderson et al. 2010; Scott, Klumpp et al. 2014; Shahrezaei and Marguerat 2015) This is because proteins constitute a large fraction of dry mass in both prokaryotes (Neidhardt,F.C. and Umbarger,H.E.,1996) and eukaryotes (e.g. yeast; see (Caballero-Córdoba and Sgarbieri 2000)) and, therefore, their synthesis is the most energetically demanding process (Warner 1999). This process is not exclusive of unicellular organisms and probably fast-proliferating tumor cells are also governed by these rules (Vander Heiden, Cantley et al. 2009; Schell, Olson et al. 2014).

The translation machinery includes the most abundant noncoding RNAs: rRNA and tRNAs. Thus the eukaryotic RNA polymerases (RNA pol) devoted to the synthesis of rRNA and tRNA (RNA pol I and III) must increase their transcription rates in parallel to the GR (Mager and Planta 1991). RNA pol II, however, transcribes a much larger set of mRNAs subjected to multiple regulatory influences, many of which lower in concentration with the GR (O'Duibhir, Lijnzaad et al. 2014).

So although a large set of mRNAs, which are highly transcribed, is also devoted to ribosome biosynthesis and translation factors (Warner 1999), the relationship between the GR and RNA pol II TR is not obviously predictable. Unlike rRNAs and tRNAs, which are stable molecules, mRNAs have a shorter half-life, and both their synthesis and decay significantly contribute to regulate their abundance (Perez-Ortin, Alepuz et al. 2013). The RNA pol II transcription rate, especially for single cell organisms, is highly variable and a proxy of their physiology and metabolism (Scott, Gunderson et al. 2010). The influence of the cell cycle (Eser, Demel et al. 2014) and cell size (Wu, Rolfe et al. 2010) on the transcription rate has been investigated in the model yeast *S. cerevisiae*. Cell cycle length and cell size are related to the GR (Wu, Rolfe et al. 2010). Transcriptome dependence on the yeast growth rate has been thoroughly investigated in D. Botstein's laboratory (Brauer, Huttenhower et al. 2008; Airoldi, Huttenhower et al. 2009; Slavov and Botstein 2011; Slavov, Airoldi et al. 2012).

These authors have found that the mRNA amount/concentration (RA) of about one third of the genes varies in a GR dependent manner.

As was mentioned, the [mRNA] of a given gene is controlled by the action of two opposite forces: synthesis by RNA pol II and degradation by several exonuclease pathways (Parker 2012)(Figure 4A). Given the appearance of several genome-wide techniques to measure the synthesis and degradation rates and the mRNA concentrations, in several model organisms, it is possible to quantify the respective contributions of transcription and degradation to the actual concentration for each individual mRNA (reviewed in (Perez-Ortin, de Miguel-Jimenez et al. 2012; Perez-Ortin, Alepuz et al. 2013), and also for the sum of them all.

Pérez-Ortín‘s laboratory has recently analysed the correlation between gene expression and growth rate in a set of mutants and environmental conditions. They found a positive and parallel correlation between both RNA polymerase II transcription and mRNA degradation with growth rates in most genes. Thus, the total mRNA concentration remains roughly constant. (Figure 4B) Some gene groups, however, regulate their mRNA concentration by uncoupling mRNA stability from the transcription rate. Ribosome-related genes modulate their transcription rates to increase mRNA levels under fast growth. In contrast, mitochondria-related and stress-induced genes lower mRNA levels at fast growth by reducing mRNA stability or the transcription rate, respectively. The former led to a higher proportion of fermentation over respiration at a higher GR, even in the same high glucose medium (Garcia-Martinez, Delgado-Ramos et al. 2016)(Figure 4C).

A

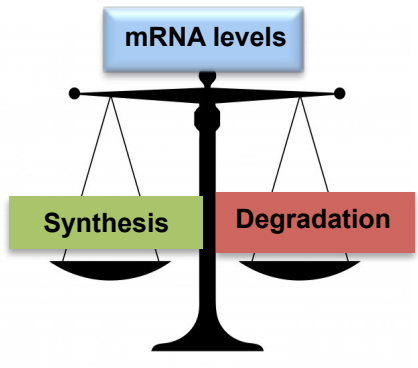

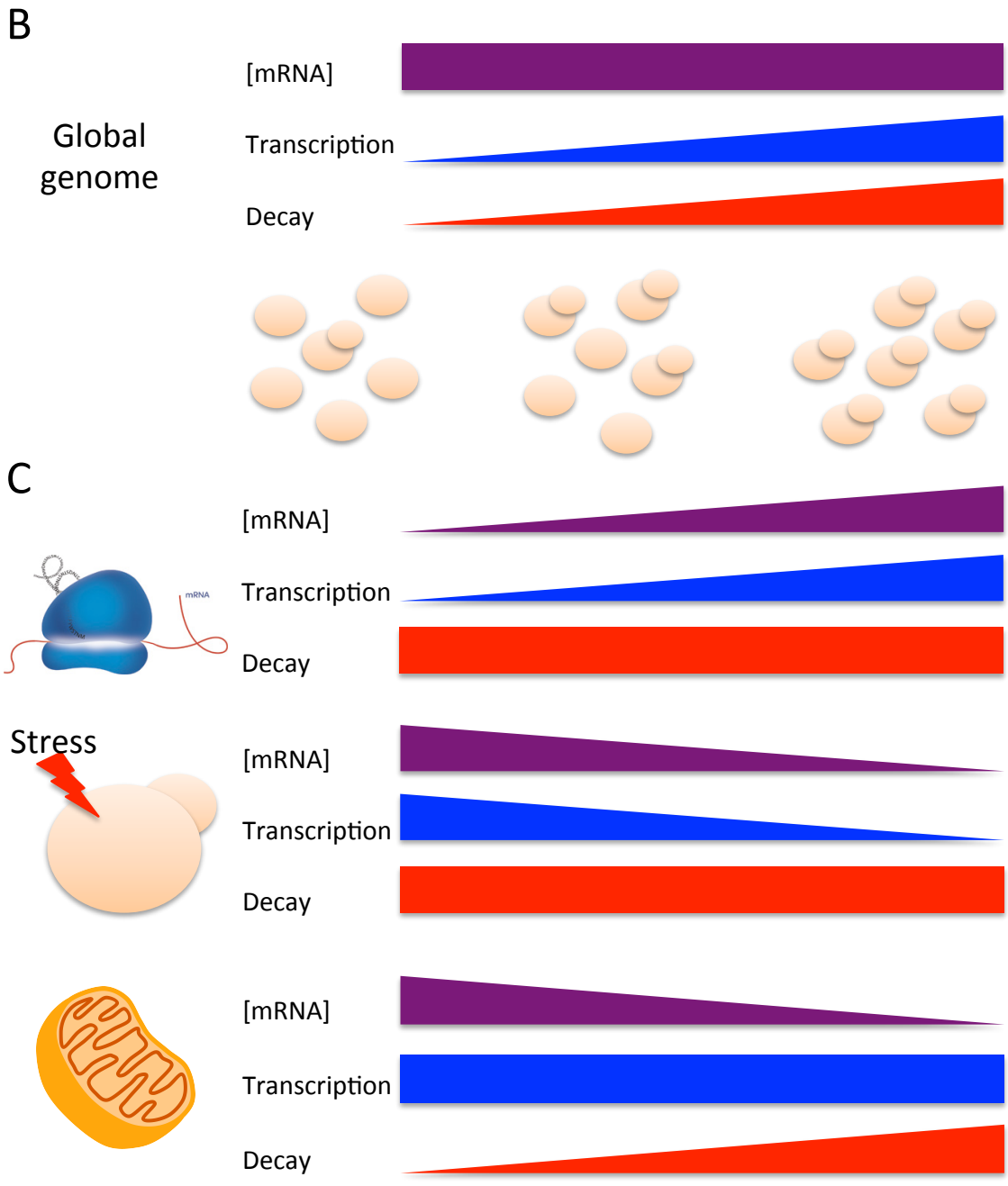

Figure 4. Growth rate and gene expression. A. Cells must adapt to changing environmental conditions to maintain fitness and to compete with other genotypes during the natural selection process. As fitness is the net growth of a genotype over time, one of the most important variables for single cell organisms is adjusting the cellular GR with gene expression. **B.** the [mRNA] of a given gene is controlled by the action of two opposite forces: synthesis by RNA pol II and degradation by several exonuclease pathways. **C.** mRNA turnover, not mRNA levels, increase with proliferation for most genes .**D.** Some groups of genes, however, regulate their mRNA

concentration by uncoupling mRNA stability from the transcription rate. As an example, mitochondria-related genes lower mRNA levels at fast growth by reducing mRNA stability.

Regulation of mRNA turnover, localization, and translation in the control of gene expression is critical for controlling protein production in eukaryotes (Derrigo, Cestelli et al. 2000; Chavez, Garcia-Martinez et al. 2016). Control elements responsible for this specific regulation of mRNA metabolism reside in the mRNA itself. All transcripts contain variable lengths of untranslated sequences (5'-UTR and 3'-UTR) which contain the binding sites for a number of RNA-binding proteins (RBPs). Most RBPs assemble on the message at the moment of transcription, thus determining the future fate of the transcript from the very beginning. Such regulatory sequences have been identified in a wide variety of transcripts in numerous organisms, including mammals, *Drosophila, Caenorhabditis elegans* and *S. cerevisae* (Derrigo, Cestelli et al. 2000; Olivas and Parker 2000; Miller, Russo et al. 2014).

It has been described two general pathways of mRNA degradation in yeast. In the main one, mRNAs are first deadenylated, which allows the mRNAs to be decapped, exposing the body of the mRNA to rapid 5′→3′ exonucleolytic degradation (Decker and Parker 1993) (Hsu and Stevens 1993; Muhlrad, Decker et al. 1994; Muhlrad, Decker et al. 1995). Alternatively, mRNAs can be exonucleolytically degraded 3′→5′ following deadenylation (Anderson and Parker 1998).

Individual mRNAs can exhibit different rates of deadenylation, decapping and 3′→5′ degradation. The identification of proteins responsible for the modulation of deadenylation and/or decapping rates on individual mRNAs is an important goal in cell biology. One of this factor is Puf3, which belongs to a widely conserved family of RNA-binding proteins that regulates diverse cellular processes by promoting translational repression and/or degradation of targeted mRNAs (Zamore, Williamson et al. 1997). At the molecular level, Puf proteins bind conserved UGU sequences within the 3’ UTR of transcripts, disrupting translation initiation complex interactions or stimulating mRNA degradation by

recruitment of decay complexes (Miller and Olivas 2011). In a some specific situations, Puf proteins can stabilize mRNA targets by promoting translation (Quenault, Lithgow et al. 2011). It has been described that *S. cerevisiae* Puf3 controls mRNA location (Saint-Georges, Garcia et al. 2008) and stability in response to the carbon source (Miller, Russo et al. 2014). In addition, Puf3 stimulates mitochondrial localization of nuclear-transcribed mRNAs containing Puf3 binding sites. The hypothesis is that Puf3 shuttles mRNA targets to the mitochondrial outer membrane surface, where they are translated and imported into the mitochondria (Figure 5).

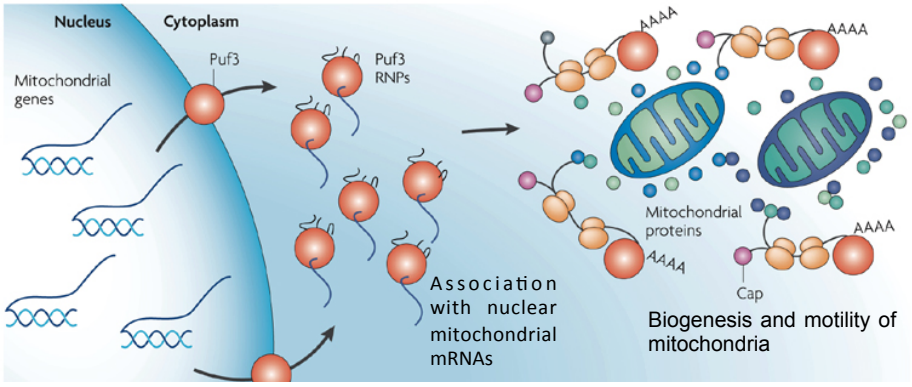

Adapted from Keene, 2007

Figure 5. The Pumilio protein Puf3. Puf3 protein (represented as a red circle) in *S. cerevisiae* forms a post-transcriptional operon that is involved in the co-regulation of protein expression, functioning in motility and mitochondrial biogenesis. Puf3 associates in the cytoplasm with nuclearly encoded mitochondrial mRNAs and favor their stabilization or decay in a some specific situations.

1.2.2 Microenvironment and phenotypical state

Based on recent studies, it has been proposed that population heterogeneity is largely determined by an interplay between the phenotypic state of a cell and its activities and the microenviromental differences that are created in growing cell populations. As an example, growing isogenic adherent mammalian cells create cell islets and regions that are sparsely or densely populated, to which cells

adapt their size, shape and rate of proliferation. This can be also seen in unicellular organism. The coupling between cell size and the timing of cell division in yeast and between cell size and the determination of phage lambda infection fate in E. Coli are examples of that (Snijder, Sacher et al. 2009) (Snijder and Pelkmans 2011).

Also, the multiple cell types existing in *Bacillus subtilis* biofilms are determined by the position the cells occupy within the biofilm. Bacteria communicate each other, form cell-cell contacts and sense the cell density and nutrient level by quorum sensing. This result in different complex patterns of multicellular behaviour, which improve the overall fitness of the population The localization and percentage of each cell type is dynamic throughout development of the community (Vlamakis, Aguilar et al. 2008) (Snijder and Pelkmans 2011).

The existence of molecular mechanism that sense local cell densities, cell–cell contacts, relative location, and nutrients in bacteria, yeast and mammalian support the importance of such population-dependent behaviour. By changes in gene transcription, protein translation, cellular growth, proliferation rate, sensitivity to apoptosis, metabolic activity, cell shape and/or cell polarization and motility, cells are able to adapt to modifications in such parameters. In turn, these changes in the most of cellular activities determine the manner in which individual cell behaves within its population. Accordingly, it contributes to shaping the population context (Snijder and Pelkmans 2011).

1.2.3 Cell cycle regulation

To control size, proliferating cells tie division to growth. In *S. cerevisiae*, which divides asymmetrically into a larger mother and smaller daughter cell, size control takes place in the first G1 phase of daughter cells (Johnston, Pringle et al. 1977). This checkpoint in which cells decided to enter in S phase is known as STAR in yeast (Hartwell 1974) and *Restriction Point* in mammals (Pardee 1974). The accurate transition from G1 phase of the cell cycle to S phase is crucial for the control of eukaryotic cell proliferation, and its misregulation promotes oncogenesis (Bertoli, Skotheim et al. 2013).

Progression through G1 is promoted by the upstream G1 cyclin Cln3 in complex

with the cyclin dependent kinase Cdc28. The Cln3–Cdc28 complex is the first to act in START (Dirick, Bohm et al. 1995). Cln3-Cdc28 phosphorylates and partially inactivates Whi5, the inhibitor of the heterodimeric transcription factor SBF (Swi4/Swi6) (Costanzo, Nishikawa et al. 2004) (Wijnen, Landman et al. 2002; de Bruin, McDonald et al. 2004) Partially active SBF, and the related transcription factor MBF (Mbp1/Swi6), promote the transcription of two further G1 cyclins CLN1 and CLN2 , which form a positive feedback loop by completing Whi5 inactivation and SBF activation committing the cell to division (Cross, Hoek et al. 1994; Flick, Chapman-Shimshoni et al. 1998; Wijnen, Landman et al. 2002; Skotheim, Di Talia et al. 2008; Ferrezuelo, Colomina et al. 2010)

The upstream position of Cln3 in the G1 regulatory network suggests that this protein is the trigger. However, its concentration does not clearly increase during G1.

A recently model has been proposed in which the dilution of the cell cycle inhibitor Whi5 controls the yeast cell size to promote G1 progression.

They found that the concentration of the cell cycle inhibitor Whi5 strongly decreases through G1, which suggests that the dilution of the cell cycle inhibitor Whi5 is a size-dependent signal promoting cell cycle progression. Such an inhibitor-dilution model represents a mechanism of cell size control that does not require a size-dependent increase in Cln3 activity and explains how growth drives proliferation.

Because Whi5 is differentially partitioned, following division, its concentration in daughter cells is consistently higher than in mother cells. However Whi5 is a stable protein, synthesized primarily during S/G2/M at a rate independent of cell size. This explains that small and large cells produce similar amounts of Whi5. This results in larger budded cells having a lower Whi5 concentration just before division. Since larger mother cells produce larger daughter cells this explains the inverse correlation between Whi5 concentration and cell size at birth, which is essential for the inhibitor-dilution size control model.

In the inhibitor-dilution mechanism, the amount of Whi5 in daughter cells does not scale with size. In contrast, the cell cycle activator Cln3 is produced in proportion to size. This differential size-dependency of cell cycle activator Cln3 and inhibitor Whi5 synthesis constitutes the basis of size control in budding yeast.

Then, according to this model, the rate at which cells pass Start is determined by the concentrations of Whi5 and Cln3. If Cln3 concentration is constant in pre-Start cells, the Whi5 concentration alone should predict the rate at which cells progress through Start (Schmoller, Turner et al. 2015) (Figure 6).

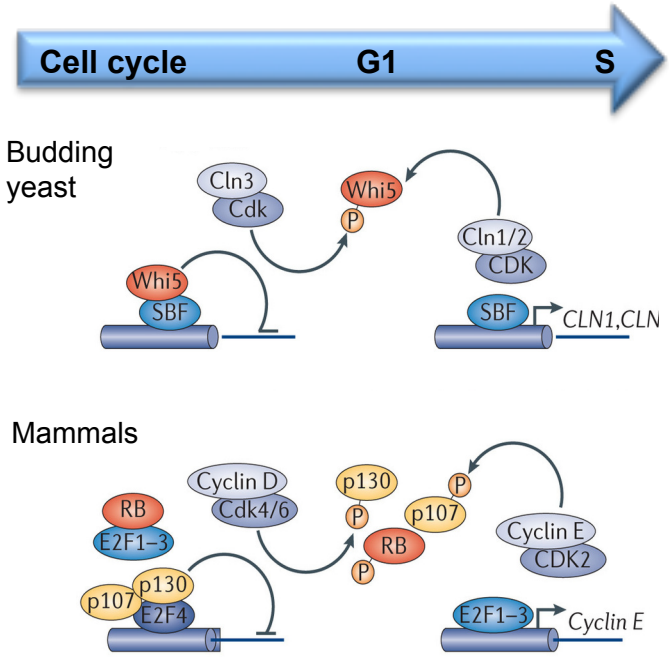

Adapted from Bertoli, Skotheim et al. 2013)

Figure 6. The G1/S regulatory network. Progression through G1 is promoted by the upstream G1 cyclin Cln3 in complex with the cyclin dependent kinase Cdc28. The Cln3–Cdc28 complex is the first to act in START . Cln3-Cdc28 phosphorylates and partially inactivates Whi5, the inhibitor of the heterodimeric transcription factor SBF . Partially active SBF promote the transcription of two further G1 cyclins CLN1 and CLN2 , which form a positive feedback loop by completing Whi5 inactivation and SBF activation committing the cell to division. In mammals, Retinoblastoma protein performs the role of Whi5 in yeast (lower panel).

1.2.4 Aging

Aging is a proven driver of heterogeneity (Avery 2006) (Glauche, I). This process is defined as a complex gradual impairment of normal biological function caused by accumulation of molecular damage, finally culminating in death (Lee, Avalos Vizcarra et al. 2012).

In the past few decades, genetic studies have identified a number of conserved pathways that regulate lifespan across species, suggesting that genes that modulate aging have been conserved in sequence and function, over a billion years of evolution (Smith, Tsuchiya et al. 2008).
In 1959, it was developed the yeast model system for aging, demonstrating that mortality rates increase with age resulting in cells with a reproducibly finite lifespan(Mortimer and Johnston 1959). Since then, yeast has served as an important model organism for studying aging, due to its short lifespan and the ease of genetic manipulation (Zhang, Luo et al. 2012)

Three different forms of aging have been defined in budding yeast. These are: (I) replicative aging, indicated by replicative lifespan (RLS), defined as the number of daughter cells produced by a mother cell before death (PNAS 2012, aging); (II) chronological aging, which is defined by the time a non-proliferating cell can survive in stationary phase (Longo, Shadel et al. 2012), and (III) clonal senescence, a consequence of disruption of telomerase enzyme complex (Smith, Wright et al. 2015). There are evidences of aging implicating a genetic component, as lifespan varies from one strain to another (Jazwinski 1990).

In this thesis we will focus on replicative aging. *S. cerevisiae* has a finite lifespan, defined by the number of times it produces a daughter cell. So individual yeast cells of standard laboratory strains can produce typically 20–30, daughter cells during a lifetime before they enter senescence (Mortimer and Johnston 1959). This process takes about 2–3 days on complex media and is one of the most rapid aging processes known. Every time a mother cell divides, it can be detected a circular bud scar composed of chitin on the mother cell surface which serves as aging biomarker (Figure 7A).

Cell replicative aging can be explained by the cell spiral model in which a virgin cell (0 generation) produces a daughter cell in every turn of the spiral (Figure 7B). During this cell cycle spiral, mother cells divides asymmetrically and generates a considerably smaller daughter cell which is born completely rejuvenated, this is, they reset their clock to zero, preventing clonal aging. That happens independently of the mother cell age at least until the last few mother cell divisions. However, the mechanism by which rejuvenation is possible is not well understood yet today. During the aging process, mother cells acquire different morphological and physiological changes as an increase in cell size, wrinkled shape, an elongation in cell cycle duration or sterility, the change many other biochemical parameters like ROS content and protein carbonyl content, they loose cell cycle checkpoint mechanisms and finally they enter in apoptosis (Breitenbach M. Et al 2015) (Jazwinski 1990; Smith, Wright et al. 2015; Yang, McCormick et al. 2015).

So cellular aging and asymmetric cell division are intimately linked. Mother cells divides asymmetrically in order to accumulate and retain damaged or lifespan-limiting materials, known as aging factors, thus allowing daughter cells to have a full lifespan. However, the daughters of very old mothers on glucose media inherit some damaged material and display a shortened lifespan, because the capacity of mother cells to divide asymmetrically decays (Smith, Wright et al. 2015). This is known as the “aging factors hypothesis”. In accordance with this, a recent study shows asymmetric distribution of several proteins between mother and daughter cells (Jo, Liu et al. 2015; Yang, McCormick et al. 2015). Moreover proteins of the translation machinery that are uncoupled form transcript levels seem to accumulate in aged cells, promoting the changes occurring in aging yeast such as metabolic changes, protein stress responses, and changes in the stoichiometry of many protein complexes (Janssens, Meinema et al. 2015). Asymmetric cell division is also a general phenomenon in mammalian cells (Zhang, Luo et al. 2012).

A

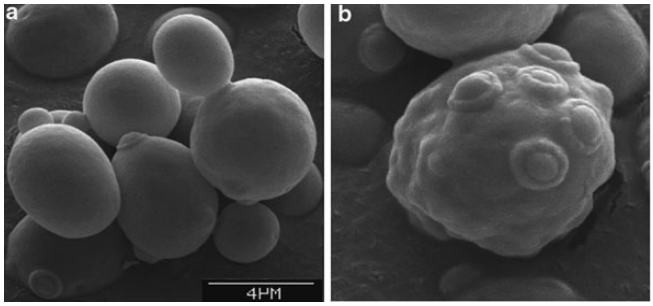

B

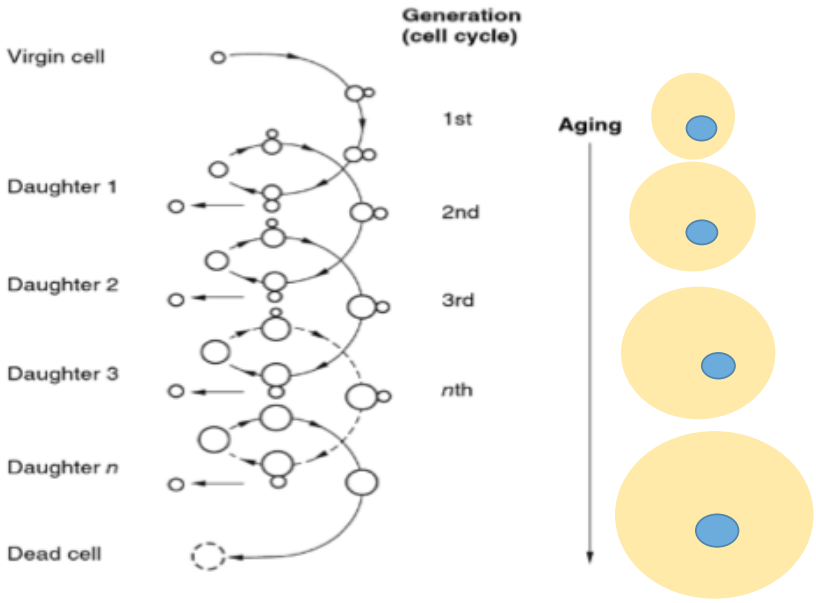

Adaptada de Jazwinski, 1990

Figure 7. Replicative aging in *S.cerevisiae*. A. Scanning electron microscopy pictures of a haploid strain (BY4741). In the left image young yeast cells can be observed. Note small size, the smooth surface and the infrequent bud scars. Virgin cells display no bud scars but only one birth scar. In the right image old mother cells of the same strain are shown. Note the large size, the irregular surface and the multiple bud scars. Both pictures are shown at the same magnification. **B.** Schematic of mother cell-specific aging. Every cell division cycle is represented by one turn of the spiral. In every generation the mother cell grows and ages, while the daughter cell is rejuvenated and increases in size only slightly. The senescent mother cell can no longer produce a bud and eventually dies and lyses through apoptosis. Adapted from Aging research in yeast.

Although *S. cerevisiae* has served as an important model for replicative aging research, the inability to track mother cells and follow molecular markers during the aging process is an important limitation to yeast aging study. The traditional lifespan assay consists is manual micromanipulation to remove daughter cells from the mother. This is a laborious, time-consuming process that does not allow long term tracking with high resolution microscopy. Recently, a microfluidic system capable of retaining mother cells has been developed making it possible to track fluorescent reporters in single cells throughout their lifespan (Janssens, Meinema et al. 2015). Nevertheless, there is a lack of techniques that facilitate the study of inheritance of aging at the level of chromatin state in clonal populations of cells.

Understanding the dynamics of epigenome variation during normal aging is critical for elucidating key epigenetic alterations that affect development, cell differentiation and diseases (Sun and Yi 2015). Recent studies have demonstrated that genome-wide DNA methylation patterns change with age and show that this age-associated epigenetic drift may have deep implications for stem-cell biology, disease development and possibly also human evolution. Thus, it has become of great interest to study the detailed epigenome dynamics landscape in response to aging. In this regard, cellular heterogeneity is one of the main issues (Yuan, Jiao et al. 2015)

1.3 How to study cell-to-cell variability

Before it can be stated that stochasticity is the reason why variability in cellular behaviour happens, one must be able to discard such confounding factors.

The population average techniques that involve the lysis of whole populations of cells, culture or tissue mask substantial information on population distribution, like the existence of subpopulations with different behaviour (Huang 2009). Otherwise, the experimental methods used to identify the responsible mechanisms of cell population heterogeneity cannot be easily apply for higher-level cellular activities (Snijder and Pelkmans 2011).

Among single-cell analysis techniques, there is a wide spectrum of methods

that differ basically in the information they provide on the nature of heterogeneity (Huang 2009).

1.3.1 Flow cytometry

This technique is one of the most powerful ones to study population heterogeneity. It is not strictly a single-cell analysis technique, but measures a specific property of a cell in an entire population at the resolution of individual cells (Huang 2009). Flow cytometry makes measurements on cells as they flow in single file past an array of detectors. In a typical flow cytometer (Shapiro, 1995), individual particles pass through an illumination site while some detectors measure the magnitude of a pulse representing the scattered light or the level of fluorescence. The scattered light provides information on the size and granularity of particles; however, the real power of this method comes from the possibility of measuring fluorescence intensity of individual cells. There are several sources of cellular fluorescence: autofluorescent pigments, the addition of fluorescent stains that bind to or react with particular molecules and the addition of specific labels such as fluorescently-tagged antibodies, oligonucleotides or lectins. Flow cytometry have several advantages over conventional cytometry. First, flow cytometry data sets often represent 10,000 to 500,000 cells for a given population leading to statistically significant results. Secondly, since flow cytometry use very sensitive electronic detectors it can distinguish very small differences in the intensity of scattered light or fluorescence. This makes possible to obtain quantitative measurements of sample heterogeneity. Finally, flow cytometry is a multiparametric technique, which means that it can measure different characteristics of each cell. Such measurements are useful because they allow to correlate the different characteristics and thus define subpopulations and/or distinguish between different cell types (Davey and Winson 2003) (Ibrahim and van den Engh 2003).

1.3.2 FACS

FACS (fluorescence-activated cell sorting) enables to sort a specific fragment of a cell population with respect to the distribution of a property of interest using fluorescence, whether it is a subpopulation or a population fraction. Then, it can be monitored how the sorted cells behave over time and distinguish if the sort fragment present a stable and irreversible state or conversely, it is in a dynamic and reversible state. Altogether, this can supply insight into the dynamics that underlie heterogeneity at the population level. In the case of macro-heterogeneity, this is, when a bimodal distribution is present, a reversible state would indicate a dynamic equilibrium, with cells transitioning between two subpopulations. However, the sorting of a population fraction from a single-peaked distribution is of special interest because such dispersion is usually considered “noise” (Huang 2009). Recent studies in our lab in yeast have demonstrated that the tail fractions exhibit different transcriptomic patterns of biological significance (Garcia-Martinez, Delgado-Ramos et al. 2016). This has also been shown in mammals, where the high or low expression levels of a stem cell marker control the cell lineage choice (Chang, Hemberg et al. 2008).

A limitation of FACS sorting is that errors in sorting could originate false-positive heterogeneity. That happens specially when there are contaminating cells with a high proliferation rate that mask the real population. It must to be separated from intrinsic population heterogeneity (Huang 2009) (Enver, Pera et al. 2009). In the other hand, FACS is a size-limited technology. Only smaller particles than 50 μm can be processed using FACS. That becomes a limitation when hydrogel carrier are analysed because those devices are susceptible to clogs. In summary, FACS has been developed for cell rather than for capsule sorting (Walser, Leibundgut et al. 2008).

1.3.3 Real time digital imaging

Contrary to flow cytometry this technique let to monitor temporal changes of a

given trait within individual cells in real time using live video-microscopy. This permit to knowing for example the changes in the cellular levels of a fluorescent protein (Huang 2009). In this way the information about fluctuations of gene expression can be obtained facilitating the discovery of novel regulatory relationships (Austin, Allen et al. 2006). However one disadvantage of the present technique is that only a hundreds of cells can be capture at a time so the amount of data produced is not sufficient to perform a robust statistical analysis. A remarkable characteristic of single cell monitoring is the capability of track the cell history and constructs the entire dell linage. Of biological interest is that single-cell monitoring allows the tracking of cell fate history and the construction of entire cell-lineage pedigrees as has been shown in the study of regeneration in mammal cells (Huang 2009) (Schroeder 2008).

1.4 Microencapsulation of living cells

Microencapsulation can be defined as the envelopment of biologically active substances inside semipermeable membranes that protect the biological structures from potential hazardous processes (Orive and Pedraz 2010). The use of microcapsules has been increasing in the last years due to its potential applications in biochemistry, biomedicine, pharmaceutics, and environmental science (Martin-Banderas, Flores-Mosquera et al. 2005). This suppose one of the most relevant biotechnological progresses in the past 25 years (Orive and Pedraz 2010).

The field of application of bioencapsulation is enormous. As an example, it has been shown that bioencapsulation is a good option to mimicking the cell's natural environment in plant cell cultures. Moreover, this method is very useful to improve the efficiency of production of different metabolites for industrial application.

The encapsulation of life organisms is also applied in fermentation processes increasing the cell density when required or improving important factors such as the aroma in wine production.

In addition, bioencapsulation has an emerging potential in medicine. For

example, it is used to protect biologically active substances or probiotics from the environment damage. It can also be used for the controlled release of drugs or other substances in specific parts of the body.

The encapsulation can be even used to encapsulate cells, which remain immobilized within the polymer, being protected against the host immune system.

Therefore, cell microencapsulation suppose a promising strategy to overcome the present difficulties related to whole organ graft rejection as well as the specific release of growth factors and drugs.

In the last few years, the main applicability of this technology has been directed to the treatment of a wide variety of diseases, including anaemia, haemophilia B , kidney and liver failure, central nervous system insufficiencies and diabetes mellitus.

More recently, microcapsules have also been used as biodegradable vehicle for stem cell proliferation and differentiation as well as in vivo administration (Orive and Pedraz 2010) .

Several methods of microencapsulation of probiotic bacteria have been reported and include spray drying, extrusion, emulsion and phase separation. However none of these reported methods are able to produce large quantities of microcapsules with a homogeneous size. The most used microencapsulation procedure is based on the calcium-alginate gel capsule formation (Kailasapathy 2002).

In the present thesis we consider this tool from a very different point of view to those previously described (diagnosis, drug delivery, etc). Thereby, we have used microencapsulation as a tool to microbial analysis, from the budding yeast *Saccharomyces cerevisiae* to filamentous fungi as *Aspergillus nidulans*.

To address this issue we have used the Flow Focusing technique (Martin-Banderas, Flores-Mosquera et al. 2005).

1.4.1 Microencapsulation by Flow Focusing

The preparation of microcapsules involves the mixing of a cell suspension and a gel-precursor solution, typically an alginate or an agarose solution (Rabanel,

Bertrand et al. 2006) (Kailasapathy 2002). This suspension is used to produce small monodroplets by one of the several available techniques (Ganan-Calvo 2004; Walser, Leibundgut et al. 2008). Next, the droplets are reinforced by gelation, by chemically induced cross linking in the case of alginates (Bienaime, Barbotin et al. 2003) (Heinemann, Meinberg et al. 2005). As a result, cells are immobilized and randomly distributed inside the microcapsules by a Poisson distribution (Nir, Lamed et al. 1990; Rosenblatt, Hokanson et al. 1997).
For high throughput experimenting, compartments containing single cells are desired to avoid ambiguous results. However, the initial number of cells per capsule can only be controlled by means of statistics. A simple way to increase the fraction of monoclonal microparticles is keeping the average degree of occupation low. This is, it is necessary to highly dilute the cells in the gel-precursor solution prior to microparticles formation. On the other hand, this high degree of dilution leads to a high number of empty microparticles and as a consequence to undesired large production volumes and long sorting and analysis times. Accordingly, high dilution is only an option if very fast analysis methods are applicable (Walser, Leibundgut et al. 2008).

Flow Focusing (FF) is a simple, fast and high throughput microencapsulation technique that started to be developed in 1994 (Gañán-Calvo 1998) (Figure 2A). The main features of this technology are: a) FF is compatible with different fluid combinations (liquid–liquid, liquid–gas) using simple liquids, polymeric solutions, emulsions, suspensions, or melted solids; b) homogeneous microparticles with a chosen size can be obtained in just one step, without additional purification steps; c) FF produces smaller particles than most other technologies, where particle size is determined by the nozzle dimension; d) the particles are scarcely stressed therefore FF is plenty suitable for the encapsulation of labile compounds (proteins, cells, and similar entities); e) FF allows the particle design so the morphology, surface treatment and composition (e.g., homogeneous particles, two-phase capsules, or hollow capsules) can be freely chosen); f) FF produces a remarkably high particle rates per orifice (Figure 2B)

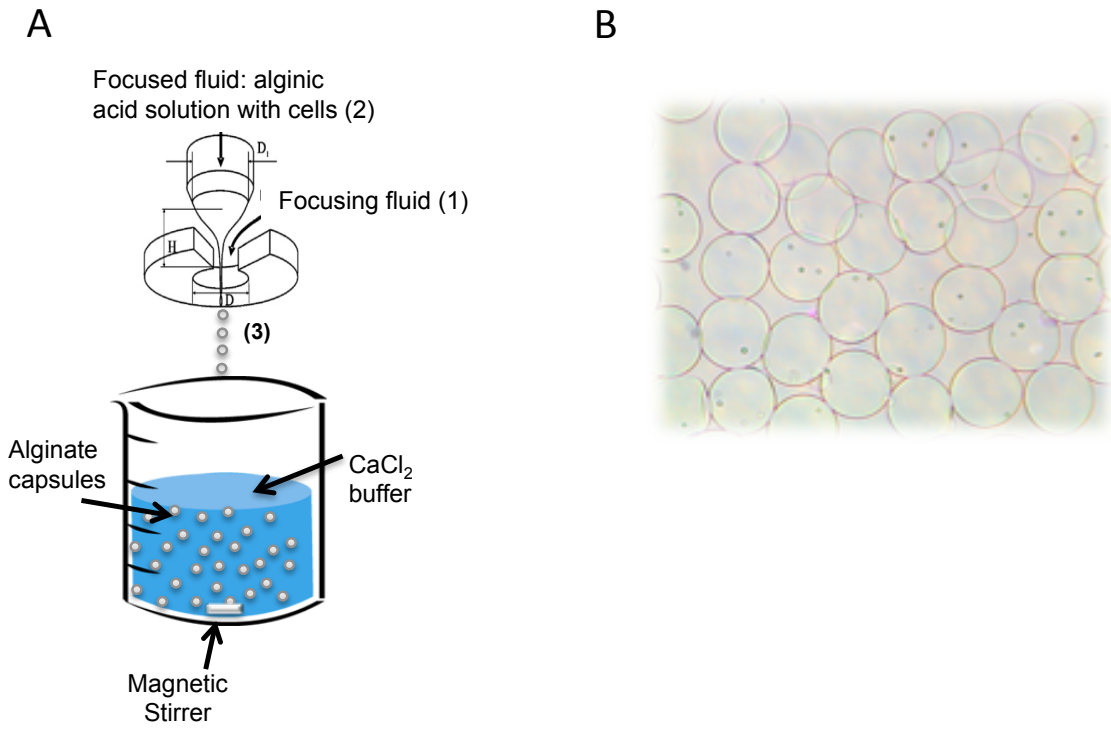

Figure 8. Microencapsulation by Flow Focusing. A. Flow-focusing atomizer. A schematic representation of the flow-focusing technology is shown. The sample is injected with a syringe pump through a capillary feed tube inside a chamber and pressurized by a continuous air supply in a Cellena encapsulator. The stationary jet breaks up by capillary instability into homogeneous droplets, which will gel in a continuously stirred calcium chloride solution at room temperature. Adapted from Martin-Banderas et al. (2005). 1) focusing fluid, 2) focused fluid, 3) meniscus. **B.** Particles produced by FF. The parcicles are very homogeneous in size and shape.

The flow focusing technology is based on the combination of hydrodynamic forces with a specific geometry (Ganan-Calvo 2004) . A FF device (Figure 2A) consists of a pressure chamber pressurized with a continuous focusing fluid supply (1). Inside, a focused fluid (2) is injected through a capillary feed tube whose extremity opens up in front of a small orifice linking the chamber with the exterior ambient. The focusing fluid stream (1) molds the fluid meniscus (3) into a cusp, giving rise to a micro- or nano jet exiting the chamber through the orifice; the jet diameter is much smaller than the exit orifice diameter. Finally,

the jet is broken into homogeneous droplets by capillary instability. The feed tube can be composed of two or more concentric needles and different liquids can be injected, thus leading to produce multilayer microcapsules with multiple shells of controllable thickness . In summary, FF assure a highly fast production of up to millions of droplets per second as the jet breaks up a rate much higher than that obtained by other microencapsulation techniques (Martin-Banderas, Flores-Mosquera et al. 2005).

1.4.2 Microencapsulation of filamentous fungi

Filamentous fungi constitute a very diverse biological group, with a great impact on human life (May and Adams 1997). Production of antibiotics, food additives, or recombinant proteins at industrial scale are good examples of the biotechnological importance of filamentous fungi (Knuf and Nielsen 2012; Brakhage 2013) (Ozcengiz and Demain 2013). Several filamentous fungal species are pathogens of plants and metazoans, including humans (Sexton and Howlett 2006). In basic research, filamentous fungal models have contributed to establish the basis of key biological aspects such as genetic information flow and metabolism (Beadle and Tatum 1941), DNA recombination (Holliday 1964)or gene silencing (Cogoni and Macino 1999). In all these fields of fungal research, genetic analysis is one of the most productive tools. Classic, forward, and reverse genetic tools are readily available for fungal models such as *Aspergillus* and *Neurospora*, and genetic approaches still remain a fundamental source for the discovery of novel biological functions. However, genetic screenings with filamentous fungi usually involve laborious, tedious, and/or time consuming procedures (for examples, see (Harris, Morrell et al. 1994; Seiler and Plamann 2003)), due to the formation of heterokaryons in organisms that undergo cell fusion and the growth mode, forming hyphae with multinuclear cellular compartments and tangled webs of mycelia instead of undergoing budding or cell fission to form two distinct uninucleated daughter cells from one mother. A good example of these limitations is cell-cycle research, a field in which the *Aspergillus* model emerged as early as the yeast ones (Hartwell, Culotti et al. 1970; Morris 1975; Nurse 1975). However, due to the simplicity of

yeast procedures, research with these single-cell organisms advanced more rapidly.

These drawbacks of filamentous fungal research can be solved, at least partially, with the use of high-throughput methods like, for instance, the combination of flow cytometry and sorting. The problem is that flow cytometry machines are not suitable for filamentous organisms. Recently, large-particle flow cytometry has been applied to fungal pellets (de Bekker, van Veluw et al. 2011), but fungal pellets usually contain a mixture of several fungal individuals, and, as such, they can be considered fungal populations rather than clonal fungal entities. In this work, we overcome all these issues with a novel method for generating isolated fungal microcolonies after the germination of microencapsulated spores, which makes possible their analysis by Flow cytometry and sorting. This method allows for positive and negative selection during genetic screenings.

2. Objectives

The aims of this thesis can be summarized in two points:

1. The development of new methodologies that facilitate microbial analysis.

2. The use of such methodology to investigate proliferation heterogeneity in *Saccharomyces cerevisiae*

3. Results

3.1 Development of new technologies that facilitate the isolation and massive analysis of clonal microscopic colonies of *Saccharomyces cerevisiae*

3.1.1 Encapsulation of Saccharomyces cerevisiae individual cells in alginate microspheres and their analysis by flow cytometry

Our first step in this project was the development of a protocol to encapsulate single cells of *S.cerevisiae* in calcium alginate particles using the Flow Focusing technology. To do that we had to optimise the nebulization parameters of the Cellena device (see Material and Methods) as well as the appropriate cell concentration to obtain the desired number of yeast per capsule. Using different proportion of culture *versus* alginic acid volumes, we were able to predict the approximate number of cells per capsule. For instance, by changing this proportion we produced particles containing either 1-5 or 30-50 cells per capsule (Figure 8A).

Once we had developed a reproducible encapsulation protocol we wondered if we were able to distinguish the particles according to the cell content by flow cytometry (Figure 8B). We made use of a COPAS and BioSorter cytometer, suitable for the optical analysis on particles larger than 50 μm. First we analysed the time of flight (TOF) of the capsules, which reflects their size. The particles exhibited a normal distribution independently of the content, and the averages of the two preparations did not change significantly (Figure 8C). So, the particles were essentially monodisperse in size and this did not change with the cell content.

The next step was to detect the possible differences in the optical complexity of the two types of particles. To address that question we quantified the extinction (EXT) of the two populations. We obtained normal distributions again with a mean value of 15 and 30 units of extinction in the 1-5 cells and 30-50 cells populations respectively (Figure 8D).

The differences in optical extinction between the two populations of particles were independent of the size of the particles, as can be clearly visualized when the two TOF *versus* EXT plots were compared (Figure 8E). With these results

we concluded that it was possible to distinguish alginate microparticles by their cellular content following large particle flow cytometry procedures.

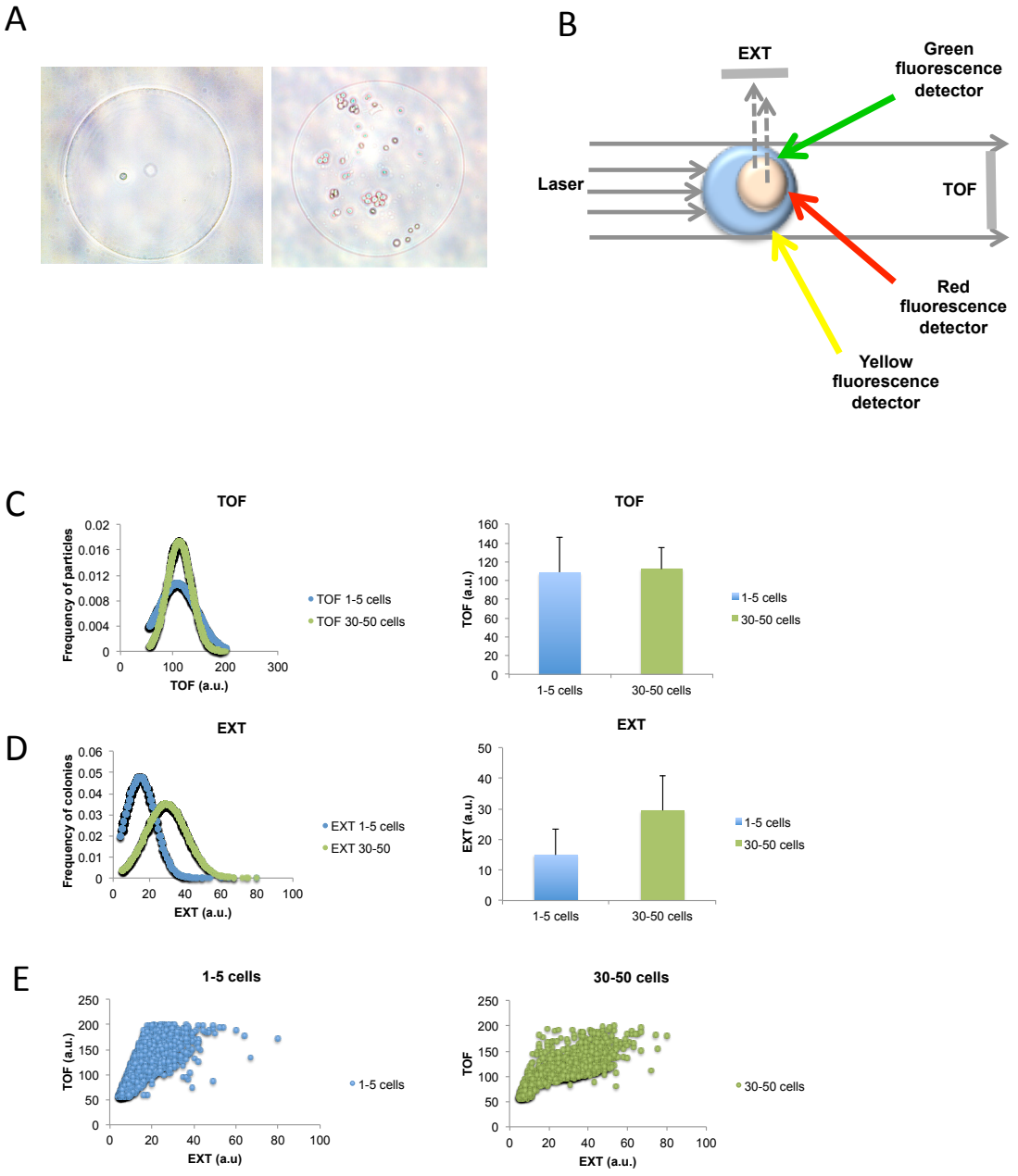

Figure 8. Flow cytometry analysis of particles containing 1-5 cells or 30-50 cells. **A.** Picture showing single or multiple encapsulated yeast in alginate capsules. **B.** Parameters that can be measured by large particle flow cytometry**.** The BioSorter allows the measurement of different physical parameters like the axial length of the object (TOF, time of flight), the optical density (EXT, extinction) and the intensity of fluorescent markers (green, red and yellow). **C.**Capsules TOF distribution and mean. It can be observed than the TOF is maintained in 110 units in both cases witch

correspond with approximately 100 µm. **D.** Particles EXT distribution and mean. **E.** TOF versus EXT was represented for particles containing 1-5 cells and 30-50 cells. It can be seen than the optical extinction depends on the cellular contain while TOF values are maintained. 2500 particles of each type were analysed.

3.1.2 Monitoring S. cerevisiae cell proliferation by microencapsulation and flow cytometry

In light of previous results we thought that it could be possible to monitor the proliferation of a *S.cerevisiae* cell population by microencapsulation and flow cytometry analysis. The use of microencapsulation for analysing the proliferation capacity of individual cells required checking that the encapsulation process did not affect the viability of yeast cells. No decrease in viability was detected after the encapsulation procedure. The number of colonies formed in YPAD agar plates by encapsulated and non-encapsulated cells was very similar (Figure 9A).

In order to follow the cell proliferation capacity of individual cells by flow cytometry, it was necessary to minimize the encapsulation of more than one cell per particle. We set the conditions to get the vast majority (94%) of the cell-containing particles loaded with only one cell (Figure 9B). Under these conditions a high proportion of particles were empty but, as shown before, this should not affect the flow-cytometry detection of the loaded capsules.

In order to detect cell proliferation, a population of encapsulated individual cells was divided into 9 equal samples: seven of them were incubated at different times (2, 4, 6, 8, 10,12 and 14 hours) in YPAD at 30 ºC. The other two samples were used as controls: one of them was maintained in YPAD at 4ºC and the last one was preserved in $CaCl_2$ at 4ºC. The observation by optical microscopy confirmed the formation of microcolonies in the samples incubated in YPAD at 30ºC. The control sample kept in $CaCl_2$ did not show any cell growth (not shown). As expected, the size of microcolonies increased with time (Figure 9C).

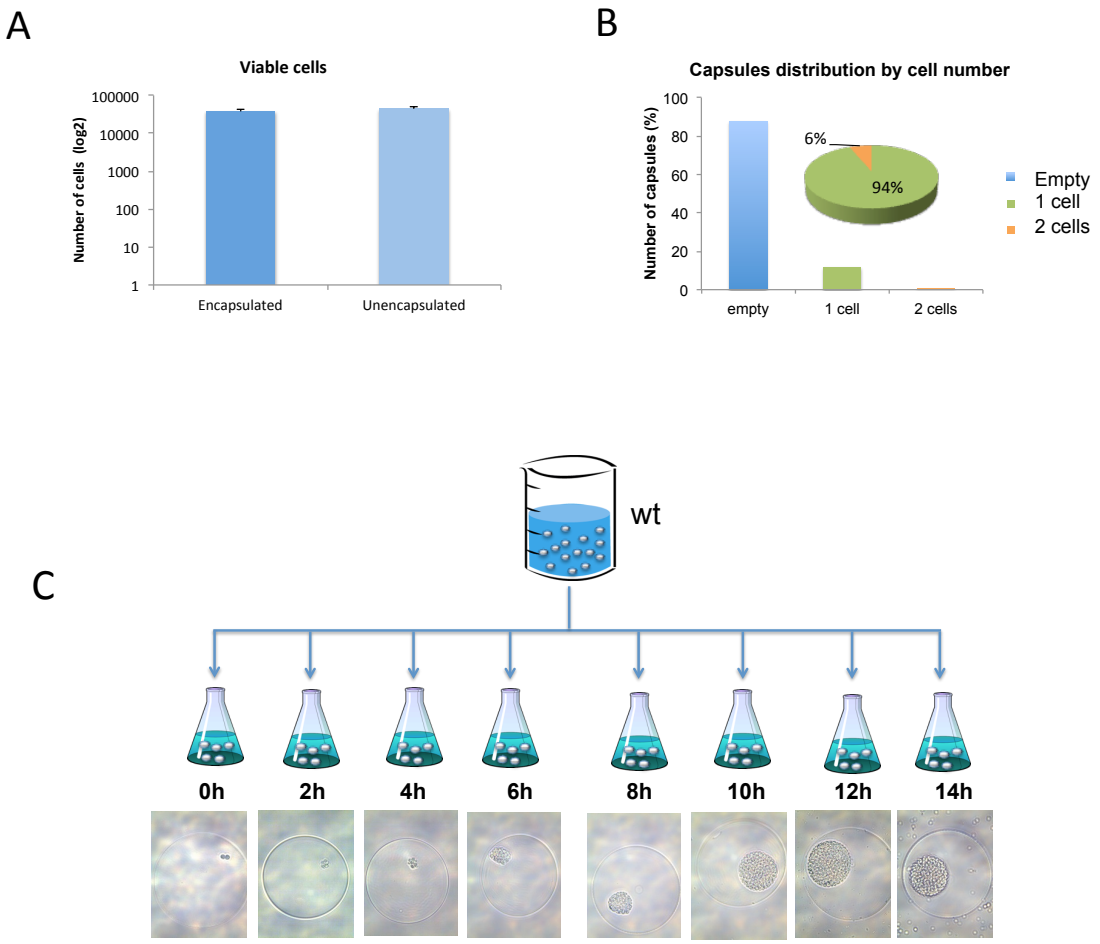

Figure 9. **Viability and proliferation of encapsulated individual cells. A**. Viability of the encapsulated cells of a standard experiment was compared with similar amount of cells, from the same culture, kept aside without being encapsulated. Cell viability was measured by its ability to form colonies on YPAD agar plates. Average and standard deviation from three independent experiments is shown. It can be observed that cells trapped in alginate particles remain fully viable. **B.** Capsules distribution by contains. A.500 capsules were analysed by optical microscopy accounting for the number of colonies inside and were classified as empty (blue), one cell (green), two or more cells (orange). It is seen that most of the capsules contained only one cell **C.** Monitoring the proliferation of *Saccharomyces cerevisiae* by microencapsulation and optical microscopy. *S.cerevisiae* cells were encapsulated under conditions that maximize the encapsulation of single cells. Encapsulated cells were incubated in rich liquid medium under standard culture conditions and were allowed to proliferate. At the different time points, (1-14 hours) samples were taken and observed by optical microscopy. Pictures taken by optical microscopy are shown (40x).

Once we confirmed the differences by optical microscopy we proceeded to analyse such populations by flow cytometry. First we checked that cell proliferation was not affecting significantly the size distribution of the particles. TOF values confirmed this prediction (Figure 10A). Then we addressed the detection of the microcolonies developed inside the particles. Since microcolonies constitute discrete entities that are optically distinguishable from the rest of the particle, we set the TOF parameters to detect them (See Materials and Methods). In this way, we got a direct approach to microcolony size. The measurements showed that detectable microcolony TOF started to increase after 6h of incubation in YPAD and continued increasing with the time of incubation (Figure 10B).

We also measured optical extinction, and the green and red autofluorescence of the particles. In all three cases we found increasing signals after 6 h of incubation (Figure 10C-E). Since the size of the particles did not change significantly during incubation (Figure 3A), we conclude that the differences detected by the other four optical parameters tested are due to the content of the microparticle and are reflecting cell proliferation and microcolony growth. Moreover, when we plotted microcolony TOF *versus* EXT, we found a clear correlation between the two signals after 6 h of incubation that was sustained in time (Figure 11A).

These increasing average values of these four optical parameters were associated to strong standard deviations (Fig 10B-E), pointing to an intrinsic heterogeneity in the proliferation of the encapsulated cells that increased with the incubation time. To check this, we graphed the distribution of the 6 h, 10 h and 14 h samples, and we observed that all of them presented a normal distribution for all the parameters that were studied. Even though, the increased amplitude of the Gaussian curves indicated a higher heterogeneity as the time of incubation increased (Figure 11B). The experimental procedure that we have developed opens, therefore, the possibility to study this proliferation heterogeneity within an apparently homogenous wild type population incubated in standard environmental conditions (see next chapter).

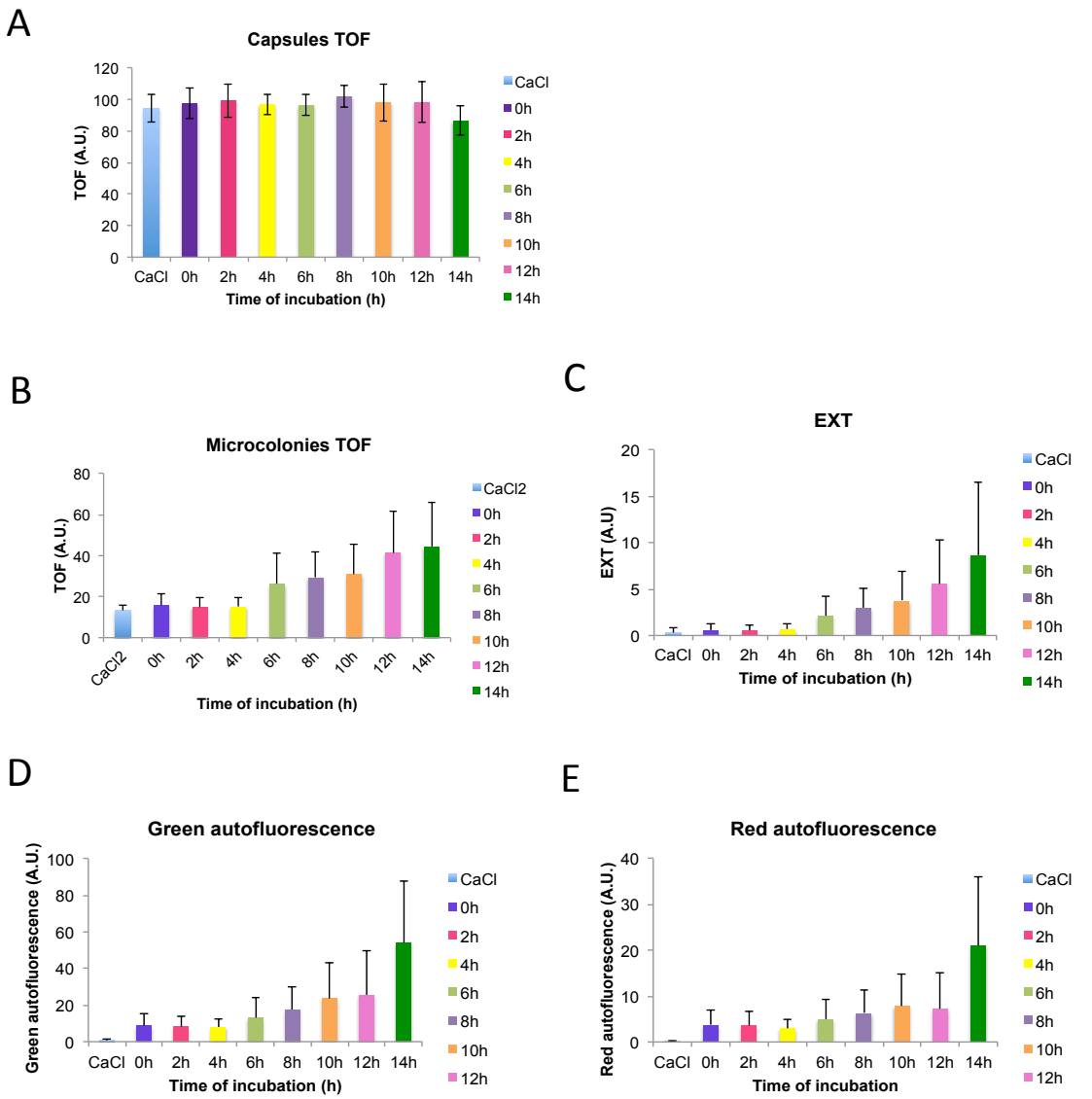

Figure 10. Flow cytometry analysis of samples showed in figure 2C. A. Control of capsules size. Specific flow cytometry parameters were set to measure the size of alginate particles in order to check their homogeneity in size (aprox 100 um) and shape. In all panels, the mean and the standard deviation of 1000 different single colonies per sample are shown. Different parameters are represented. B. TOF (time of flight), corresponding to the axial length of the colony. C. EXT (extinction), the optical density of the detected colony. D. Green self-fluorescence and E. Red self-fluorescence. The mean and the standard deviation for TOF, EXT, Green and Red self-fluorescence are represented for the 9 samples of the experiment. Data were filtered by TOF (10> TOF >100). The strong standard deviations (Figure 10 3B-E), pointing to an intrinsic heterogeneity in the proliferation of the encapsulated cells.

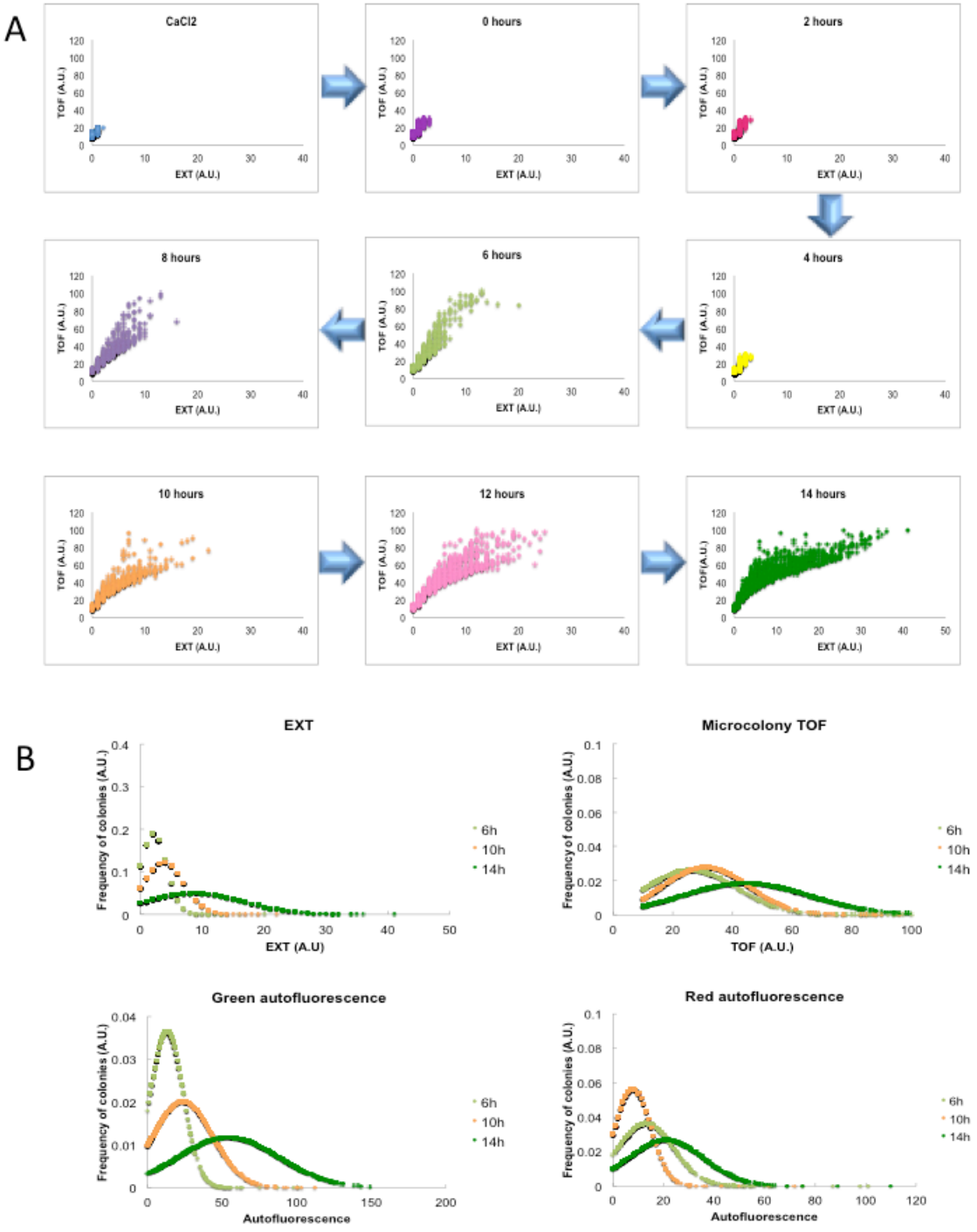

Figure 11. Detection of proliferation of the encapsulated cells by large particle flow cytometry. A. Two different populations of microparticles can be detected. The one situated to the left is corresponded with empty microparticles or microparticles with cells that did not proliferate. The right one is represented by microparticles containing yeast microcolonies in different proliferation states. **B.** An intrinsic heterogeneity that

increased with incubation time can be observed in the Gaussian curves distribution representation. Only three representative time points are showed (6h, 10ha nd 14h).

3.1.3 Application of microencapsulation technology to the study of the genetic interaction between DST1 *and* SFP1

With the aim to check the usefulness of the microbial analysis by microencapsulation and flow cytometry, we decided to apply this technique to clarify the genetic interaction between the *DST1* and *SFP1* genes, which was being studied in our lab. *DST1* encodes the transcriptional factor TFIIS which is an eukaryal and archaeal type of the RNA cleavage factor that stimulates the cleavage of the 3' -end of nascent RNA by RNA polymerases, when they are arrested after backtracking (Fish and Kane 2002). TFIIS is not essential through the *S. cerevisiae* life cycle (Nakanishi, Nakano et al. 1992). However, the *dst1*Δ mutant is highly sensitive to drugs that impair the *de novo* synthesis of NTP, such as 6-azauracil (6AU) and mycophenolic acid (MPA) (Exinger and Lacroute 1992).

Previous work in the lab allowed the isolation of mutants that suppressed the sensitivity of *dst1*Δ *to* 6AU and MPA (Gomez-Herreros, de Miguel-Jimenez et al. 2012). One of these mutants was affected in *SFP1,* related to the transcriptional regulation of those genes that encode ribosomal components [rRNAs and ribosomal proteins (RP)]. As shown in figure 12A, the double *sfp1*Δ *dst1*Δ mutant is able to growth in a medium with a 6AU concentration in which the single mutant *dst1*Δ is clearly sensitive (Gomez-Herreros, de Miguel-Jimenez et al. 2012). Nevertheless, the slow growth of the single *sfp1*Δ mutant, under any condition, made difficult the interpretation of an experiment that required a large number of generations. In order to overcome this inconvenience, we applied our proliferation assay, based on microencapsulation and flow cytometry, which reduces the observation time from 4 days (visible *sfp1*Δ colonies on plates) to 20 h (detectable *sfp1*Δ microcolonies in microcapsules). Four isogenic strains were encapsulated: wt, *dst1*Δ, *sfp1*Δ and the double mutant *dst*Δ*sfp1*Δ, and were incubated for 20h in the presence of 25 µg/ml 6AU. Observation by optical microscopy indicated that 6AU had no significant effect on the wild-type

proliferation capacity and the effect was also minimal for the *sfp1*Δ and *dst1*Δ*sfp1*Δ cells, whereas the *dst1*Δ cells underwent a dramatic growth arrest by the drug, resulting in aberrant microcolonies (Figure 12B).

The eight populations of microcolonies were analysed by flow cytometry. We detected different proliferation patterns in the absent of 6AU for the wt and the *dst1*Δ on one side and for the *sfp1*Δ and the double mutant on the other side, showing the last one a lower proliferation rate. These patterns were practically identical in the presence of 6AU except for the *dst1*Δ mutant, which presented a drastic reduction in growth (Figure 12C). Despite the intrinsic defect in cell growth that the *SFP1* deletion generated, when incubated in the presence of 6AU half the cells from the double mutant were able to develop bigger microcolonies than any of those produced by the *dst1*Δ cell population under the same conditions (Figure 12D). So, the proliferation assay based on microencapsulation and flow cytometry demonstrated the existence of an epistatic relationship between *SFP1* and *DST1*, which allows the suppression of the 6AU-sensitivity phenotype of *dst1*Δ by *sfp1*Δ.

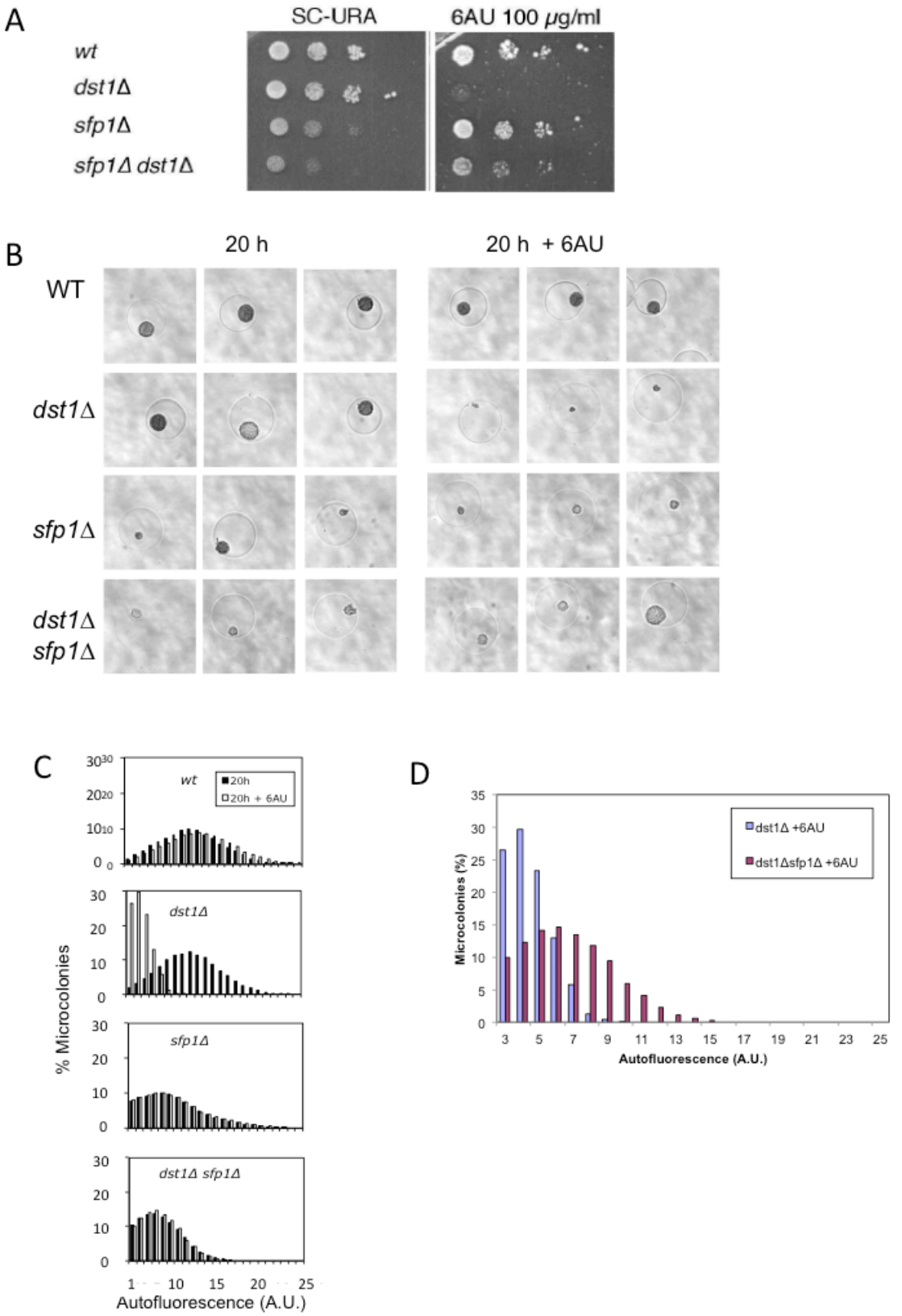

Figure 12. Genetic interactions analysis between DST1 and SFP1 genes by microencapsulation and flow cytometry. **A**.6AU effect over the growth in the four

strains analysed. The high sensitivity in the dst1Δ mutant can be observed in this drop assay . Sensitivity of dst1Δ to 6AU can be partially suppressed by mutations that alter the transcriptional regulation of RP genes as is observed in the double mutant dst1Δsfp1. **B.** Size distribution of the microcolonies developed by isogenic yeast cells with the indicated genotypes (BY4741 genetic background), in the absence or presence of 25 mg/ml 6AU. Deletion of SFP1 suppresses the sensitivity of dst1Δ to 6AU in the microcolony assay Images of representative microcolonies are shown. **C.** Individual cells were microencapsulated in alginate, incubated for 20 h and analysed in a flow cytometer utilizing autofluorescence as an indicator of cell size. **D.** Comparison of the size distributions of the microcolonies developed by the isogenic dst1Δ and dst1Δsfp1Δ cells incubated in the presence of 25 µg/ml 6AU for 20h .See Figure 1 for additional details.

3.1.4 Sorting of encapsulated microcolonies according to their proliferation rates

The results shown so far suggest that microencapsulated microcolonies can be sorted in order to select a subpopulation of cells according to their proliferative phenotype. In order to test this prediction, we encapsulated individual cells from wt and *dst1*Δ cultures as described above, and incubated them in minimal medium in the presence or absence of 6AU. As expected, flow cytometry analysis of the two populations displayed very similar results in the absence of 6AU, whereas produced clearly different patterns in the presence of the drug (Figure 13A), suggesting that this condition would allow differentially sorting the two genotypes.

We mixed the two populations and established the sorting frames in the flow cytometer for selecting wild-type and *dst1*Δ cells, according to the four optical parameters previously used (microcolony TOF, EXT, red autofluorescence and green autofluorescence; Figure 6B). Optical microscopy of the sorted capsules indicated a successful result, in terms of microcolony size (Figure 13C). In order to quantify the efficiency of these two types of sorting selection, we plated the sorted microcapsules allowing microcolonies to grow into visible colonies. Half of each sorted sample was plated in YPD media containing G418, which selected for the Kan^r marker of *dst1*Δ, and the other half in YPD without drug,

allowing growth of both *dst1*Δ and the wild type. For the wild-type selection we got a sorting efficiency of more than 90%. In the case of the selection for *dst1*Δ the sorting efficiency was 75% (Figure 13D). We concluded that flow-cytometry sorting of encapsulated microcolonies is an efficient procedure for the physical isolation of cell subpopulations with differential proliferation capacities.

A

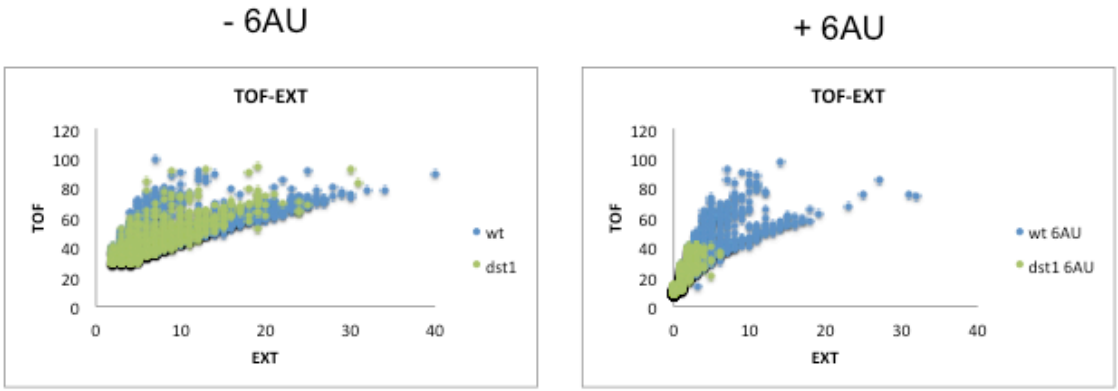

B

Wild type selection

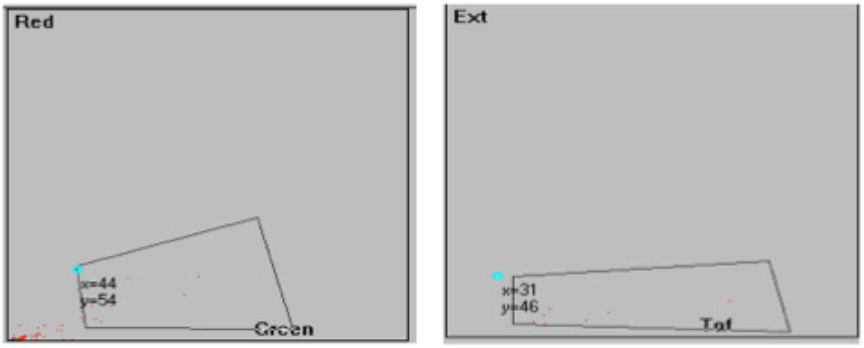

*dst1*Δ selection

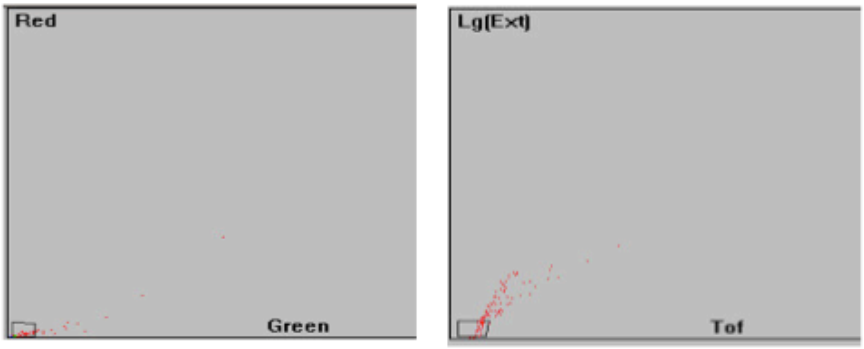

C

Wild type selection

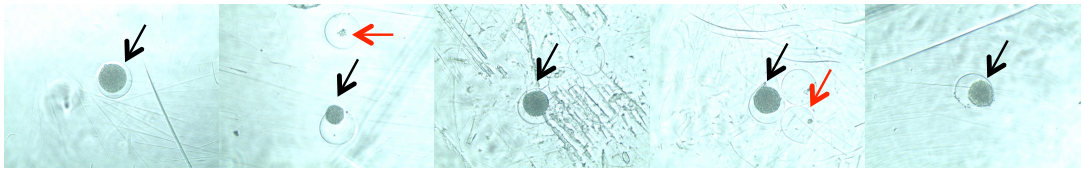

dst1Δ selection

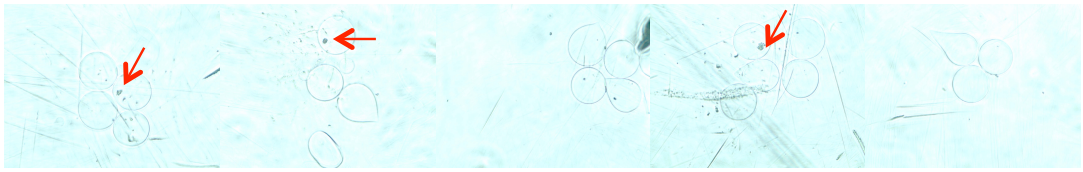

D

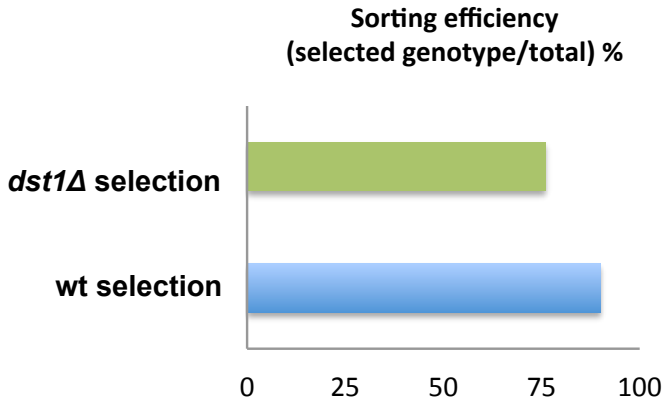

Figure 13 Sorting of encapsulated microcolonies according to their proliferation rates. A. Flow cytometry analysis of wt mixed with *dst1Δ* population. Note the decrease in TOF and EXT values in *dst1Δ* in the presence of the drug. this condition would allow differentially sorting the two genotypes . B. TOF versus EXT and Red versus Green autofluorescence parameters were plotted to select the region that should belong to the wt or mutant colonies (black box in the grey screen). C. Microwells showing the sorting result. An inverted microscope took the pictures. D. Efficiency of the sorting process, defined as the proportion of correct capsules with respect to the total of classified capsules

3.2 Flow cytometry of microencapsulated colonies for genetics analysis of filamentous fungi

In this chapter we present the combination of single spore microencapsulation and large particle flow cytometry as a powerful alternative for the genetic analysis of filamentous fungi. Individual spores were embedded in monodisperse alginate microparticles and incubated in the appropriate conditions. Sorting of the microparticles containing the clonal fungal mycelia proved the power of this method to perform positive and/or negative selection during genetic screenings.

3.2.1 Generation of fungal microcolonies by spore microencapsulation

Fungal spores were microencapsulated in calcium alginate beads with conditions adjusted to obtain single-spore capsules. This procedure gave microcapsules with a regular spherical shape and a homogenous size close to 400 um (Figure 14A). Microcapsules were first inoculated into liquid media to test the capacity of two selected fungal species, *Trichoderma reesei* and *Aspergillus nidulans*, to grow inside the alginate microcapsules (Figure 14, B and C). Samples were taken at regular intervals, and fungal growth was monitored by light microscopy. Alginate beads are transparent, which allowed for fungal visualization under the light microscope. Germination of spores inside the microcapsules could be observed 8 hours after inoculation. Fungal growth proceeded normally inside the alginate microcapsules by apical extension and branching. Proliferation inside the capsules could be measured by flow cytometry using the COPAS technology . Particles exhibiting higher optical density increased with the time of incubation (Figure 15, D and E). Cumulative distribution of optical density indicated that after 14 hours mycelia accumulation was heterogeneous, suggesting that some microcolonies were growing faster than other, as was also observed with microscopy (Figure 14, B-E). The parallelism between microscopic observation and flow cytometry measurement indicates that the combination of spore microencapsulation and COPAS

technology is a valid high throughput method for the analysis of filamentous fungal growth.

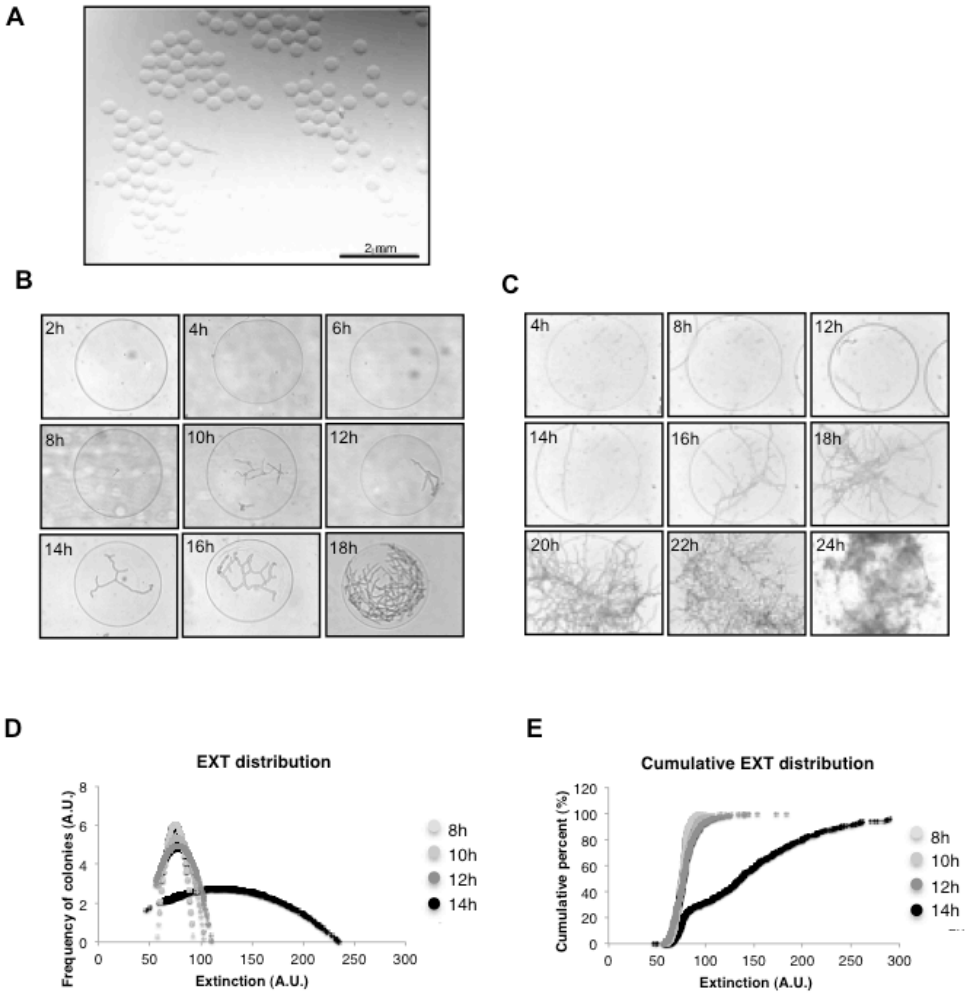

Figure 14. Monitoring the proliferation of *T. reesei* and *A. nidulans* spores by light microscopy and flow cytometry. A. Spherical size-monodispersed alginate microcapsules fabricated in the microencapsulator. **B-C.** Pictures of encapsulated spores during germination. In this test the spores were encapsulated in 400um, 3% alginate capsules. After encapsulation the beads were incubated in shaking flasks and samples were recovered after different time of incubation. **B.** *T. reesei*. **C.** *A. nidulans*. **D-E.** Flow cytometry analysis of encapsulated spores *T. reesei*. Aliquots were analysed by COPAS SELECT flow cytometry allowing the measurement of different optical parameters: size (TOF), optical density (EXT), green self-fluorescence and red self-fluorescence signals. The germination of spores is associated with an increase in density. These measurements are represented in the graphs showing the increase of

EXT over time (left) and the EXT distribution within the bead (right)

3.2.2 Detection of commonly used phenotypes of microencapsulated fungi

To test the reliability of this method and its utility for genetic analysis, different assays were performed. First, we tested whether microcapsules were suitable systems for detecting common fungal phenotypes. Proliferation of an auxotrophic *A. nidulans* mutant (pyroA4 pyrG89) was only detected in the microcapsules when the corresponding supplements were present in the medium (Figure 15A). In agreement with previous observations (Osmani et al. 2006), the auxotrophic spores could germinate in the absence of U2, but growth soon stopped, resulting in very short hyphae. Similarly, strains resistant to two different fungicides (pyrithiamine and glufosinate) were capable of colonizing microcapsules in the presence of the drugs, whereas isogenic non-resistant strains were unable, as expected (Figure 15, B and C). Finally, strains expressing fluorescent-tagged proteins were visualized when growing inside the microcapsules (Figure 15D).

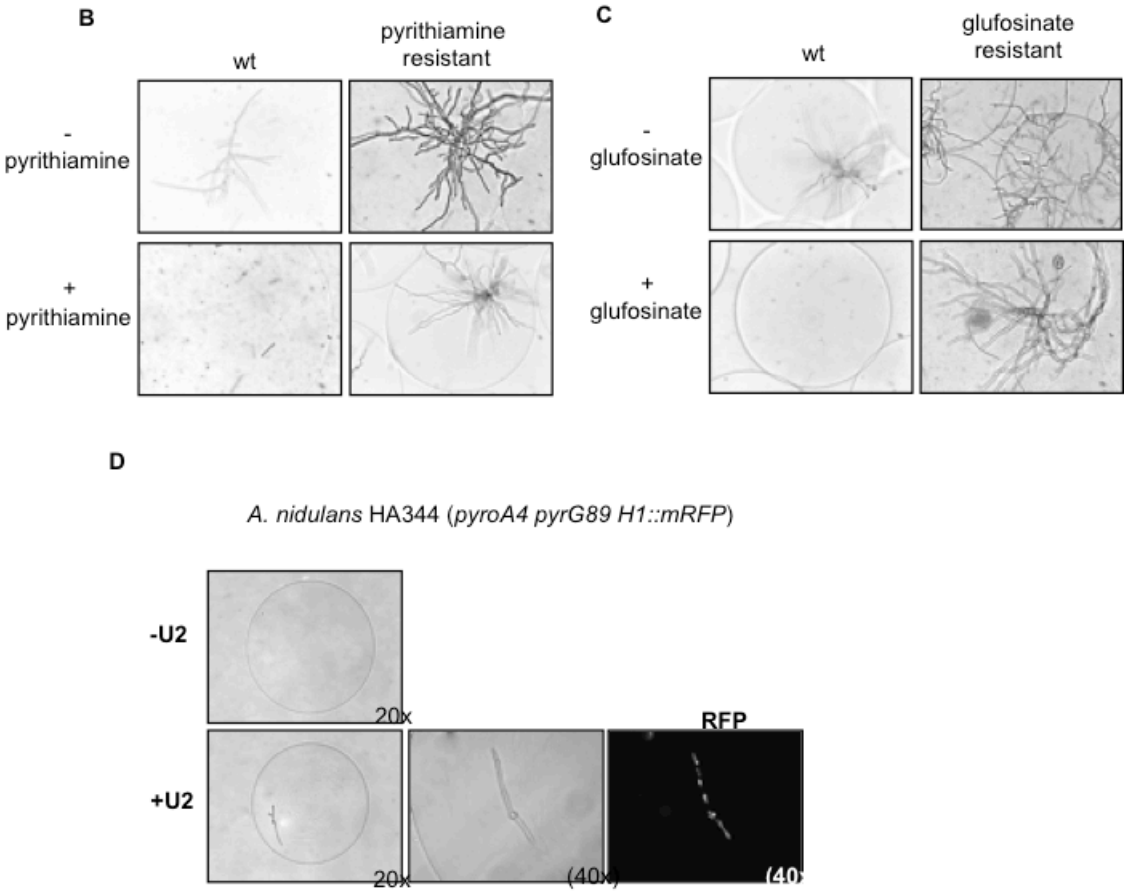

Figure 15. Fungal phenotypes can be detected in microcapsules. Encapsulation allows to screen for growth / no growth and/or fluorescence. **A.** the auxotroph mutant HA344: H1::RFP pyrG89 pyroA4 is not able to grow in the absence of pyridoxine or U2 (uracil + uridine). When both requests were added to the medium, the spores started to germinate as is shown by optical and fluorescence microscopy **(C)**. This screening can be extended to search for resistance to different compounds. For each case, we utilized a fungicide resistant strain obtained by transformation of a resistance cassette in the genome and the corresponding isogenic strain. **B.**Capsules containing spores were incubated in minimal medium in the presence or absence of pyrithiamine (left panel) and glufosinate (right panel) for 25-30 hours.

3.2.3 Flow cytometry analysis of encapsulated fungal microcolonies

COPAS flow cytometry allowed the analysis of these phenotypes across the microencapsulated population in a quantitative manner. Cytometric analysis detected a population of wild-type microcolonies with increased optical density that was missing in the microcapsules containing auxotrophic pyrG89 spores (Figure 16). In contrast, a prominent population of microcapsules with increased optical density was detected when the auxotrophic mutant was incubated in the presence of uracil and uridine (Figure 16). In the presence of U2, we were able to detect signal in the red channel in the case of the pyrG89 strain arising from all the H1-RFP2 tagged nuclei. Despite of the wild-type growing, signal in the red channel was not observed (data not shown).

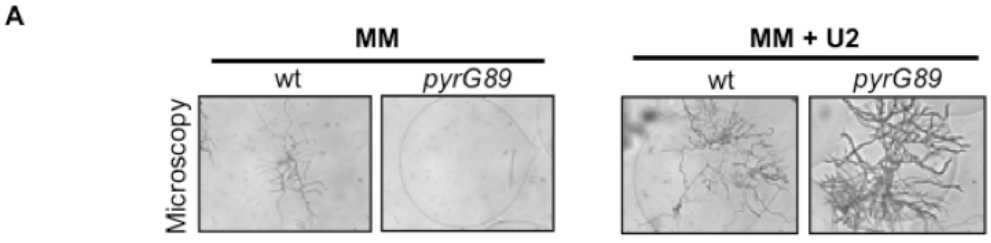

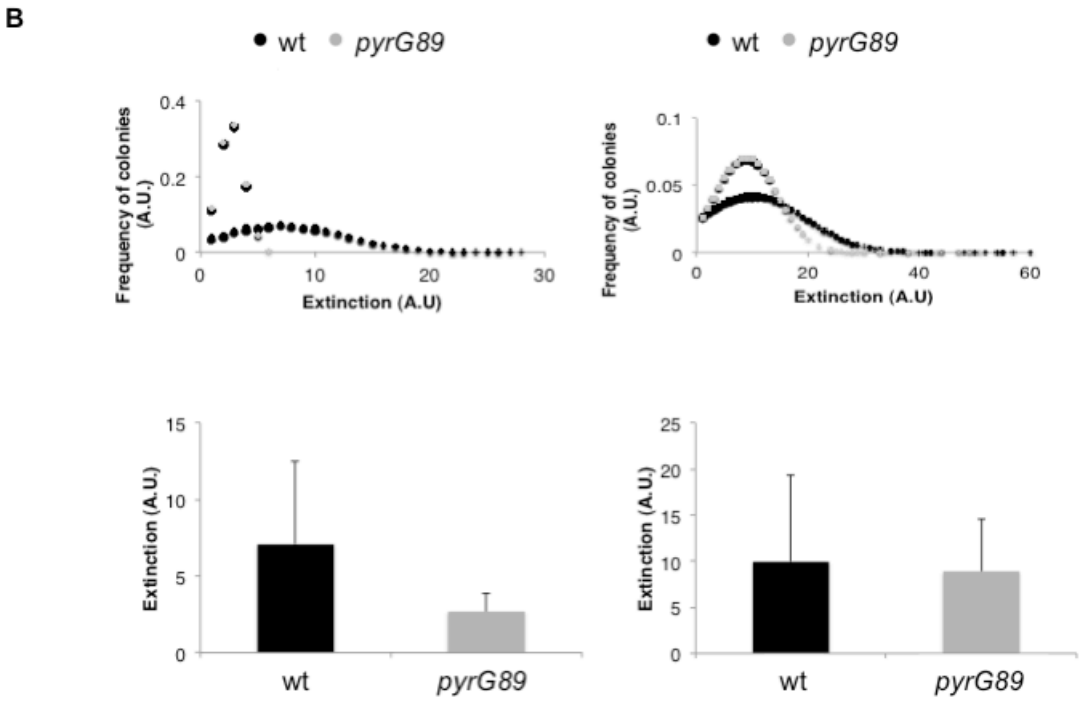

Figure 16. Screening for fungal growth or fluorescence. Pictures of encapsulated *A. nidulans* spores after growing in different media and flow cytometry analysis of the particles. A pyrG89 strain (auxotrophic for uracil and uridine) carrying the histone H1-RFP fusion and a non-fluorescent wild type strain were grown in minimal media in the absence or in the presence of U2 for 20 h. Fungal growth in the microcapsules was visualized by light microscopy (A) and quantified by COPAS flow cytometry showing the extinction levels (B).

3.2.4 Genetic screening of microencapsulated fungi by large particle flow cytometry

Thermosensitive mutants (ts) are very useful tools for studying the function of essential genes (Govindaraghavan et al. 2014). However, isolation of such mutants requires extremely laborious replica plating of large number of mutants (Harris et al. 1994). We figured that our procedure could be used for the isolation of ts mutants in essential genes. As a proof-of-concept we used a ts mutation in the nimX gene, which encodes the cyclin-dependent protein kinase involved in cell cycle control CDK1/CDC2 (Osmani et al. 1994). Wild-type and ts

mutant strains were capable of proliferate in the microcapsules at the permissive temperature, as visualized by light microscopy and detected by COPAS flow cytometry. In contrast, only the wild-type microcolonies were detected at the restricted temperature. As expected, the wild type grew faster at 42 than at 30 ºC (Figure 17, A-C). In a parallel experiment, these two types of microcapsules, containing spores of either the wild type or the mutant, were mixed together and incubated at the restrictive temperature for 18 hours. Two populations were identified when the mixture of microcapsules was analyzed by COPAS flow cytometry, based on their optical parameters. One was distinguished by its high optical density and time of flight values; the other one was low values for both parameters (Figure 17D). Both populations were sorted independently. To check the quality of the sorting, microcapsules were visualized under a stereo microscope revealing that most of the microcapsules of one of the populations carried grown mycelia opposite to the other population, in which microcapsules did not carry grown mycelia (Figure 17E). Both strains could be easily distinguished by their fluorescence. The wild-type strain carried a H1::RFP fusion, whereas the ts mutant carried a H1::GFP fusion (Figure 17D). Visualization of the sorted microcapsules under the fluorescent microscope confirmed that the population of grown mycelia contained the wild-type strain (red fluorescent), whereas the non-grown population contained the ts short hyphae of the mutant strain (green fluorescent) (Figure 17F).

These microcapsules could then be plated on regular Petri dishes and incubated on complete media at the permissive temperature to recover the desired strains, either wild type or mutant (data not shown).

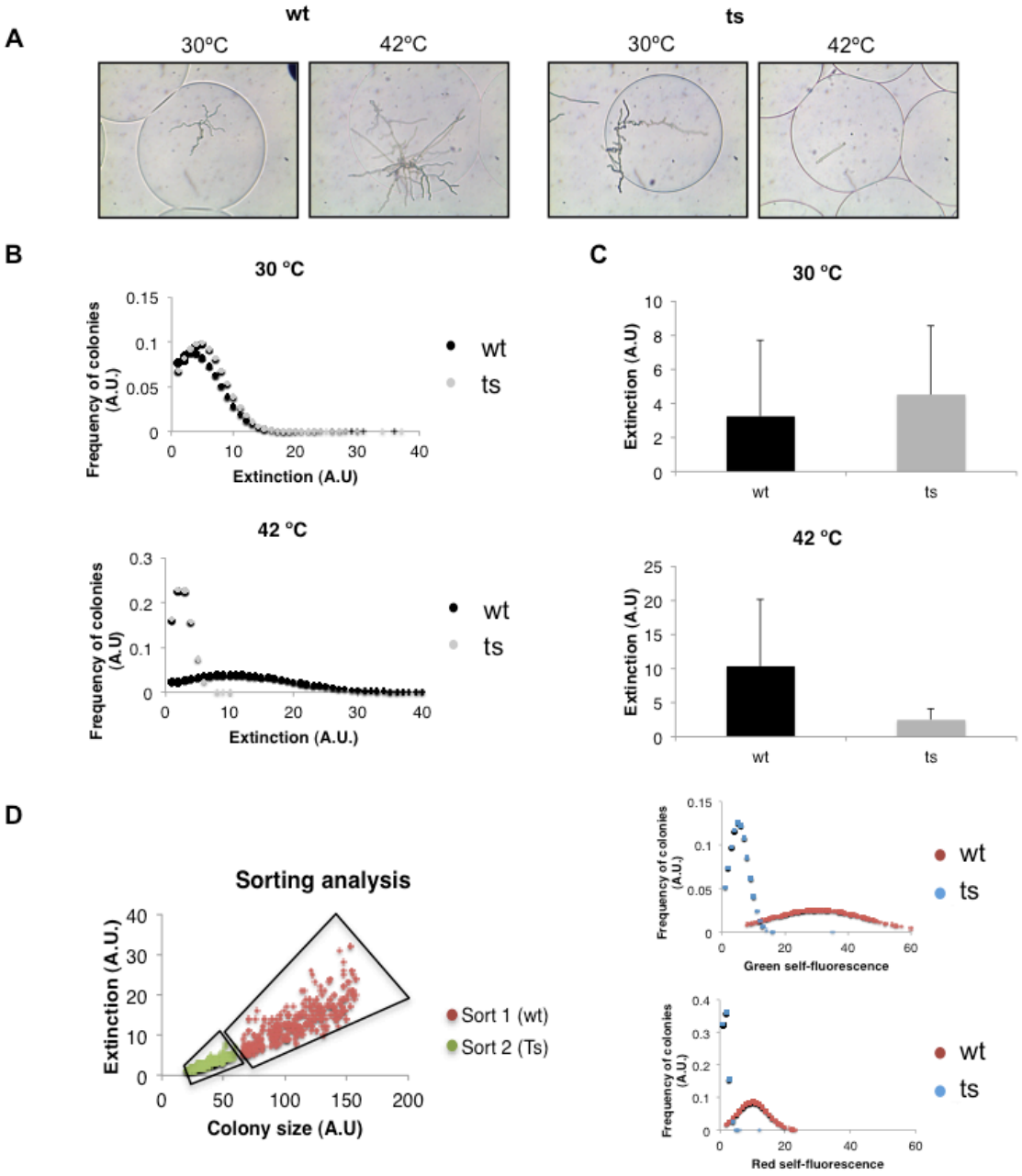

This method allows for the analysis of clonal fungal colonies grown in liquid media by flow cytometry. The power of this method relies on the capacity to do genetic screenings and make both positive and negative selection, for example, allowing to sort strains carrying ts alleles of essential genes, which could be later recovered by growing at the permissive temperature. Performing this method skips the laborious and time-consuming requirement of replica plating. In addition, this method can be extended to screenings for regulators by employing GFP genes under the control of a promoter of interest. It makes this method powerful and versatile.

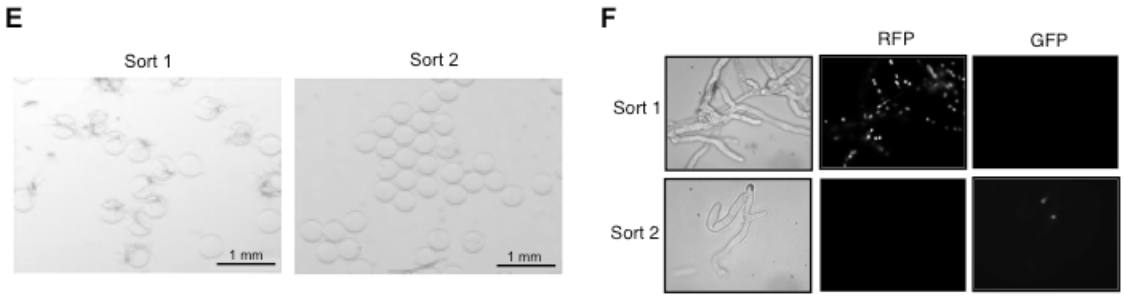

Figure 17. Screening for conditional mutants using thermosensitive (ts) alleles. A. Analysis of ts mutants by microencapsulation. In the left box is shown the growth of single spores of the wild-type (wt). **B-C.** *A. nidulans* at permissive and restrictive temperature, and in the right the ts strain is shown. (B-C) Flow cytometry analysis of encapsulated wt and ts *A. nidulans* spores after growing at different temperatures showing the measurement of optical density (EXT) at both temperatures. **D.** Sorting analysis of wt and ts mutant. The spots depict the population of interest in both cases, showing green and red autofluorescence (diagrams on the right).**E.** Pictures of the cell-sorting results of both strains grown at restrictive temperatures: sort 1 (wt strain) and sort 2 (ts atrain) under optical microscope. **Co**nfirmation of the identity of the strains after sorting was performed taking advantage of the H1::chRFP (wt) and HH1::GFP (ts mutant) fusion proteins under fluorescence microscope. EXT, extinction.

3.3 Analysis of cellular heterogeneity in clonal populations of *S. cerevisiae* by microencapsulation, flow cytometry and massive RNA sequencing

From the experiments in the Chapter 1 we could verify the existence of colony size heterogeneity within an isogenic wild-type population of *S.cerevisiae* growing in constant environmental conditions (Figure 18A). Although this phenomenon has been previously described by several authors (Acar, Mettetal et al. 2008; St-Pierre and Endy 2008; Snijder, Sacher et al. 2009), very little is known about the mechanisms that cause this heterogeneity. In the present chapter we report the use of a combination of yeast microencapsulation, flow-cytometry sorting and massive RNA sequencing to help understanding this process.

3.3.1 Microcolony heterogeneity is not due to the microparticle size or to its position within the microparticle

As has previously been described in the introduction, extrinsic noise has a very important role in the regulation of population heterogeneity. Although alginate microencapsulation allows the free diffusion of nutrients and is fully compatible with yeast proliferation we considered that it was necessary to test whether the different microcolony size was related to the actual size of the microparticle itself. We found no correlation between the colony size and that of the capsule (Figure 18B). We also found no correlation between the microcolony size and its distance to the microcapsule surface (Figure 18C). Therefore, we concluded that proliferation heterogeneity was not due to extrinsic noise related to the microencapsulation procedure but to intrinsic biological reasons.

Microcolony size heterogeneity could also be due to an unequal lag phase. The increasing statistical dispersion shown by microcolony size during the time-course experiments, maintaining a symmetrical size distribution, was hardly compatible with this possibility (Figure 11B). Moreover, our results are in agreement with previous reports on proliferation heterogeneity conducted under optimal culture conditions in *S. cerevisiae*, and detected with technical

approaches that did not involve encapsulation [24].

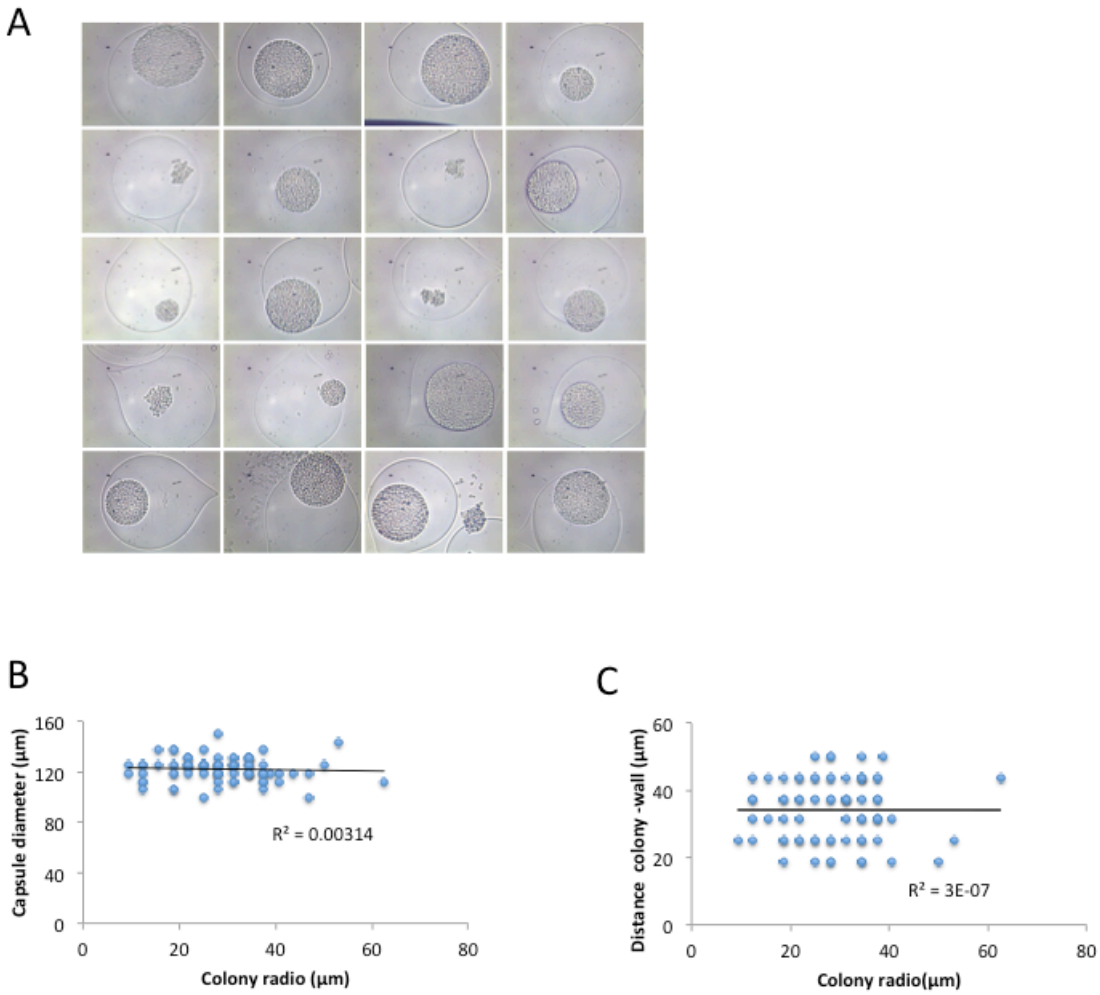

Figure 18. Intrinsic proliferation heterogeneity of encapsulated cells. A. The microcolonies developed from the encapsulated single yeast cells exhibited a wide size range after incubation in YPAD medium, as detected by optical microscopy (Figure 2). The more prominent heterogeneity was observed at 13 hours of incubation. All the pictures come from the same sample (13 hours of incubation). **B** Size of 50 microcolonies grown during 13 hours in YPAD medium was compared to the size of their particles. No correlation was found. Tendency lines for linear regression and correlation coefficients are shown. **C.** Cells trapped in alginate particles develop microcolonies without being influenced by the particle size or its location within the particle. Size of 50 microcolonies grown during 13 hours in YPAD medium and their distance to the external border of the alginate particle were measured and compared. No correlation was found.

3.3.2 Sorting of big and small microcolonies

As shown above, the combination of microencapsulation and large particle flow cytometry allows sister microcolonies to be physically separated by sorting. We isolated the 10% top and bottom subpopulations of microcolonies according to their size (Figure 19A). We considered the follow ranges of diameter to define the particles as small, medium or big: small (10-20μm), medium (20-50μ) and big (50-100μm) (Figure 19B). The sorting efficiency was quite high as can be seen in the set of pictures of figure 8C. The resulting sorted subpopulations exhibited very different mean sizes and standard deviations that exclude any significant overlaping in terms of size (Figure 19D).

To estimate the number of cells in the sorted microcolonies we counted the number of cells of a set of disgregated microcolony by optic microscopy, and related them with the microcolony diameter in a calibration curve (Figure 20A). This simple procedure allowed us estimating the average number of cells in the two sorted subpopulations, asuming a constant cell volume in all microcolonies (see later). The two subpopulations (small and big microcolonies) exhibited an average cell number of 32 and 2519, respectively (Figure 20B), which involve apparent doubling times of approximately 162 and 76 min according to the incubation time under growing conditions (Figure 20C). The average cell number and apparent doubling time of non-sorted microcolonies gave intermediate values. However, when all the analysed microcolonies were considered as a single cell population, the resulting population doubling time was approximately 90 minutes, comparable to standard liquid cultures (Figure 20C). Note that the population doubling-time of the whole population is largely dominated by big microcolonies due to the substantially higher fraction of the cells belonging to them. Taken together, these results indicate that size heterogeneity correlates with an evident variation in the proliferation capacity within a clonal population: cells from a small microcolony present lower proliferation capacity. Therefore, we can conclude that a proliferative heterogeneity exists in a clonal population of *S. cerevisiae.*

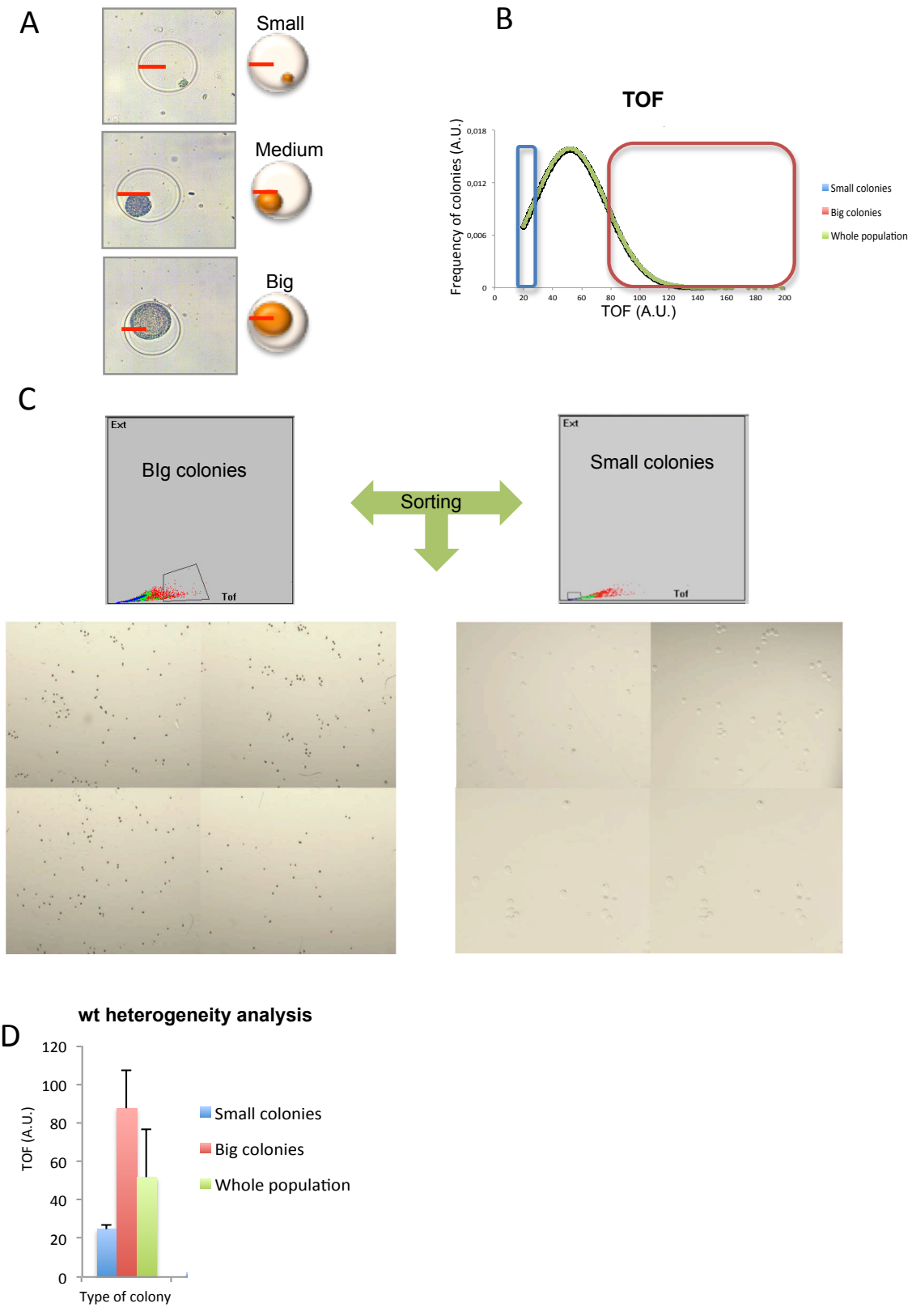

Figure 19. Selection and sorting of big and small microcolonies. A. Microcolonies are classified according to their size in small, medium or big microcolonies. As capsule diameter is stable, microcolonies which surpass the capsule radio are considered big (50-100µm); those whose size ranges from half the ratio and the ratio are considered

médium (20-50µ) microcolonies. Those smaller than half the capsule ratio are considered small microcolonies (10-20µm). **B.** Representation of the areas that were selected for sorting compared with the whole population. (Blue, small colonies. Red, big colonies. Green, whole population.. **C.** The two different populations were classified using the COPAS device. EXT and TOF were used as the parameters to make the selection. While sorting, particles were collected in tubes. The sorting efficiency was quite high as can be seen in the set of pictures. **D.** TOF mean and standard deviation of the three studied populations exclude any significant overlaping in terms of size.

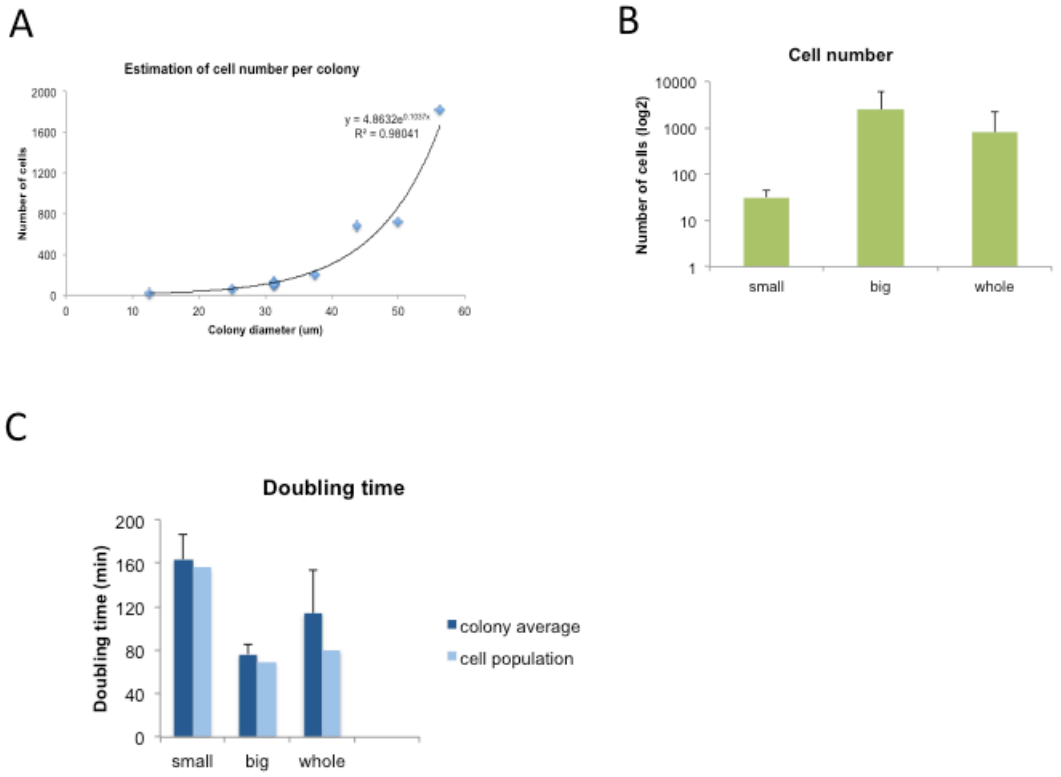

Figure 20. Characterization of sorted microcolonies. A. Cell number estimation per colony by cell counting under microscope (see Materials and methods). The subpopulations that corresponded to the smallest and biggest microcolonies were sorted after 13 hours of incubation. Cells were extracted from 50 particles of each type and from the non-sorted colonies (whole), and were counted under the microscope. **B.** Cell numbers average and standard deviations are shown for the three analysed populations. **C.** Apparent doubling times were estimated from these data. Population doubling times were also calculated by considering the sum of all the cells present in the analysed colonies. Note that the population doubling-time of the whole population

is largely dominated by big microcolonies due to the substantially higher fraction of the cells belonging to them.

3.3.3 Transcriptomic analysis of fast- and slow-proliferating colonies of S. cerevisiae

Once we classified the microcolonies by the different growth rate we wanted to characterize the possible transcriptomic differences between small and big colonies. The final objective is to understand the mechanism(s) responsible for this proliferation heterogeneity. To do that, mRNA preparations were isolated from the sorted microcolonies and their transcriptomes, after RNAseq, were compared. We had RNASeq data from all types of colonies with at least three replicates of each one and from some controls. The controls consisted in not encapsulated cells and not ethanol-fixed culture at 0.5 O.D., just to discard or have into account the possible microencapsulation and fixation effects, respectively. We also extracted mRNA from a saturated culture (2 O.D) to check if the nutrients starvation could lead to a slow grow phenotype.
Our purpose was to analyse all this data and study the potential transcriptomic change in any kind of microcolonies.
We proceed to isolate RNA from different samples as described previously.
RNAs were amplified and sequenced using a method to identify poly-A sites in a genome-wide and strand-specific manner. This method, termed 3' T-fill (see Materials and methods), initially fills in the poly-A stretch with unlabeled dTTPs, allowing sequencing to start directly after the poly-A tail into the 3' -untranslated regions (UTR) (Wilkening, Pelechano et al. 2013).

The log2 fold change within pairs of samples was represented. We found that the small and big colonies were transcriptionally different. The same happened when small and whole population were compared whereas big colonies and whole population were quite similar. This result means that the big colonies are reflecting what is happening in the average population (Figure 21). When the ethanol-fixed whole population was compared with a non-fixed sample we found important differences at transcriptomic level. These differences were expected,

however ethanol fixation is instantaneous so we supposed that all the transcripts should be well preserved both in small and big colonies . Looking at the comparison of an exponential culture at 0.5 O.D and a saturated culture (2 O.D.) we did not find much differences. So we conclude that the small colonies are not smaller (or don´t have a growth defect) because of a limitation of nutrients.

In the light of these results we decided to focus in small versus big colonies comparison.

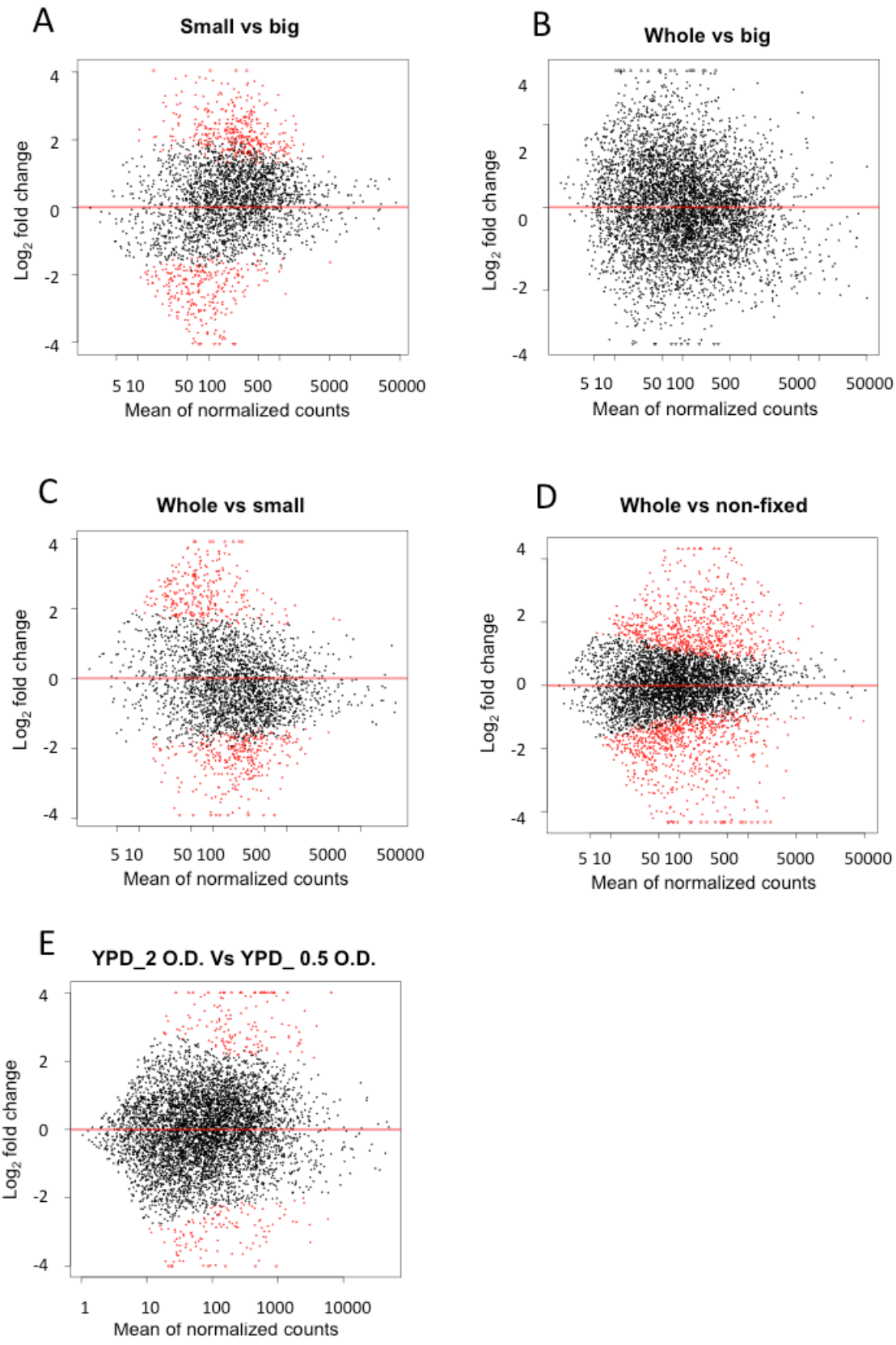

Figure 21. Overview of the transcriptional differences among the sequenced samples. Transcription level differences as log_2 fold change (y-axis) and the mean of

all normalized counts (x-axis) are represented. Red dots correspond to those genes that are differentially expressed whereas black dots are not differentially expressed genes. Different comparisons are shown. **A.** Small colonies versus big colonies. **B.** Whole population versus big colonies. **C.** Whole population versus small colonies. **D.** Whole fixed versus whole non-fixed population. **E.** Saturated (2 O.D) versus exponential (0.5) non-encapsulated and non fixed cultures. All the samples were grown in YPAD. In the case of encapsulated cultures samples were recovered after 13 hours of incubation. The unenapsulated samples were recovered when the desired O.D. was reached.

3.3.4 Quality analysis of RNA-seq data

In order to check the quality of the samples and its replicates we used some standard procedures to compare either within different replicates of the same sample or between different samples (Small *versus* Big).

First we checked the read number for each sample. In RNA-Seq, the number of reads is used to gather the expression of a transcript. The length is not taking into account because we will use the data for a comparison analysis. So the number of reads between samples and more important between replicates must be very similar (some authors talk about no more than 10% of size difference). So first we checked the overall number of all transcripts and then we filtered as Gordon Smyth suggest discarding low expressed genes (the one than affect the most at the FDR calculation). As recommendation , all transcripts with less than 5 reads per million in at least 2 samples wasn't taken into account.
Because of the low number of reads in the third small colonies replicate (Small 3) we decided to discard it of the analysis (Table2). After do that we could still see that there was a high difference in the sequencing deep within samples. These values, oscillating between 350K and 25 millions, where different enough to need a downsampling . Thus, after downsampling we had the number of reads showed in figure 22A.

Table 2. Library sizes.

Sample	Library size
Big 1	2651332
Big 2	3448491
Big 3	2540765
Small 1	3000000
Small 2	1490985
Small 3	9779

Library sizes, referred to number of reads, for each of the samples.

Multi-Dimensional Scaling plot measures the similarities of the samples and plots in two dimensions. The distance between each pair of samples (columns) is the root-mean-square deviation (Euclidean distance) for the top top genes. Distances on the plot can be interpreted as leading log2-fold-change, meaning the typical (root-mean-square) log2-fold-change between the samples for the genes that distinguish those samples (Figure 22B).

Given the small RNA amounts isolated, in particular from slow-growing microcolonies, we analysed the consistency of the results obtained. As expected, wider variation was found among the RNA samples obtained from small colonies. We needed to check if this was related with the different number of reads or with a different biological situation so we tried with a boxplot (Figure 22C)

When a boxplot was represented we saw again that the three big samples are very similar (small differences in Big 2) but the small ones are quite different. Thus, we proceed with an expression clustering to check if the two kinds of samples clustered together (Figure 22D). Yet despite this variation, the cluster analysis very consistently separated big-colony samples from small-colony samples. Finally, we used a heat map as a false color image with a dendrogram added to the left side and to the top. Typically, reordering of the rows and columns according to some set of values (row or column means)

within the restrictions imposed by the dendrogram is carried out. We drew a heat map for all the transcripts in the experiment and we found two different clusters, one for small colonies samples and another for the three big colonies samples (Figure 22E).

The RNA samples obtained from the non-sorted microcolonies (whole population) were also analysed, and only minor differences were detected for the big-colony samples.

At this point we could say that although the appreciable differences within the small colonies replicates, both the dendrogram and the heat map separate clearly this two kinds of samples. Accordingly, the two sets of samples are different at transcriptional level.

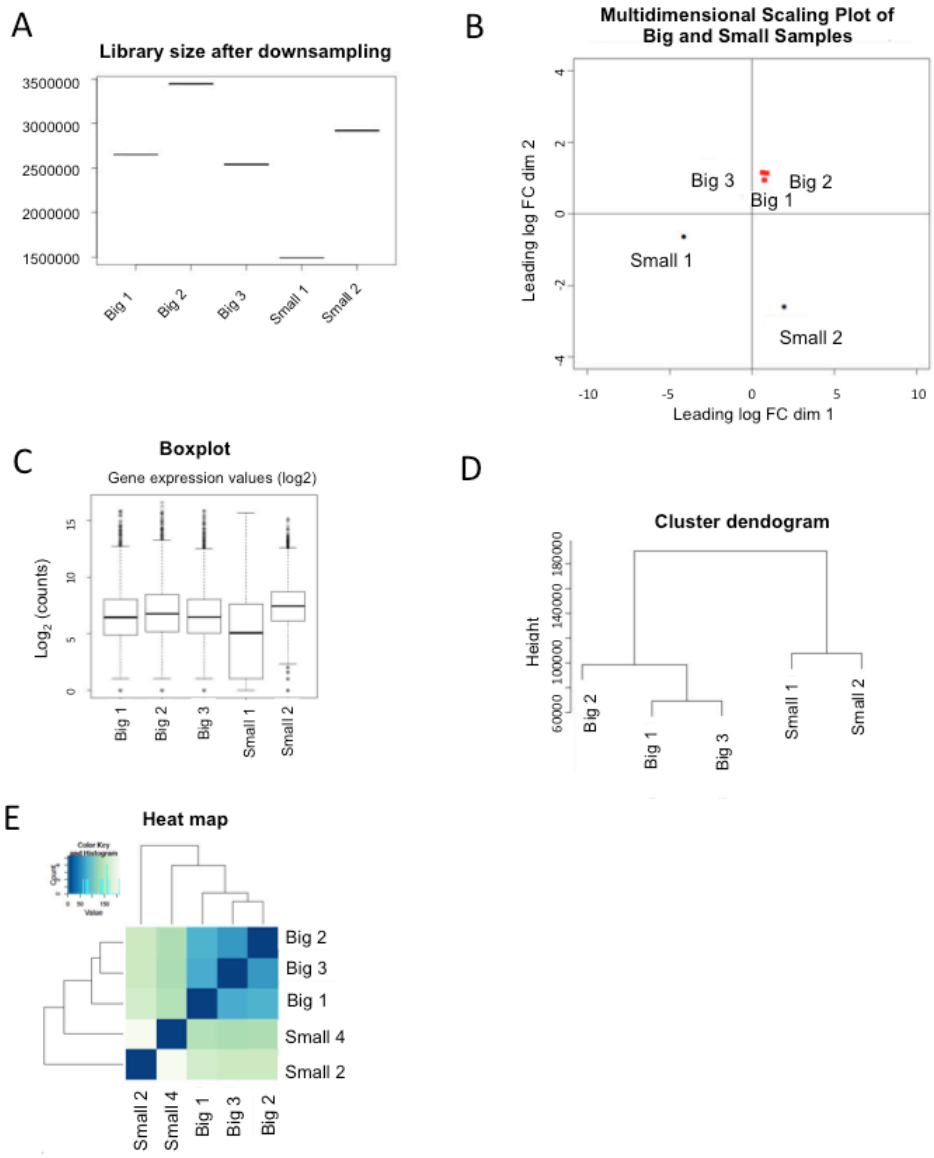

Figure 22. Quality analysis of RNAseq data. A. Library size, referred to number of reads, for each of the samples after the downsampling. Because of the low number of reads, we decided to eliminated the sample small 1 for the following analysis. **B.** Multi-Dimensional Scaling. It can be observed how the big samples appears together. This is not the case for the small replicates so we proceed with a boxplot and clustering to check if they clustered together. **C.**Boxplot. **D.** Cluster dendogram. **E.** Heat map for all analysed genes.

Altogether the prevailing view is that complex phenotypes are not the result of changes in a single gene expression but reflects abnormalities in the entire cellular network/pathways. A better understanding of how gene expression, at multiple loci throughout the genome, work together to influence the presentation of a complex phenotype may lead to the discovery and characterization of unknown biological processes.

We will study differences at pathway level (Through GO Molecular function and KEGG pathways) and cellular complex level (Through GO cellular complex) using enrichment and functional analyses from RNASeq data in the context of the proliferation heterogeneity.

3.3.5 Differential gene expression in small *versus* big microcolonies

We quantified the gene expression from the mapped reads using the HTSeq-count package (Anders, Pyl et al. 2015) in order to obtain counts of mapped reads per gene.

Many genes showed a significant differential expression when small (slow-proliferating microcolonies) and big (fast- proliferating microcolonies) growing cell populations were compared (Table 3 and 4). Top differentially expressed genes included several regulators of cell proliferation (Table 3), like G1-S transition inhibitor *WHI5* , which is consistent with the differential cell cycle regulation of fast- and slow-proliferating microcolonies. Accordingly, the “Mitotic cell cycle” gene ontology category (GO0000278), which includes genes involved in cell division, was significantly underrepresented in the mRNA

population of slow-growing microcolonies (p-value 0.03 for the Mann-Whitney U-test). In addition, genes encoding for the transcription machinery and energy metabolism were also differentially expressed. More to the point, mitochondria-related genes were significantly overexpressed and ribosomal protein genes were under expressed in small microcolonies as could be expected (Table 5). We conclude that even in the absence of genetic or environmental variation, cells can adopt different GRs, which were distinguished by the typical mRNA signatures of fast or slow proliferation which generates, respectively, big and small microcolonies.

Table 3. mRNAs overrepresented in small microcolonies

Gene	Symbol	Log_2FoldChange	P-value
WHI5	YOR083W	7.048833589	6.98026E-06
CMR1	YDL156W	7.210912382	1.53696E-05
SRO9	YCL037C	5.294470488	3.42462E-05
PCA1	YBR295W	5.744866858	3.92648E-05
RPO21	YDL140C	4.370957694	8.08913E-05
AGE1	YDR524C	5.057438477	8.24273E-05
FPK1	YNR047W	5.354758102	9.16954E-05
YML082W	YML082W	4.862561176	0.000120482
ALR2	YFL050C	4.947952391	0.000132546
PET123	YOR158W	5.339210086	0.000147304
BRE1	YDL074C	5.231493819	0.000246201
HIR3	YJR140C	4.726380917	0.000262981
RRP12	YPL012W	3.929367002	0.000305346
ARO9	YHR137W	4.39026416	0.000390452
PPZ1	YML016C	4.678586267	0.000405159
MAD3	YJL013C	4.387105719	0.000448006
RPL40A	YIL148W	4.103774155	0.00046916
PRP39	YML046W	4.611053291	0.000563323
SSA4	YER103W	4.180940644	0.000574475

PRP6	YBR055C	4.34505999	0.000583935
SIP4	YJL089W	4.973975862	0.000616517
FET5	YFL041W	3.99210332	0.00063317
MCK1	YNL307C	3.82623474	0.00063743
YBR230W-A	YBR230W-A	4.563145059	0.000639699
ALD5	YER073W	4.448224437	0.000643781
NUF2	YOL069W	3.923206635	0.000674679
OMS1	YDR316W	4.195176721	0.000792431
PIN4	YBL051C	3.646882337	0.000802205
ERT1	YBR239C	3.995301562	0.001009505
FOL1	YNL256W	4.287752277	0.001087331
YGL082W	YGL082W	3.719830852	0.001102317
MRPL33	YMR286W	5.209544511	0.001103214
YER034W	YER034W	4.510018424	0.00117443
EDC2	YER035W	4.510018424	0.00117443
KOG1	YHR186C	4.000052721	0.001223059
CLG1	YGL215W	4.683192214	0.001337805
ATC1	YDR184C	3.617463407	0.001391366
YER079W	YER079W	3.886530891	0.0014024
PUF3	YLL013C	3.428516055	0.001437528
KIN1	YDR122W	3.479849295	0.001536036
NKP1	YDR383C	3.52603352	0.001607852
TCA17	YEL048C	3.605841026	0.001691836
VPS52	YDR484W	3.669711553	0.001753976
TIF2	YJL138C	3.502226812	0.001766756
YKL050C	YKL050C	3.744231573	0.001811585
YPK3	YBR028C	3.557608379	0.001849172

Mitochondria-related (blue) and cell cycle-related genes (green) dominate this list.P values correspond to the Mann-Whitney U-test.

Table 4. mRNAs overrepresented in big microcolonies.

Gene name	ORF name	Log_2 fold change	P-value
MIG3	YER028C	-8.975	4.25E-05
POX1	YGL205W	-6.650	7.15E-05
YJR146W	YJR146W	-7.034	8.75E-05
HMS2	YJR147W	-7.034	8.75E-05
ELA1	YNL230C	-9.115	1.14E-04
YLR179C	YLR179C	-8.642	1.64E-04
CTF19	YPL018W	-9.039	1.79E-04
YCR087C-A	YCR087C-A	-8.478	2.02E-04
YNL092W	YNL092W	-6.589	4.92E-04
STP3	YLR375W	-5.626	6.38E-04
EMP65	YER140W	-6.148	7.22E-04
CMD1	YBR109C	-5.143	8.11E-04
NUP53	YMR153W	-6.090	1.03E-03
YLR312C	YLR312C	-7.882	1.03E-03
YPT53	YNL093W	-4.982	1.10E-03
CUE4	YML101C	-5.895	1.42E-03
HOT1	YMR172W	-7.410	1.43E-03
DON1	YDR273W	-4.214	1.91E-03

Table 5. differentially expressed categories in small versus big microcolonies.

Gene Ontology category	P-value (Mann-Whitney)
Ribosomal protein ↓	9.6×10^{-23}
Aerobic respiration ↑	3.6×10^{-11}
Mitotic cell cycle ↑	3.0×10^{-2}

The mRNAs differentially expressed in the small and big microcolonies belong to several GO categories, including ribosomal protein coding genes, aerobic respiration, and mitotic cell cycle. Aerobic respiration and mitotic cell cycle genes were significantly overexpressed and ribosomal protein genes were under expressed in small microcolonies. P values correspond to the Mann-Whitney U-test.

3.3.6 The mRNA profile of small microcolonies indicates a respitatory metabolism controlled by Puf3

As we can see in Table 2 and 4, slow-growing cells in small microcolonies displayed a respiratory profile due to the higher expression of respiratory genes. These overexpressed genes included three regulators of the energy metabolism during the transition from fermentation to respiration: *SIP4* (Lesage, Yang et al. 1996; Vincent and Carlson 1998), *ERT1 (Gasmi, Jacques et al. 2014)* and *PUF3* (Miller, Russo et al. 2014). The relevant function of these three genes in energy metabolism made them potential interesting genes to study.

The most differentially expressed gene related with respiration metabolism itself was *SIP4*, whose protein has been described years ago as a C6 zinc cluster transcriptional activator that binds to the carbon source-responsive element (CSRE) of gluconeogenic genes. Sip4 is involved in the positive regulation of gluconeogenesis, is regulated by Snf1p protein kinase and localized to the

nucleus (Lesage, Yang et al. 1996).

ERT1 gene (Ethanol Regulated Transcription factor 1) was recently described as a gene encoding a putative zinc cluster protein that acts as a factor involved in the regulation of gluconeogenesis as well as a key fermentation gene by the repression of PDC1, encoding an important enzyme for fermentation. So *ERT1* is redundant with SIP4 (Gasmi, Jacques et al. 2014).

Finally, from our RNA seq results we highlight the *PUF3* gene, encoding a protein of the mitochondrial outer surface. Puf3 links the Arp2/3 complex with the mitochore during anterograde mitochondrial movement. More interestingly, Puf3p has been reported to favour the translation of a set of mitochondria related genes under respiratory conditions and also binds to and promotes degradation of mRNAs for select nuclear-encoded mitochondrial proteins (Keene 2007) (Lee and Tu 2015). As the Puf3 protein is a transcript-specific regulator of mRNA degradation in yeast (EMBO 2000, Olivas and Parker), we thought that Puf3 could be playing a role in the mRNA stability regulation in the slow proliferating (small) microcolonies.

Due to low biological material abundance that is obtained from small microcolonies, we were unable to measure mRNA stability in this isolated microcolonies. As an alternative approach, we reasoned that we could use the relative abundance of the alternative mRNA isoforms with a different stability and RNA-binding protein sites as a proxy for their post-transcriptional life (Gupta, Clauder-Münster et al. 2014).

Specifically we analyzed the relative distribution of 3' polyadenylation mRNA isoforms by exhibiting different lengths of their 3' end in the two populations of microcolonies. Some of these isoforms contained well-known interaction sites for factors that modified mRNA stability upon binding (Riordan, Herschlag et al. 2011). We found that the isoforms that contained the Puf3- binding site were enriched in slow-growing (small) microcolonies compared to alternative isoforms for the same genes that did not contain this binding site (Figure 23A).

Moreover, when we restricted our analysis to the eight gene members of the Puf3 regulon, which presented significant numbers of reads of alternative isoforms (with and without Puf3-binding sites), in both small and big microcolonies, we found that seven genes presented greater enrichment in the small subpopulation for those isoforms that contained Puf3-binding sites (Figure

23B). These results suggest that the higher Puf3 expression in the slow-growing microcolonies brought about an increase in the levels of its target genes, mediated probably by the stabilization of their mRNAs.

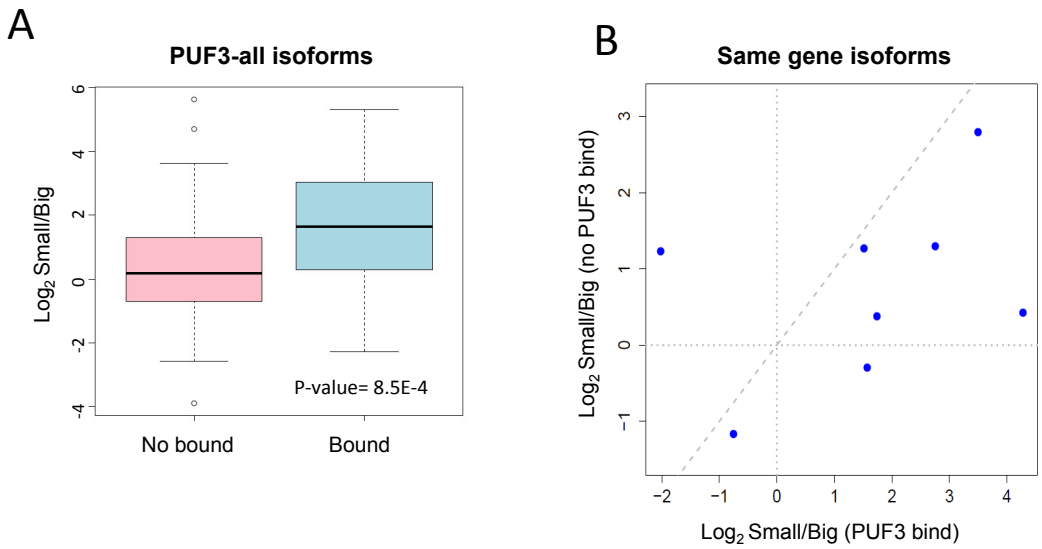

Figure 23. mRNA bound by Puf3 are overrepresented in small microcolonies. A. Boxplot comparing the relative mRNA amount of genes that contain annotated Puf3-binding sites in their 3'UTR. The alternative polyadenylation isoforms that contain Puf3-binding sites (bound, in blue) are (Porrua and Libri 2015)significantly enriched in small microcolonies compared to the isoforms, excluding Puf3-binding sites (not bound, in pink). **B.** Analysis of the eight gene members of the Puf3 regulon, which presented simultaneously alternative polyadenylation isoforms both with and without Puf3-binding sites in both small and big microcolonies (minimum of 10 reads). Seven genes presented greater enrichment in the small subpopulation for those isoforms that contain Puf3-binding sites. Altogether, These results suggest that Puf3 stabilize the mRNAs of its target genes producing an increase of their levels in the small microcolonies.

We also found others RNA binding proteins whose target genes are significantly different distributed in small versus big microcolonies (Figure 24). This suggests that other regulatory proteins may differentially control mRNA abundance in response to the GR by acting on mRNA stability. Thus, significantly lowered levels in small microcolonies were also found for the genes that were targets of three other RNA binding proteins: Nab2, Nsr11 and Nrd1, involved in nuclear

RNA decay (Porrua and Libri 2015). Overall, we conclude that RNA stability was also differentially regulated in wild-type cells with distinct proliferation rates, and that this regulation could be related to the respiratory metabolism of slow-growing cells.

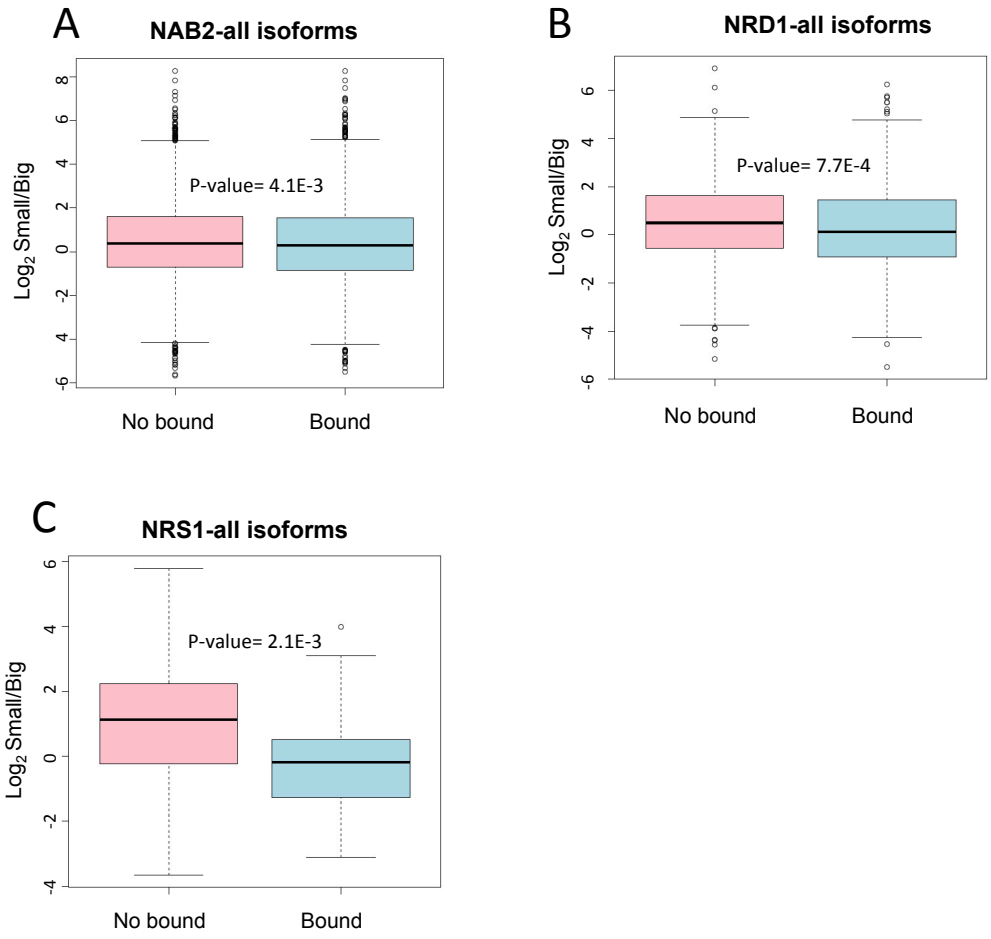

Figure 24. Others RNA binding proteins whose target genes are significantly differentially distributed in small *versus* big microcolonies. A. Boxplot comparing the relative mRNA amount of genes that contain annotated Nab2. **B.** Nrd1 and **C.** Nsr1-binding sites in their 3'UTR. All of them are involved in nuclear RNA decay. The relative distribution (small/big) of mRNA 3' isoforms containing binding sites for the indicated factors, compared to non-bound isoforms are represented.

3.3.7 Cells from small microcolonies are delayed in the G1/S transition

As described above in this work, different size microcolonies have different proliferation capacity, as the number of cells present in a small microcolony is much lower than in a big one. In order to determine if the reduced proliferation in small microcolonies was due to an abnormal cell cycle progression, a flow cytometry analysis and recount of the cells from this small microcolonies was performed. We sorted the small microcolonies fraction after the encapsulation of a wt strain after growing during 13 hours, then the alginate capsules were broken and cells were analysed by flow cytometry to study their cell cycle profile. As a control, cells coming from the whole encapsulated population (containing small, medium and big microcolonies) were also analysed for a cell cycle characterisation (Figure 25)

We could observe a slight accumulation of cells in G1 phase in the slow proliferating microcolonies in comparison with the whole cell population (Figure 25B). Flow cytometry profiles were unclear in most of the replicates due to the poor amount of cells obtained after capsule breaking and microcolonies disaggregation. As a consequence, propidium iodide cell staining and cytometry profiles acquisition was not efficient. Then, in order to confirm the cell cycle phases distribution, we performed cell counting under a microscope (Figure 25A). It is remarkable the increase in the number of cells in G1 (unbudding cells) and the consequent decrease in S/G2/M (budding cells) in the small colonies compared to the whole population of encapsulated cells.

Altogether these results indicate that cells derived from small microcolonies exhibit a longer G1/S transition.

A

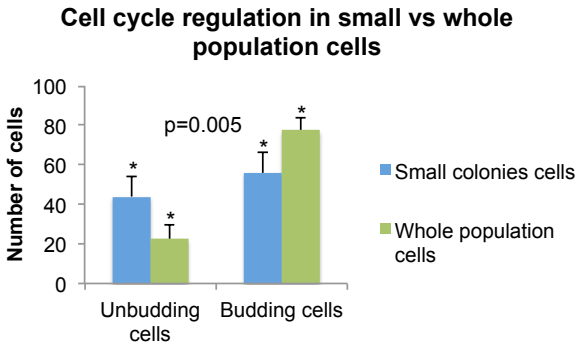

B

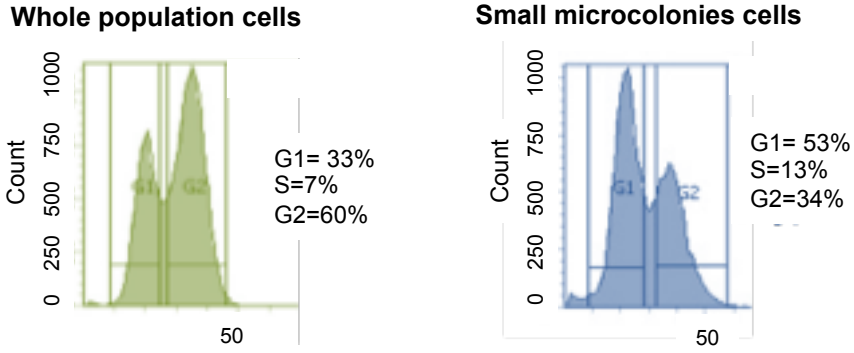

Figure 25. Cell cycle regulation of microencapsulated cells. A. Cells extracted from small microcolonies show a differential cell cycle regulation compared with the whole population. Counting of cells according to their cell cycle phase was performed in 5 independent replicas. 100 cells were counted in all cases. Mean and standard deviation are shown. **B.** Flow cytometry analysis of one of the replicas is shown. A longer G1 phase can be appreciated in cells extracted from small microcolonies. It could be a consequence of WHI5 overexpression detected in the slow growth microcolonies.

3.3.8 WHI5 contributes to proliferation heterogeneity

The RNAseq results from the slow (small) and fast (big) proliferating microcolonies suggests the involvement of several regulators of the cell cycle in the regulation of cells heterogeneity. In fact, the most upregulated gene in small microcolonies is the G1/S transition inhibitor WHI5 (Table 3). This gene

encodes a transcriptional repressor that inhibits both SBF (SCB-binding factor) and MBF (MCB-binding factor) transcription factors during G1/S transition (Costanzo, Nishikawa et al. 2004; de Bruin, McDonald et al. 2004; Pramila, Wu et al. 2006). The *whi5* deletion mutant passes through Start at about half the size of wild-type cells, thereby accelerating the G1/S phase transition (Simon, Barnett et al. 2001; Jorgensen, Nishikawa et al. 2002; Zhang, Schneider et al. 2002). Conversely, overexpression of WHI5 causes both a G1 delay and an increase in cell size in wild-type cell.

In order to investigate whether Whi5 is involved in this heterogeneity phenomenon we used the *whi5Δ* mutant, which lacks the *WHI5* gene.

When the proportion of fast and slow proliferating microcolonies was analysed by flow cytometry after single cell microencapsulation and growth, we found that the ratio small (slow proliferating) *versus* big colonies (fast proliferating) decreased in the absence of *WHI5* comparing with the wt. The *whi5Δ* mutant showed a lower proportion of small microcolonies than the wt as expected (Figure 26A)

To check this result we also counted the number of small and big colonies under the microscope (Figure 26B) and calculated the small/big ratios from these data (Figure 26C). The same result was obtained.

However, when the small/big ratios were calculated for the *puf3Δ* mutant and compared with the wt, we did not observed a decrease in the number of small colonies (Figure 26D).

Altogether these results indicates that cells derived from small microcolonies exhibit a longer G1 phase and reinforce the possible role of Whi5 protein in the regulation of the population heterogeneity though its control on the G1/S transition.

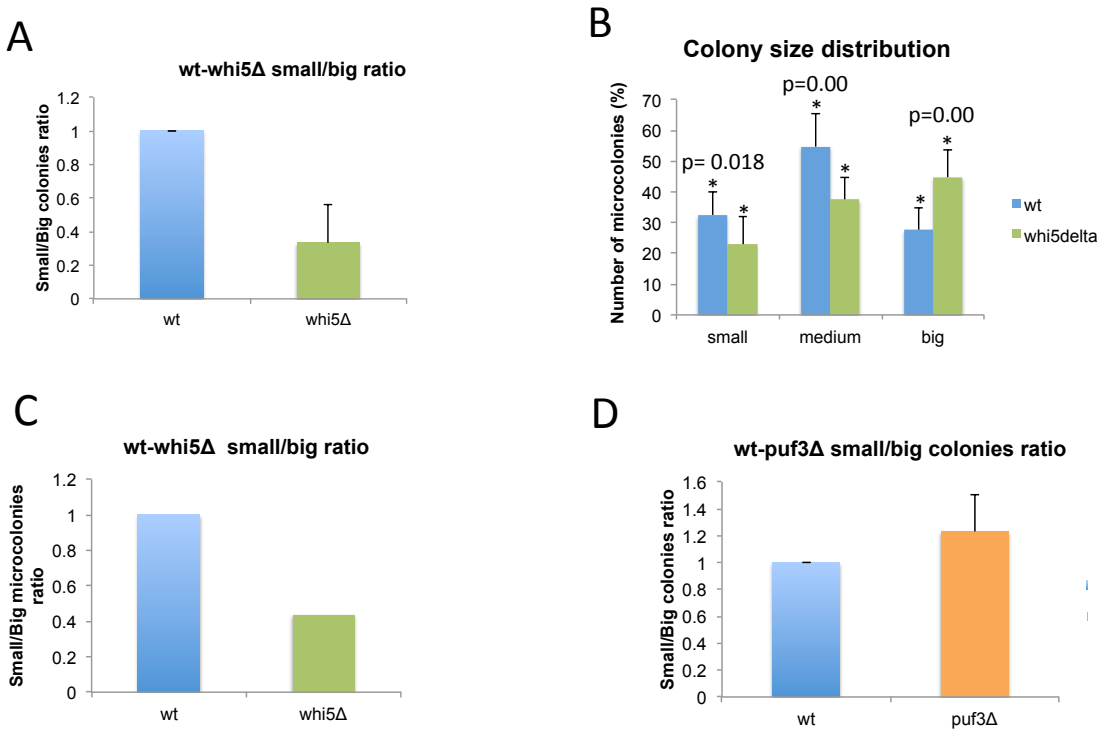

Figure 26. A. Small/Big colony ratio in wt and *whi5Δ*. A. Ratios calculated after flow cytometry analysis. 5000 microcolonies were analysed in three independent replicates cases.. A decrease in the small/big colonies ratio can be observed in the *whi5Δ* mutant. **B.** Microcolonies counting under microscope. 1000 microcolonies were counted in ten independent areas of different samples. Mean and standard deviation are represented. **C.** Small/big colonies rations were again calculated from the counting in B. These data confirm that *whi5Δ* exhibits a different colony distribution compared with the wild-type. **D.** Small/Big colonies ratio in *puf3Δ* mutant. It can be observed how this mutant does not behave as the *whi5Δ* when the Small/Big ratios were calculated. This suggest that the respiratory phenotype in small microcolonies is a consequence of the slow growth.

3.4 Replicative aging contributes to proliferation heterogeneity

Normally, a G1/S transition delay is associated with an increase in cell size. In this work, we have previously shown that this is the case in small microcolonies where cells are larger. On the other hand, the increased cell size phenotype it has been also related in some cases with aging (Smith, Wright et al. 2015). Thus, we wondered whether the slow proliferating (small) microcolonies were also enriched in aged cells.

3.4.1 Identification of microcolony founding cells by bud scar counting

To know whether replicative aging was implicated in the appearance of small microcolonies phenotype, we count the bud scar numbers in small microcolonies coming from a wt culture growing during 13 hours. To address that we performed a calcofluor staining in yeast cells, which enables us to count the bud scars after analysis with confocal microscopy (Figure 27 and Figure 28). A bud scar is a crater-like ring of chitinous located on the surface of the mother cell. It is formed after the newly emerged daughter cell separates thereby marking the site of cytokinesis and septation. The number of bud scars that accumulate on the surface of a cell is a useful determinant of replicative age Thus, the bud scars counting let us to identify the microcolonies-founding cell as the cell which contains the largest number of these marks. In almost every founding cell analysed, a large number of bud scars were observed (Figure 28 and Table 6). However, this number does not correlate with the total number of divisions needed to generate the number of cells belonging to the microcolony. Namely, the number of bud scars in the small microcolonies-founding cell was higher than expected based in the number of cells present in the microcolony. In the other way around, the total number of cells forming the small microcolony was smaller that expected based on the number of bud scars of the founding cell.

As the microcolonies cell number indirectly indicates the maximum number of divisions of the founding cell, we could calculate the theoretical number of bud scars in the funding cells when it is just encapsulated. A comparison between the theoretical and the observed bud scars number is shown in Table 6.

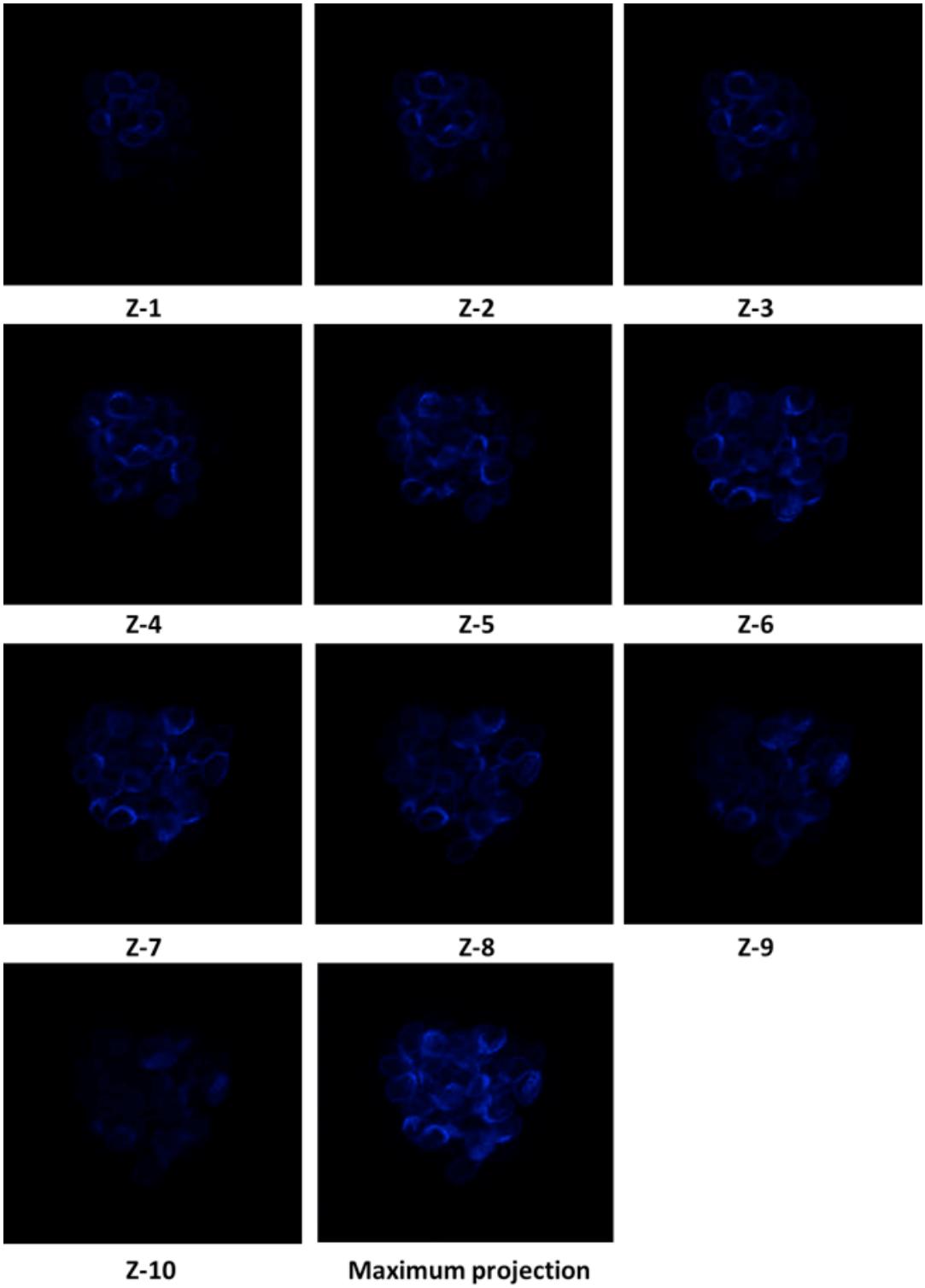

Figure 27. Calcofluor staining of a small microcolony using confocal microscopy. Here are displayed Z sections of a small microcolony from Z1-Z10 and the maximum projection of all Z sections. This enables bud scars and colony cells counting through the colony.

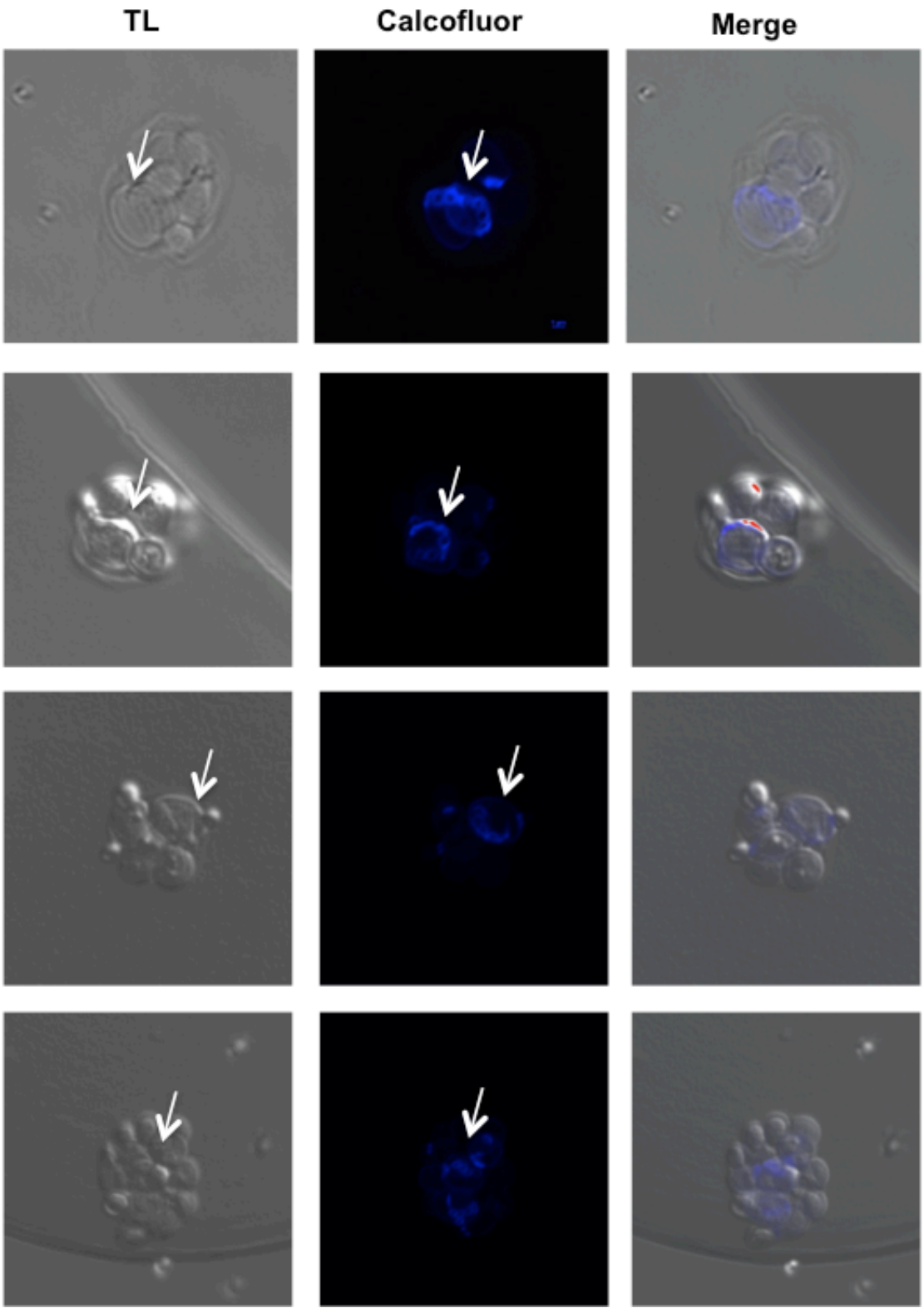

Figure 28. Identidication of the founding cell by bud scar counting. 6 different small colonies are showed. White arrows indicate the founder cell.

Table 6. Observed and expected number of bud scars comparison.

Colony ID	Nºcells/colony	Bud scars expected	Bud scars observed
1	22	4	4
2	5	2	5
3	20	4	4
4	20	4	5
5	18	4	4
6	16	4	6
7	14	4	4
8	30	5	5
9	16	4	7
10	28	5	6
11	12	4	8
12	18	4	6
13	22	4	6
14	20	4	8
15	18	4	4
16	6	3	9
17	12	4	6
18	18	4	6
19	8	3	6
20	8	3	7
21	4	2	6
22	10	3	5
23	12	4	5
24	8	3	8
25	6	3	5
26	8	3	7
27	6	3	5
28	6	3	6
29	12	4	6

30	5	**2**	6
31	16	**4**	6
32	8	**3**	5
33	10	**3**	7
34	12	**4**	5
35	8	**3**	6
36	4	**2**	5
37	22	**4**	8
38	8	**3**	7
39	6	**3**	4
40	16	**4**	8
41	8	**3**	5
42	32	**5**	7
43	22	4	4
44	4	**2**	6
45	16	**4**	7
46	12	**4**	6
47	8	**3**	7
48	6	**3**	7
49	20	**4**	9
50	12	**4**	7

Fifty colonies were analysed. The rows show the observed and expected number of bud scars in the founding cell and the number of cell forming the colony. From the last one, the expected number of bud scars was estimated. In white, small microcolonies whose founding cells show more bud scars than expected.

3.4.2 Small microcolonies founding cells were aged when they were encapsulated

Taken into account the previous results shown in Table 6, we calculated the cell age of the small microcolonies founding cell. To address that, the theoretical number of bud scars of the founding cell was subtracted from the observed number. This difference could be only explained as the number of bud scars already present in the founding cell before being encapsulated. We found that in the most of the colonies analysed, the founding cells had undergone some divisions before they were encapsulated. Thus, they would not have the division capacity of a daughter cell, but lower. This may explain why these cells produce smaller colonies when encapsulated.

After calculate the microcolonies founding cells age, we compared it with the cell age distribution of a wt exponential culture that was not encapsulated as a control. The data obtained with this culture were consistent with already published cell age distributions (Lee, Vizcarra et al. 2012). However, we found that cells from small microcolonies present a very clear increase in the bud scars number. Whereas in a non-encapsulated exponential culture the majority of cells are virgin cells or present 1-2 bud scars, in the small microcolonies cells with 3, 4 or 5 bud scars are more abundant. These data are resumed in Figure 29.

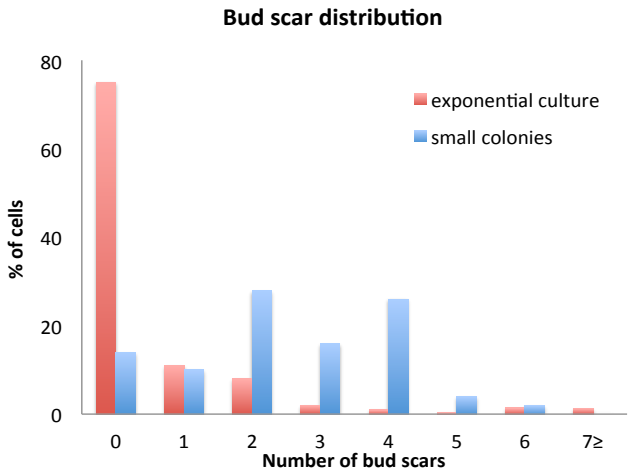

Figure 29. Bud scars distribution in small microcolony founding cells and in a liquid exponential culture. In red, percentage of small microcolonies founding cells with a specific age (represented by the bud scars number) at the moment of encapsulation. In blue, bud scars distribution in a exponential non encapsulated culture of the same strain. P value <0,001.

4.Discussion

4.1 Microencapsulation is a useful tool to study cell and mycelium proliferation

We have demonstrated in this thesis that microencapsulation is an easy, useful and efficient method to study cell proliferation. The classical way to analyse proliferation consist on cultivating cells until forming visible colonies which are used in subsequent steps (e.g. genetic screenings (Wan, Yu et al. 2006)) (Walser, Leibundgut et al. 2008). However, the huge complexity of living systems makes necessary the development of high throughput technologies. Thus, sample numbers exceeding 10^6 per day require new technologies for sample miniaturization and parallelized processing. Such technologies must be sensitive, robust, informative and economically feasible (Inglese, Johnson et al. 2007; Pereira and Williams 2007).

In this context, microencapsulation supposes an alternative time and space-saving method for cell separation and growth in which the colonies derived from the encapsulated cells remain trapped in the gel microparticles. Such microparticles allow the exchange of nutrients or reactants through the polymer as the same time that they retain cells inside. These microcarriers comprise the key properties for microorganisms cultivation, specifically allow biomass to grow under monoseptic conditions (Walser, Leibundgut et al. 2008).

After comparing encapsulation with conventional methods for microorganism analysis two main advantages can be highlighted: the savings in the time necessary to detect growth and the possibility to perform a high-throughput analysis by measuring the microcapsules by flow cytometry. About the former, while to detect growth in a Petri dish as less 20 generations are required, by cell microencapsulation the growth under the microscope can be detected in a few hours, depending on the microorganism. Moreover, the population homogeneity is much higher in the microcolonies. The cells clonality is maintained because of the low number of cellular divisions, which makes more reliable the results obtained by this technique.

Second, the microparticles produced by Flow Focusing exhibit the proper optical and morphological features to be detected by large particle flow cytometry using the complex object parametric analyser and sorter (COPAS or BioSorter) technology that contrary to the FACS allows for the analysis of big particles (20-1500um) (Figure 8). COPAS and BioSorter devices automates the analysis, sorting and dispensing of large objects such as stem cells (Tarunina, Hernandez et al. 2014), cell clusters (Fernandez, Hatch et al. 2005), large cells (de la Cruz and Edgar 2008), beads, seeds and small model organisms (Maruyama, Grevengoed et al. 2011; Zugasti, Thakur et al. 2016). The BioSorter allows the measurement of different physical parameters like the axial length of the object (TOF, time of flight), the optical density (EXT, extinction) and the intensity of fluorescent markers (green, red and yellow). Because of the low rate of object per second it serves as a tool for the differentiation between monoclonal, polyclonal or empty microparticles after cell cultivation (manual BioSorter, (Walser, Leibundgut et al. 2008) (Figure 8B).

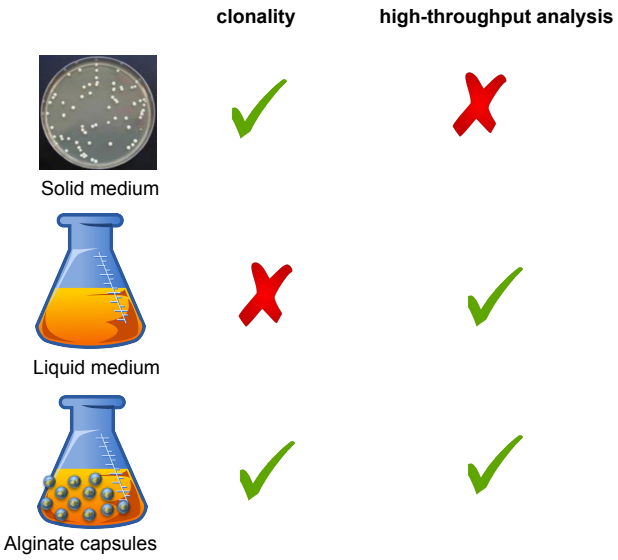

Figure 30. Advantages of cells microencapsulation *versus* the conventional methods of microorganism culture.

We have been able to answer different biological questions taking advantage of the facilities providing by the Flow Focusing technique: homogeneous capsules

of a chosen size can be produced, the cells suffer minimal mechanical stresses and the capsules production rate is higher than most other encapsulation technologies (Martin-Banderas, Flores-Mosquera et al. 2005). Then, combining microencapsulation with large particle flow cytometry, the number of applications we can uncover are multiplied. A key point of the technique optimized in this thesis, is the efficient encapsulation of individual cells. In this way, the analysis of progression from isogenic isolated cells is possible.

In this way, we have demonstrated that this technique is suitable for genetic screenings as well as genetic analysis in isolated cells in different mutants, both in yeast (Gomez-Herreros, de Miguel-Jimenez et al. 2012) and filamentous fungi (Delgado-Ramos, Marcos et al. 2014)

In both cases, the power of this method relies on the capacity to do genetic screenings and make both positive and negative selection, for example, allowing to sort strains carrying thermosensitive alleles of essential genes, which could be later recovered by growing at the permissive temperature. Performing this method skips the laborious and time-consuming requirement of replica plating. In addition, this method can be extended to screenings for regulators by employing GFP genes under the control of a promoter of interest. It makes this method powerful and versatile.

A classic problem in population and evolutionary biology is to understand how a population enhance its fitness in nature, a continuously changing environment. Recent studies demonstrating the importance of phenotypic heterogeneity in genetically identical cells have renewed an interest in studying this phenomenon. By the transition among multiple phenotypes, an isogenic population of cells ensure that some cells are always prepared for the possible environmental fluctuations (Acar, Mettetal et al. 2008) (Sanchez-Romero and Casadesus 2014). However there has been historically a technical limitation to study this processes. Combining microencapsulation with flow cytometry we have been able to follow the progression of a population through the encapsulation of their single cells. Our results give new insight towards the knowledge of those processes that govern heterogeneity in isogenic populations, particularly in small colonies formation. We have give experimental evidences of the existence of deterministic regulatory processes that in principle

could be though to be stochastic. So we have found a connection between metabolism, cell cycle, replicative aging and microcolony phenotype.
In summary, using microencapsulation of individual isogenic vells, we showed the existence of a size microcolonies heterogeneity that was caused by a proliferative capacity heterogeneity. Thus, small microcolonies correspond to cells with lower proliferation capacity than cells present in big microcolonies. In other words, cells from small microcolonies present a slow growth rate (GR) while cells from big ones have a fast GR.

4.2 Saccharomyces cerevisiae adapts its energy metabolism to the growth rate

Usually, most experiments study cell populations in cultures, in which the growth rate (GR), gene expression and mass changes represent population averages assuming that the observed cell to cell variability is because of noise (Newman, Ghaemmaghami et al. 2006). However, our experiments demonstrate that different GR can be observed in a clonal cell population under homogeneous conditions. This way, one clear conclusion drawn from our experiments is that *S. cerevisiae* adapt its energy metabolism to the GR.
Yeast slow growth (observed in small microcolonies) was accompanied by a rise in the mRNA levels of the mitochondrial and respiratory genes, which, in turn, provoked a relative increase in respiratory metabolism (Fig. X)). In fact, the overexpressed genes in small microcolonies included three regulators of the energy metabolism during the transition from fermentation to respiration: *SIP4* (Lesage, Yang et al. 1996; Vincent and Carlson 1998), *ERT1* (Gasmi, Jacques et al. 2014) and PUF3 (Miller, Russo et al. 2014). Correspondingly, faster growth (present in big microcolonies) was associated with a relative increase in fermentative metabolism as well as they present an upregulation of ribosomal genes. Our data are supported by Lu *et al*. (Lu, Brauer et al. 2009). Based on chemostat experiments, they suggested that slow growth might be accompanied by higher respiration. They found a shift in the transcriptome toward a mild stress response and oxidative metabolism. These authors also observed poor ethanol production and higher glucose consumption per biomass

unit produced at high GRs. Also, van Dijk et al, (van Dijk, Dhar et al. 2015) reached a similar conclusion using a different colonies isolation approach, which reinforce again our results.

The inverse correlation between the GR and respiration in carbon-fermentable media is interesting because *S. cerevisiae,* and other Crabtree-positive yeasts are assumed to have adopted a fast fermentation of glucose to ethanol as an evolutionary strategy to compete with other microorganisms (Lagunas 1986) (Dashko, Zhou et al. 2014). It seems, therefore, that yeast equates a higher GR with fermentation for competitive purposes and a lower GR with energy restriction and respiration, and a more energy-efficient metabolism. This is, although is commonly assumed that free-living microorganisms have evolved to grow as fast as possible as the simplest behaviour that firs Darwinian natural selection for single cells (Bosdriesz, Molenaar et al. 2015), there are some exceptions that maybe improve the population fitness. Under some slow growth conditions, yeast cells are subjected to a yeast metabolic cycle in which respiratory and fermentative metabolism phases alternate (Tu, Kudlicki et al. 2005; Slavov, Airoldi et al. 2012). In this cycle, mitochondria and respiration genes have RNA amounts (RA) peaks in the high oxygen consumption phase. It is noteworthy that yeast metabolic cycle seems to lower, or is even absent, at a high GR (Tu, Kudlicki et al. 2005). Thus, the increasing importance of respiration (and the genes related to it) at a low GR may be a direct result of the ever-increasing importance of metabolic cycling. Our conclusion on the interdependence of the growth rate and respiration-related genes expression was based on our microcolony assay in which all the cells were wild-type, had the same genome and were culture in the same environment avoiding any bias caused by using mutants, and supported by the meta-analysis of (mainly) mutant collections (Garcia-Martinez, Delgado-Ramos et al. 2016).

Interestingly, the *S. cerevisiae* growth strategy has a counterpart in cancer cells, which use high glycolytic rates (fermentation to lactate) instead of respiration in the presence of both glucose and oxygen (i.e. “Warburg effect (Vander Heiden, Cantley et al. 2009) (Diaz-Ruiz, Rigoulet et al. 2011))

For a high GR, cancer cells need the fast production of precursors for nucleotides, amino acids and fatty acids, and NADPH for the synthesis of macromolecules. These precursors are not generated directly during

respiration. Thus *S. cerevisiae* and cancer cells have both probably acquired regulatory mechanisms that allow the fine-tuning of the respiration:fermentation ratio to suit GR requirements. At least in yeast, this mechanism seems to act by controlling mainly the mRNA stability of mitochondria related genes as will be discussed later.

4.3 Change in mRNA stability contributes to gene expression regulation by growth rate

The mRNA levels of the respiration and mitochondria-related genes lowered at higher GRs (big microcolonies with fast proliferation) (Table 3 and 5).Although, this was previously reported (Brauer, Huttenhower et al. 2008; Airoldi, Huttenhower et al. 2009) our results, together with hose produced by Pérez-Ortín and co-workers (García-Martínez et al, 2016) show, for the first time, that change in mRNA levels was not due to a change in the synthesis rate, but to mRNA destabilization (Figure 23). Many mitochondria related genes belong to post transcriptional regulons, which are controlled at the degradation level (Keene 2007). A group of these mRNAs has binding sites for the Puf3 protein within their 3 'UTR. This protein controls mRNA location (Saint-Georges, Garcia et al. 2008) and stability in response to the carbon source (Miller, Russo et al. 2014). From our RNA seq experiment we obtained that Puf3 was significantly upregulated in the slow grow microcolonies. Thus it is likely that Puf3 is partially responsible for the destabilization of the respiration and mitochondria-related genes at a faster GR (Figure 23 A) and their stabilization at a slow GR. Using the most extensively cited study (Gerber, Herschlag et al. 2004), we found a significant enrichment ($P < 0.05$) of Puf3 targets among the destabilized genes at a faster growth. It was also interesting to note that, among the Puf3-regulated genes, only the long mRNA isoforms with potential Puf3-binding sites (Riordan, Herschlag et al. 2011) were asymmetrically enriched in slow- versus fast-growing microcolonies (Figure 23 B). This result is supported by (Gupta, Clauder-Münster et al. 2014) whose experiments show that PUF3 binds and destabilizes specific polyadenylation isoforms. Moreover, our experiments highlight the importance of mRNA polyadenylation isoform choice. In fact, two different studies in yeast have shown that even single‐nucleotide differences

in 3′ UTR length can often lead to drastic changes in transcript stability and translation efficiency (Geisberg, Moqtaderi et al. 2014; Gupta, Clauder-Münster et al. 2014). It is therefore possible that cell‐to‐cell variation in 3′ UTR choice contributes to phenotypic diversity. In mouse cells, the 3' UTR choice has been described as a mechanism dependent of the developmental state of the cell and it has been demonstrated that cell identity can be retrieved using information on 3′ end usage alone (Velten, Anders et al. 2015).

The regulatory model that arose from these and other published results was the following: a low GR activated PUF3 expression, which would favour its role in the expression of its target genes.

An important consequence of the general dependence of mRNA turnover of the GR is that genes cannot be annotated by their characteristics mRNA half-lifes since these values depend on the GR (Chavez, Garcia-Martinez et al. 2016)

Altogether, this results support the fact that in yeast, transcription and degradation rates are coupled by cross-talk mechanisms that imprint mRNAs during their transcription in the nucleus so as to determine their fate in the cytoplasm, as has been recently shown by (Goler-Baron, Selitrennik et al. 2008; Harel-Sharvit, Eldad et al. 2010; Haimovich, Medina et al. 2013; Sun, Schwalb et al. 2013)

It is important to stress that, in this model, *PUF3* expression is activated as a consequence of the low growth rate present in the small microcolonies. Therefore, the *PUF3* overexpression is a response to this growth rate. This aspect will be discussed in more detail below.

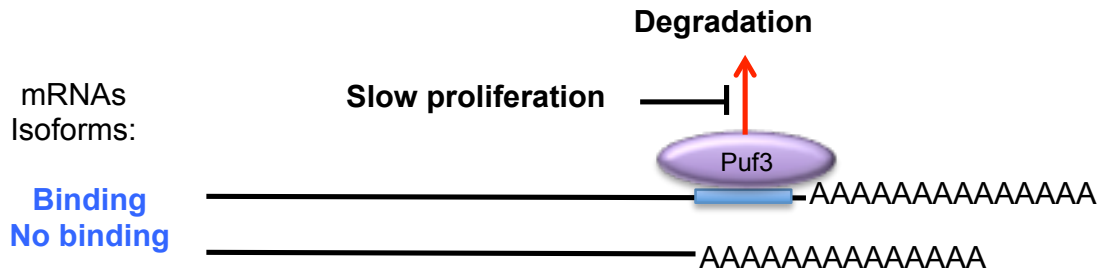

Figure 31. Proposed mechanism of action of Puf3 in slow proliferating microcolonies. A low growth rate promotes Puf3 expression in small microcolonies.

Puf3 binds their targets mRNAs in an isoform specific manner. The binding promotes the stabilization of such isoforms in slow proliferation conditions. Thus it is likely that Puf3 is partially responsible for the destabilization of the respiration and mitochondria-related genes at a faster growth rate and their stabilization at a slow growth rate. This could explain the respiratory phenotype showd in the small microcolonies.

4.4 The intrinsic proliferation variability in wild-type yeast populations seems to be due to a metastable expression program

The existence of intrinsic expression variability in wild-type yeast populations has been previously shown and allows cells to anticipate environmental changes (Venturelli, Zuleta et al. 2015; Wang, Atolia et al. 2015). However, it has not been shown whether this variability is just caused by the random cell-to-cell variation of gene expression, or if it is constituted a metastable expression program that can be inherited through the mitotic cycle. Our results indicates that this is the case since noisy fluctuations of gene expression, without transmitting through cell division, would not likely explain the existence of slow and fast proliferating subpopulations with specific transcriptomic signatures. The coexistence of two populations with different energy metabolisms in a single yeast population led to an alternative reinterpretation of diauxic transition, as observed in yeast cultures when glucose declined in the medium. The change from fermentative to respiratory metabolism, rather than cell reprogramming, could result from the differential effect that glucose exhaustion would have on fast and slow proliferating cells. Whereas the former would stop growing, the latter would take the lead of the culture by just continuing their slow proliferation based on respiration.

4.5 *Cell cycle regulation is involved in proliferation heterogeneity.*

The heterogeneity analysis that was performed in this thesis demonstrated first that the differences in size microcolonies were due to heterogeneity in

proliferative capacity of the cells. Thus, cells from small microcolonies have slower proliferation capacity than cells from big ones.

The transcriptomic analysis revealed an overexpression of the cell cycle progression antagonist Whi5 in small microcolonies. Whi5 specifically inhibit the G1/S transition. Interestingly, cells from small microcolonies show a delay in G1/S transition, which is consistent with such overexpression previous results. Moreover, the heterogeneity analysis of a *whi5Δ* mutant showed a decreased population of small microcolonies. This result suggests an interesting role of Whi5 in generating the small microcolonies phenotype. On the contrary, this is not the case for some studied respiratory mutants. In the case of *puf3Δ* strain, the ratios small/big colonies are much higher in comparison with the wild type. This reinforce the hypothesis that the respiratory phenotype showed in small microcolonies is a consequence and not a cause of being small because of their specific cell cycle regulation (Fig x and x). All these results suggest that the cell cycle regulator Whi5 could play an important role in heterogeneity generation and maintenance and is involved in small microcolony phenotype. A recent publication highlights the role of Whi5 in the cell division control and propose a model in which the Whi5 concentration alone should predict the rate at which cells progress through Start. This relevant role of Whi5 support our hypothesis of Whi5 as a cell population heterogeneity regulator based on Whi5 concentration (Schmoller, Turner et al. 2015).

It is difficult to think that the inactivation of a single gene leads to a change of heterogeneity at the level of cell population. However, a few examples have been described in mammalian systems. This is the case of p21 protein. This protein is a CDK inhibitor in G1 phase (Harper, Adami et al. 1993) and it is transcriptionally activated by p53 after DNA damage (el-Deiry, Tokino et al. 1993). Apart from its role in cell cycle arrest in DNA damaged cells, it has been revealed a direct role for low basal levels of p21 in non-damaged cells in controlling population heterogeneity in cell cycle activity (Overton, Spencer et al. 2014). This has a huge significance in cancer biology. While a therapeutic agent may be effective against one fraction of a population, it may be less effective against another fraction. So population heterogeneity can change the point of view in the treatment of tumor. In fact, in the light of the p21 results it has been suggested that, instead of using CDK inhibitors (CKIs) in cancer therapy, CKIs

themselves should be targeted (Overton, Spencer et al. 2014).

4.6 Proliferation heterogeneity is related to aging

As has been previously described, our experiments give rise to think in Whi5 as the main player that makes the cells to express a slow growing expression program through a G1/S transition delay. This is, the different cell cycle regulation, that could be epigenetically inherently thought the mitotic cell cycle, should be the responsible of the observed population heterogeneity.

Whi5 orthologous in mammals, Retinoblastoma (Rb), is known to be induced in response to DNA damage and also leads to cell senescence, establishing and maintaining the typical senescence growth arrest. Cellular senescence has been proposed to a possible contributor to ageing or loss off regenerative capacity of cell in vivo. In fact, the number of senescent cells increases with age and are present at sites of age- related pathology (Campisi and d'Adda di Fagagna 2007). Because of the existing link between cellular senescence, controlled in part by Rb, and ageing in mammals, we hypothesized that the observed proliferation heterogeneity in *S.cerevisiae* could be related to ageing and controlled somehow by Whi5 protein levels. In fact, from our aging experiments, we found that aging is also an important mechanism contributing to small colonies formation, where Whi5 is overexpressed. First, we analysed the bud scar distribution by bud scar calcofluor staining in small microcolonies and compared the results to a non-encapsulated exponential culture of the same strain. We observed that the small microcolonies bud scar distribution was sloped to larger numbers of bud scars. Furthermore, the small microcolonies founding cells had more bud scars than expected from the number of cells in the colony, that is to say, founding cells were already aged when they were encapsulated before founded the small microcolony. These results were very consistent with the hypothesis that, at least in part, aging may explain smaller colony sizes.

Taken together all the results, we propose a model in which we establish a link between aging and proliferative capacity through the regulation of Whi5 levels. In this model aging would play a role in the increase in Whi5 levels in yeast cells.

Cell damage has been recently described to be accumulated in slow grower colonies as a result of the existing oxidative stress (van Dijk, Dhar et al. 2015). We propose that this DNA damage can be the result of aging and may accumulate and activate Whi5 cell cycle inhibitor. This Whi5 increase leads to a larger G1 phase, as Whi5 dilution takes longer to reach the threshold needed to enter S phase (Schmoller, Turner et al. 2015). Due to this, cells show slow growth. So Whi5 may play the same role in yeast that Rb in mammals as a contributor to senescence.

As we have discussed above, an aged founded cell generates a small microcolony. From our results, can also be inferred that some epigenetic mechanism is necessary to transmit the “aged state” to the new daughter cells to maintain the low proliferative capacity over different generations and generate, in this way, a small microcolony.

Our results take relevant importance because they open up the possibility to further research aging as a candidate linked to size heterogeneity in yeast population. Also, this technique represent an alternative to the low efficiency of the replicative lifespan assay based on micro-dissection and offers the possibility to perform large-scale genetic screening for lifespan phenotypes as well as to track molecular markers during aging.

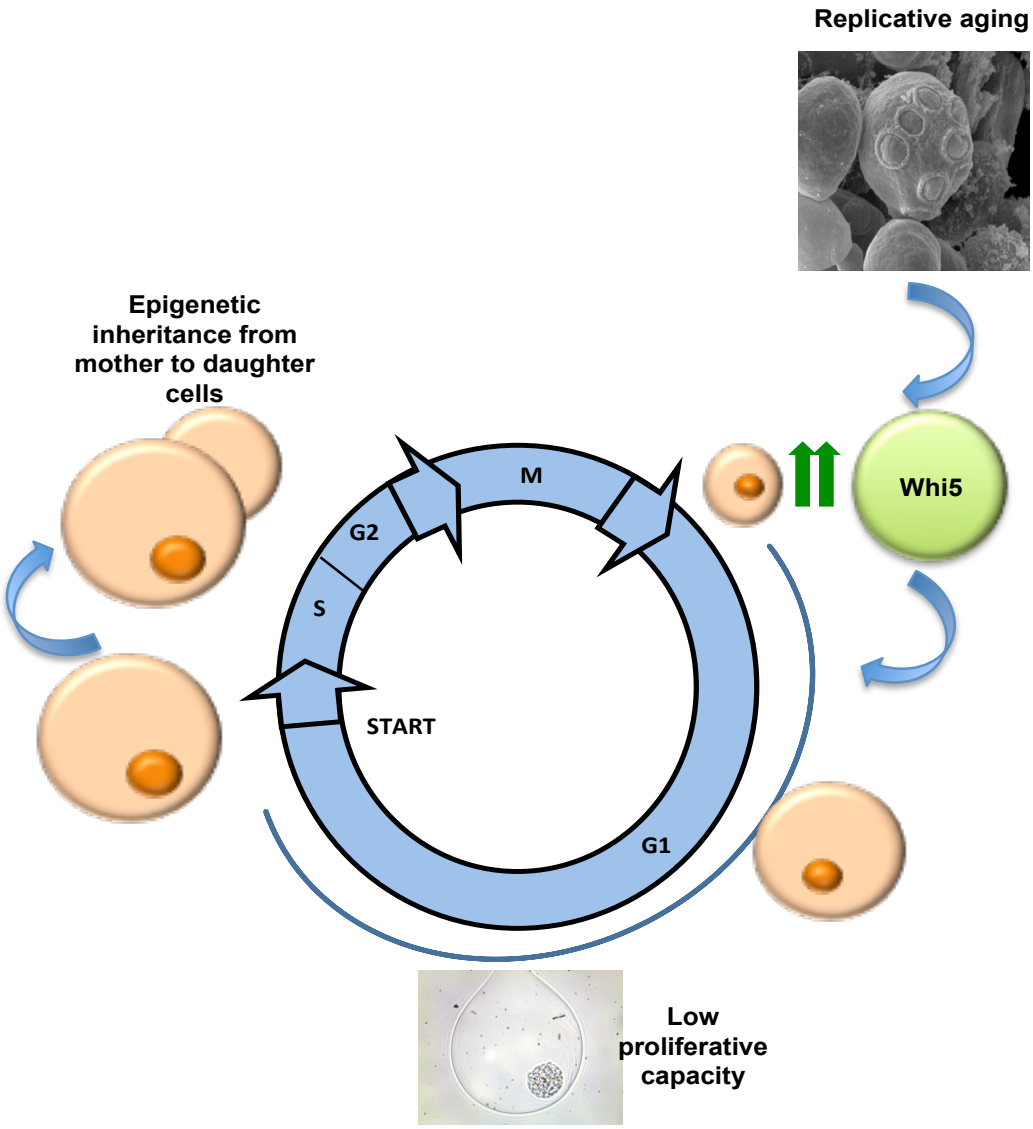

Figure 32. Working model to explain the link of replicative aging to proliferation heterogeneity Cell damage has been recently described to be accumulated in slow grower colonies as a result of the existing oxidative stress (van Dijk, Dhar et al. 2015). We propose that this DNA damage, that extend G2 phase, can be the result of aging and may accumulate and activate Whi5 cell cycle inhibitor, expressed in G2, in the small microcolonies. As Whi5 dilution takes longer to reach the threshold necessary to cell division, this Whi5 increase leads to a larger G1 phase, (Schmoller, Turner et al. 2015). Due to this, cells show slow growth. So Whi5 may play the same role in yeast that Rb in mammals as a contributor to senescence. However, if it only happens in the mother cell, it could not be explained the small microcolony phenotype and the detection of Whi5 overexpression. Thus, we propose the existency of a epigenetic mechanism inherited from the mother to the daughter cells that maintain the high levels of Whi5 in the progeny.

5. Conclusions

1. Cell microencapsulation is a useful microbiological tool that can be easily coupled to large particle flow cytometry, allowing the high throughput analysis of cell and mycelium microcolonies.

2. In the absence of genetic or environmental variation *S. cerevisiae* cell populations show intrinsic proliferation heterogeneity.

3. Fast- and slow-proliferating subpopulations exhibit differential transcriptomic patterns. This suggests the existence of a metastable expression programs that can be transmitted through the mitotic cycle.

4. Slow-growing microcolonies express respiration and mithocondria-related genes, even in the presence of high glucose concentrations. This is likely due to the stabilization of their mRNAs in a Puf3-mediated manner.

5. The regulation of the G1-S transition by Whi5 plays a role in the control of cell proliferation heterogeneity.

6. Aging of the founding cell favours a reduction in the proliferation capacity of its lineage.

6. Materials and methods

6.1 Strains and growth conditions

Escherichia coli strains

DH5 alpha competent cells

Saccharomyces cerevisiae strains

All the Saccharomyces cerevisiae strains utilized were in the BY4741 backgroung. Strains were grown at 30ºC in the indicated media.

DNY51 strain was used for liquid aging assays. It was previously described in Lindstrom & Gottschling 2009 (Lindstrom and Gottschling 2009). This strain presents a construction that allows a selection against newborn daughter cells through a “mother enrichment program” or “MEP” . Cre-EBD78, a novel version of a fusion protein between the Cre recombinase from bacteriophage P1 and the estrogen-binding domain of the murine estrogen receptor that is strictly dependent on β-Estradiol for activity. PSCW11-cre-EBD78 is integrated at the ho locus and specifically expressed in newborn cells, using a daughter-specific promoter derived from SCW11. Target genes were constructed at their endogenous loci by introduction of loxP sites. Target genes are UBC9 and CDC20, both necessary elements for cell cycle progression. In β-Estradiol treatment conditions, Cre recombinase translocates to the nucleus and, as a consequence of its activity, target genes are removed only in newborn cells, as PSCW11-cre-EBD78 expression is restricted to those.

Table 7. Yeast strains used in this work

Yeast strain	**Relevant genotype**	**Reference**
BY4741 (wt)	MATa *his3Δ1 leu2Δ0 met15Δ0 ura3Δ0*	Euroscarf
MMY9.2 (*dst1Δ)*	MAT *a met15Δ hisΔ1 leu2Δ ura3Δ YGL043w::kanMX4 lys-*	(Gomez-Herreros, de Miguel-Jimenez et al. 2012)

Y05312	BY4741 sfp1::kanMX4	Euroscarf
FGY43.1B (*dst1Δsfp1 Δ)*	BY4741 *dst1::kanMX4 sfp1::kanMX4*	(Gomez-Herreros, de Miguel-Jimenez et al. 2012)
DNY51	MAT a *can1::PSTE2-Sp_his5+ leu2Δ lyp1Δmet15Δ hoΔ::PSCW11-cre-EBD78-NATMX loxP-UBC9-loxP-LEU2 loxP-CDC20-Intron-loxP-HPHMX his3Δ:KAN*	Lindstrom et Gottschling, 2009.
Y1859	BY4741 *whi5::kanMX4*	Euroscarf
Y1501	BY4741 *puf3::kanMX4*	Euroscarf
Y1334	BY4741 *sip4::kanMX4*	Euroscarf
Y3379	BY4741 *ert1::kanMX4*	Euroscarf
Y605	BY4741 *rsf1::kanMX4*	Euroscarf

Trichoderma reesei strains

Strain QM9414

Aspergillus nidulans strains

Experiments performed with thermosensitive strains were carried out at 30 or 42 ºC as indicated. Glucose was used as sole carbon source, and ammonium tartrate was used as sole nitrogen source. Strains were obtained by following standard procedures (Pontecorvo et al. 1953).

Table 8. Aspergillus strains used in this work.

Strain	Relevant genotype	Reference
FGSC4	Wild-type strain, *veA+*	FGSC
DKA63	*biA1*	M. Peñalva
DKA4	*pyroA4 pyrG89 wA2*	
DKA95(AGB288)	*ΔcryA::ptrA veA+ G.*	Braus
DKA200 (FGSC A1096)	*pabaA1*	FGSC
DKA13(MH11057)	*pabaA1niiA4 ΔnkuA::bar yA1*	M. Hynes
HA344	*H1-chRFP::Afpyro pyrG89 (pyroA4; argB2?) ΔnkuA::argB*	S. Osmani
DKA180	*nimX2F233L, yA2, nicB8, pyroA4; HH1-GFP-Afpyro+; ΔnkuA (?)*	This study
Strains used only for crossings		
FGSC A1126	*nimX2F233L nicB8 pyroA4 yA2*	Osmani et al. (1994), obtained from FGSC
LO 1945	*pyrG89 riboB2 pyroA4 nkuAΔ HH1-GFP-Afpyro+*	B. Oakley

Growth assays

For growth assays, yeast cultures were diluted to O.D. $_{600nm}$ 0.5 and serial dilutions (1:10) were spotted onto plates.

6.2 Growth media and reagents

Yeast growth media

YPAD rich medium: 1% yeast extract; 2% bactopeptone; 2% glucose, 0,2% adenine.

-YPED rich medium: identical to YPAD but supplemented with x um of beta-estradiol.

- SC minimal medium: 0.17% yeast nitrogen bases (YNB); ammonium sulphate; 0,5 % ammonium sulphate; 2% glucose and supplemented with the amino acids leucine, tryptophan, histidine, leusine and the nitrogenous bases adenine and uracile. It is specified when one or more of these requirements had been omitted from the medium.

Solid media were prepared by the addition of 2% agar before autoclaving

Bacterial growth media

-LB rich medium: 0.5% yeast extract; 1% bacto-tryptone; 1% NaCl.

-LB + Amp rich medium: LB medium supplemented with ampicillin (100mg/l) after autoclaving.

Solid media were prepared by the addition of 2% agar before autoclaving.

Filamentous fungi media

Strains were grown in complete (CMA) or minimal (MMA) media containing the appropriate supplements (Cove 1966).

Antibiotics, drugs, enzymes, inhibitors and others reagents

- Alginate (Sigma) : poliyaccharide used to produce gel microparticles

- Ampicilin (Amp) (Sigma): beta-lactam antibiotic that inhibits Escherichia coli celular división by preventing the synthesis of the cell Wall. It was used for the selection of plasmid carrying cells.

- Calcium chloride (Sigma): salt used in a solution that help the microparticle

gelation.

- Calcofluor (Sigma): special fluorescent stain that binds strongly to structures containing cellulose and chitin. Used to stain bud scars.
- Sodium citrate: salt used in Flow cytometry to clean the samples. It is also used to break the alginate microparticles.
- DL-Dithiothreitol (DTT) (Promega): reducing agent.
- Dynabeads M280 Streptavidin (Invitrogen): magnetic beads that capture the 3' terminal cDNA fragments.
- ERCC RNA Spike-ins (Invitrogen): external RNA controls (polyadenilated transcripts) that enable performance assessment of a variety of technology platforms used for gene expression experiments.
-10X PCR Buffer w/ 15mM MgCl2 (Applied Biosystems): optimazed buffer used for PCR
- RNASin plus (Promega): RNase Inhibitor is a recombinant mammalian RNase inhibitor.
- SuperScript III (Invitrogen):
- Exonuclease I (NEB)
- 100mM dATP (Peqlab)
- RNAse H (Invitrogen)
-TdT enzyme (Roche)
- 2x Terra diret PCR Buffer (Clontech)
- Terra DNA Polymerase (Clontech): used in polymerization chain reaction.
- PCR Clean Beads (Magbio)
- 10x Transcription Reaction Buffer (Roche)
- T7 RNA Polymerase (Roche)
- 10mM NTP (Invitrogen)
- 10x First Strand Buffer (Invitrogen)
- Actinomycine D (Invitrogen)
- SuperScript II (Invitrogen)
- DNA Polymerase I (Fermentas):
- Dynabeads M280 Streptavidin (Invitrogen)
- NEBNext End Repair Buffer (NEB)
- NEBNext End Repair Enzyme Mix (NEB)

- Klenow Fragement (3'->5' Exo-) (NEB)
- T4 DNA Ligase (NEB)
- 10x T4 DNA Ligase Buffer (NEB)
- Phusion Fidelity Master Mix
- E-Gel 2% Sure Select
- Zymolyase 20T (USB): Mix of enzymes of Arthbacter luteus used to digest the cell Wall os S.cerevisiae (20U/mg)
- Zymolyase 100T (USB): Mix of enzymes of Arthbacter luteus used to digest the cell Wall os S.cerevisiae (100U/mg)
- Glufosinate: it was prepared from Basta (Bayer CropScience) and used as previously described (Nayak et al. 2006).
- Pyrithiamine 0.1 mg/mL (Sigma)
- 6 azauracil

6.3 Molecular biology methods

Oiigonucleotides

Table 9. Oligonucleotides used in this work.

Primer	**Sequence 5'→3'**	**Use**
WHI5-UP	ATA TAA TTC CTC GCG CTG CC	PCR
WHI5-LOW	CGG CGG ATA CGC AGA GAT AA	PCR
SIP4-UP	AGA AAG CTT TCT GCC TCT CC	PCR
SIP4-LOW	AGA AAC GGT GAC CAA TCC GG	PCR
RSF1-UP	ACT ATT ATC GCG TAA ACC AA	PCR
RSF1-LOW	TCT CAT CTG CGC TTT AAT TA	PCR
ERT1-UP	AAG AGC CGG TGC AAC GGC AT	PCR
ERT1-LOW	ACC AGA ATG AGC AGA CGC CT	PCR
PUF3-UP	AGA TAG GAA CAT TGA AAG GC	PCR
PUF3-LOW	ATG GAC AAG AGT AGA TAT CA	PCR
P5_dT16VN	[Btn]AATGATACGGCGACCACCGAGATCTACAC TCTTTCCCTACACGACGCTCTTCCGATCTTTTTT	3'T-fill (Reverse transcription

	TTTTTTTTTTVN	step)
P7MPX_linker_for	GTGACTGGAGTTCAGACGTGTGCTCTTCCGATC*T	3'T-fill (Ligation step)
P7MPX_linker_rev	[Phos]GATCGGAAGAGCACACGTCTGAACTCCAGTCAC[AmC7]	3'T-fill (Ligation step)
PE1.0	ATGATACGGCGACCACCGAGATCTACACTCTTTCCCTACACGACGCTCTTCCGATC*T	3'T-fill (PCR amplification step)
PE2_MPX_05	CAAGCAGAAGACGGCATACGAGATCACTGTGTGACTGGAGTTCAGACGTGTGCTCTTCCGATC*T	3'T-fill (PCR amplification step, Big1)
PE2_MPX_03	CAAGCAGAAGACGGCATACGAGATGCCTAAGTGACTGGAGTTCAGACGTGTGCTCTTCCGATC*T	3'T-fill (PCR amplification step, Big2)
PE2_MPX_04	CAAGCAGAAGACGGCATACGAGATTGGTCAGTGACTGGAGTTCAGACGTGTGCTCTTCCGATC*T	3'T-fill (PCR amplification step, Big 3)
PE2_MPX_01	CAAGCAGAAGACGGCATACGAGATCGTGATGTGACTGGAGTTCAGACGTGTGCTCTTCCGATC*T	3'T-fill (PCR amplification step, Small 2)
PE2_MPX_03	CAAGCAGAAGACGGCATACGAGATGCCTAAGTGACTGGAGTTCAGACGTGTGCTCTTCCGATC*T	3'T-fill (PCR amplification step, Small 4)
T7 promoter	AGT GAG TCG TAT TA	Subcloning
M13 Forward (-20) Primer	CTG GCC GTC GTT TTA C	Subcloning

6 nt barcodes are colored

[Btn] biotinylated nucleotide

[Phos] 5'Phosphorylation

Plasmids

The plasmid used for subcloning was the pCR 2.1-TOPO (Invitrogen)

Subcloning

The subclone was used as a final quality check before sequencing the library coming from the big and small colonies sets.
5 ul directly from the PCR (20 ng aprox) were mixed with 0.6 ul of A-tailing buffer and 0.4 ul of Klenow fragment. The mixture was incubated 30 minutes at 37ªC. Then 1 ul of topo vector plus 1 ul of salt solution was added. The sample was incubated 25 minutes at room temperature. Finally, a transformation in a max efficiency *E.coli* was carried out as described later.

Bacterial transformation

100 ul of DH5 alpha *E.coli* competent cells were mixed with 20 ng of DNA and the mixture was incubated on ice for 30 minutes. Cells were subsequently incubated at 42ºC for 45 seconds. Then, cells were incubated for 2 minutes on ice. 1 ml of LB medium was added, and cells were incubated at 37ªC for 60 minutes shaking at 225 rpm. Three dilutions of the transformation (1:100, 1:10, 1) were plated on LB+Amp medium.

Colony PCR

50 ul of water were mixed with a colony and incubate 5 minutes at 95 ºC. The PCR mix was prepared as follow: 0.75 ul of primers mix (M13 for/rev 5um), 6.2 ul of 5x Phire Buffer, 0.62 l of dNTPs 10 mM, 21.23 ul of water, 0.2 ul of Pol Phire and 1 ul of cell suspension. The reactions were incubated in a thermocycler. The program is escribed in the PCR session.

Polymerase chain reaction (PCR)

The reaction was prepared by mixing 42 ul of water, 5 ul of 10X polymerase buffer, 1ul dNTPs mix (10mM each), 1 ul primers mix (0.1 nmoles/ul each), 1ul

template DNA and 0.4 ul Expand High Fidelity polymerase or 0.7 ul Taq polumerase. The reactions were incubated in a thermocycler. The program was: 1 cycle of 2 minutes at 95ºC; 35 cycles consisting of a) 30 seconds at 95ºC, b)30 seconds at the specific annealing temperature of the primers used, c) min/kb of PCR product at 72ºC; ad 1 final cycle of 10 minutes at 72ºC.

RNA isolation

RNA was isolated following the acid phenol protocol described in (215 Tesis Gon). 10 ml of yeast culture growing exponentially was harvested by centrifugation and washed with water. Cells were resuspended in TES buffer (10 mM Tris-HCl pH 7.5; 10 mM EDTA pH 8; 0,5% SDS. An equivalent volume of acid phenol was added and samples were incubated at 65ªC for 45 minutes. Samples were mixed by vortexing every 10 minutes. Samples were then centrifuged, and the upper aqueous phase was recovered. After washing the samples with chloroform, RNA was precipitated in 2.5 volume of 96% ethanol plus 0.1 volume of · M sodium acetate pH 5.3. samples were washed with 70% ethanol, dried for 10 minutes at 65ºC and resuspended in 50 ul of double-distilled water. RNA samples were quantified using the NanoDrop spectrophotometer.

6.4 Cell cycle analysis

Cell cycle analysis by morphology under microscope

The morphology analysis of S.cerevisiae let to distinguish if cells with 1C DNA content (haploid) are in G1 phase, previous to START or if the have already passed through START and they are in a early replication phase. So if cells have iniciated the replication phase, they should present a small bud that will give rise to the daughter cell. However, if they are in a phase previous to START they appear with a round shape, without bud. When cells are in G2 phase, they present a big bud.

Cell cycle analysis by flow cytometry

For exponential cultures flow cytometry 500 µl of cells fixed using 70% ethanol were collected and centrifuged (5 minutes, 13.000 r.p.m). Cell pellet was resuspended in 1ml sodium citrate (50mM). This was centrifuged again and the pellet was resuspended in a solution of sodium citrate (50mM) and RNAse at 100 µg/µl concentration and incubated overnight at 37º. Then 500µl of a solution of sodium citrate (50mM) and propidium iodide (4 µg/ml) was added and this was incubated for 30 minutes at room temperature. 3 cycles of sonication were applied in the Ultrasonicator Biorruptor®. The flow cytometry was performed in the flow cytometer FACSCantoTM II (BD Bioscience).
For cells derived from microcapsules, the propidium iodide solution used for the staining was ten times less concentrated.

6.5 Microencapsulation and microcolony analysis

Microencapsulation of yeast

Yeast cells of a culture in YPAD at an approximate O.D600 of 0.5 were microencapsulated in calcium alginate beads (100-120 µm) in a Cellena microencapsulator device (Ingeniatrics). First, the culture (O.D600 0.5) was mixed with calcium alginate and YPAD in the following proportions: 10µl of the culture, 290 µl of YPAD and 2.7 ml of alginate 1.66% to complete a total of 3 ml. The sample was then injected with a syringe pump through a capillary feed tube inside a chamber and pressurized by a continuous air supply. The stationary jet broke up by capillary instability into homogeneous droplets, which gel in a continuously stirred 3% calcium chloride solution at room temperature. The specific encapsulationconditions are as follow: 50 mbar air pressure, 1ml/h pump pressure and continuous stirring at 400 rpm. Once completed, the capsules were collected with a sterile spoon and inoculated in 50ml of YPAD medium. They were cultured 13 hours at 30ºC and then collected again and fixated in a solution of 1:1 YPAD and 70% ethanol. The final sample was preserved at 4ºC.

Microencapsulation conditions were adjusted to obtain single-yeast capsules, which ensures that all the cells growing inside the microcapsules are clonal.

Microencapsulation of fungal spores

Fungal spores were microencapsulated in calcium alginate beads following the same protocol described previously but with several differences. Because of the mycelia size we used a nozzle that produce capsules of 400um. Microencapsulation conditions were adjusted to obtain single-spore capsules, which ensures that all the mycelia cells growing inside the microcapsules derived from one single spore and consequently, they are clonal. This procedure gave microcapsules with a regular spherical shape and homogenous size, which contained one spore inside the beads (Figure 2A). Spore suspensions were adjusted at 0,160 units at O.D. 600 nm, and 10 mL of each suspension was mixed with 290 mL of water and 2.7 mL of alginate 3%.. The capsules were stored in the same solution at 4 ºC with agitation for at least 1 hr or until they were used, then they were filtered and washed with distilled water to remove excess of calcium chloride. Then, microcapsules were inoculated with a sterile spoon into liquid media and incubated under the appropriate conditions.

Light and fluorescent microscopy

Size colonies and cell morphlogy were studied using an optical microscope Leica DM750. Images were taken using a Leica ICC50 W digital microscope camera. Microcolonies are classified according to their size in small, medium or big microcolonies. As capsule diameter is stable, microcolonies which surpass the capsule radio are considered big; those whose size ranges from half the ratio and the ratio are considered medium microcolonies. Those smaller than half the capsule ratio are considered small microcolonies.

The capsules containing fungal strains were grown in CMA or MMA liquid medium with appropriate supplements at the indicated temperature. Capsules

were examined using light or fluorescent microscopy and visualized on a Leica DMR fluorescent microscope with the appropriate filter sets and equipped with a Leica DC350F camera, or Leica DM1000 light microscope equipped with a Leica EC3 camera. Shape and homogeneity of the capsules and results after sorting were analyzed in a Leica M125 stereo microscope equipped with a Leica DFC450C camera.

Confocal microscopy

Capsules and cells stained with calcofluor were visualized in an A1R Confocal Nikon Microscope. Cells and bud scars images were acquired using DAPI filter and 60x objective. Each acquisition was taken every 0.5µm in Z axis.

Calcofluor staining of yeast culture

1mL of an exponential culture is centrifuged (5 minutes at 6000 r.p.m). The pellet is resuspended in 0.5 mL of calcofluor (0.1 µg/ µl in PBS) (Sigma-Aldrich) for 5 minutes at room temperature. This is washed 2-3 times with 1mL PBS (centrifugations at 6000 r.p.m for 5 minutes) and finally resuspended in 100 µL of PBS.

Calcofluor staining of capsules

Fixated beads (in 15ml YPAD + 15 mL 70% ethanol) are filtrated and collected. They are washed with a trisHCl-CaCl2 solution (2:1) to avoid the capsule breaking. Beads are then inoculated in 0.5 mL of calcofluor at 0.1 µg/ µl concentration for 5 minutes at room temperature. The beads are filtrated and collected again and are washed with trisHCl-CaCl2 solution 2-3 times. Finally they were collected and preserved 0.5-1mL of the same solution.

Capsule disgregation

Fixated beads (in 15ml YPAD + 15 mL 70% ethanol) are centrifuged for 15 minutes at 4000 r.p.m. The pellet is resuspended in 10mL of sodium citrate 10% for 5 minutes at room temperature and then washed with sterile water. Cells can be preserved at -20ºC.

Ratios of bud scars in microcolonies and founding cell age estimation

In order to count the number of bud scars in cells, images acquired in confocal microscope were used. As calcofluor stains bud scars in yeast cells, we were able to count the number of bud scars per cell in small colonies and in yeast cultures.

First the ratios of bud scars between small colonies and a common culture of the same strain in exponential phase was calculated. In order to do this, images of 50 small colonies and of an exponential culture of a wild type yeast (360 cells in total) stained with calcofluor were acquired in the Confocal Nikon Microscope. For the small colonies, the number of bud scars of each cell in each colony was counted. The same was performed for the exponential culture. The total number of cells with a certain number of bud scars was the calculated for both groups and then compared. A chi-squared test was performed to validate the results.

To estimate the age of the founding cell in small colonies, the founding cell must be identified, which is the cell with the highest number of bud scars. Then, the total number of cells in the colony is manually counted and, considering this, the theoretical number of bud scars of the founding cells is defined following this premise: a founding cell with “x” bud scars may form a 2^x cells per colony.

This theoretical number is subtracted from the observed number of bud scars of the founding cell to obtain its age at the moment it was encapsulated and started forming the colony.

Large-particle flow cytometry

Yeast

Microencapsulated colonies was analysed in a BioSorter flow cytometer (Union Biometrica). Relative microcolony size was monitored by measuring the axial length of the object (TOF, time of flight), the optical density of the detected object (EXT,optical extinction) and fluorescence under the following photomultiplier tube settings: green (1100), yellow (600), and red (1100). The time of flight was fixed at a minimum of 40, and the extinction signal was 1.0. Sample cup pressure was adjusted to 0.30-0.35 psi to maintain a frequency of 5-15 events per second and diverter pressure was 7.00 psi. For the sorting assay, the optimal parameters were fixed to perform the selection of the population of interest as required. After sorting, the particles were collected in Petri dishes and analysed by visualization under light microscopy to check the size.

Filamentous fungi

Microencapsulated fungal spores were grown in the indicated media. After we confirmed hyphal growth by light microscopy, the population of microencapsulated colonies was analyzed in a Complex Object Parametric Analyzer and Sorter (COPAS) SELECT Flow cytometer (Union Biometrica) (Figure 1C). Relative microcolony size was monitored by measuring the axial length of the object (time of flight), the optical density of the detected object (optical extinction) and fluorescence under the following photomultiplier tube settings: green (1100), yellow (600), and red (1100). The time of flight mínimum was fixed at 150, and the extinction signal was 3.1. Sheath fluid pressure was adjusted to 4.40–5.20, whereas sample fluid pressure was set to maintain a frequency of 15–25 events per second.

For the sorting assay, the optimal parameters were fixed to perform the selection of the population of interest as required. After sorting, the particles were collected in Petri dishes and analyzed by visualization under stereo and fluorescent microscopy. To recover the encapsulated strains, particles were

plated on complete solid media and incubated at 30_ (permissive temperature) for 324 d.

6.6 Transcriptomic analysis of microcolonies

The total RNA extracted from the sorted microcolonies and from the non-sorted controls, following the method previously descriibed, was sequenced following the 3'T-fill protocol as previously described (Wilkening, Pelechano et al. 2013). The starting material used was 500–3000 ng of total RNA.

- This protocol has been designed to process multiple samples simultaneously. It is advisable to use 0.2mL PCR-strips or 96-well plates for library preparation in combination with multichannel pipettes.
- A thermocycler with a heated lid is used for all incubations above room temperature.
- Throughout the protocol, different volume to sample ratios of Agencourt AMPure XP beads (Beckman Coulter Genomics) are used. The different ratios between bead solution and sample alters the final polyethylene glycol (PEG) concentration (present in the bead buffer), resulting in a size-specific capture. In general, lower amounts of bead solution will capture longer DNA molecules (Lundin et al., 2010). Follow the manufactures protocol (http://www.beckmangenomics.com/products/dna_purification_and_cleanup/agencourt_ampure_xp.html).

To obtain the final DNA library, subsequent steps are required.

Fragment Total RNA

As this protocol is designed to sequence the terminal fragments of the RNA molecules, the first step involves the fragmentation of the total RNA, from which the 3' terminal mRNA fragments are selected at later steps.

1. Mix 10µg of DNA-free total RNA with 4µL of 5X RNA fragmentation buffer (200mM Tris-acetate, pH 8.1, 500mM KOAc, 150mM MgOAc) in 0.2mL PCR strips or a 96-well plate. Optionally, add 4µL Spike-in IVT stock solution for quality control (see below).
2. Adjust the total volume to 20µL with RNase-free water and incubate the sample at 80ºC for 5 min.
3. Transfer the sample to ice immediately and proceed to the purification step.
4. Cleanup with 1.5X Ampure XP beads (add 30uL to the 20 µL fragmented RNA), elute in 12.8 ul EB (10 mM Tris-HCl, pH 8). See manufacturer protocol.

Reverse transcription

The first step of the library preparation protocol consists of synthesizing biotinylated cDNA molecules by priming the poly(A) tail with a sequencing-compatible oligo dT primer (compatible with the PE 1.0, Illumina).

1. Mix 11.2µL of the fragmented RNA with 1µL biotinylated oligo dT primer (P5_dT16VN (1 µM) = 2.5 pmol) and 1µL 10mM dNTP Mix. If less starting material is used, the amount of oligo dT primer should be adjusted accordingly.
2. Incubate the sample for 5 min at 65ºC to disrupt secondary structures and place on ice.
3. Add 4µL 5X First Strand Buffer (Invitrogen), 2µL DTT (0.1M), 0.32µL Actinomycin D (1.25 mg/mL) and 0.5µL RNasin Plus (Promega) to each

sample.

4. Mix each tube and put in a thermocycler at 42ºC.
5. After 2 min, add 0.5µL Superscript II (200U/µL, Invitrogen) to each tube. It is critical to do so at 42ºC to prevent mispriming of the anchored oligo(dT) primer.
6. Incubate the samples at 42ºC for 50 min, and then inactivate the enzyme by incubating the samples at 72ºC for 15 min.
7. Cleanup with 1.5X Ampure XP beads and elute in 40 ul EB (10 mM Tris-HCl, pH 8). This will clean the excess of unused biotinilated oligo.

Second strand synthesis

To generate the second strand of cDNA, we use RNase H, which nicks the RNA in the cDNA/RNA hybrid, and DNA polymerase I, which produces the second strand of the cDNA by nick translation.

1. Mix 40µL cDNA from the previous step with 5µL 10X DNA polymerase I buffer (Fermentas) and 2.5µL dNTPs (10mM) on ice.
2. Add 0.5µL RNaseH (5U/µL, NEB) and 2µL DNA polymerase I (10U/µL, Fermentas).
3. Incubate the tubes at 16ºC for 2.5 hours.
4. Cleanup with 0.9X Ampure XP beads and elute in 20 ul EB. This will remove the enzymes and the short DNA fragments.

Capture of the 3' terminal cDNA fragments

Once the cDNA fragments have been produced, it is necessary to select those molecules that contain the biotinylated sequencing primer at their 3' ends. This is accomplished by using magnetic beads coated with streptavidin. It is important to remember that from this step until the enrichment PCR, the sample is bound to the magnetic beads, unlike in the Ampure bead purification where the sample is in the supernatant.

Prepare streptoavidin beads

First, it is necessary to prepare the magnetic beads according to the manufacturer's instructions.

1. Use 20µL Dynabeads M-280 Streptavidin (Invitrogen) for each sample (good for binding 4pmol of biotinylated oligo(dT)).
2. Transfer the tubes to a magnetic stand and remove the supernatant.
3. Take the tubes from the magnetic stand and resuspend the beads in 200µL 1X bind and wash buffer (1X B&W buffer, containing 5mM Tris-HCl pH=7.5, 0.5mM EDTA and 1M NaCl).
4. Transfer the tubes to a magnetic stand and remove the supernatant.
5. Repeat the wash with 200µL 1X B&W buffer.
6. Transfer the tubes to a magnetic stand and remove the supernatant.
7. Resuspend the beads in 20µL 2X B&W-buffer (10mM Tris-HCl pH=7.5, 1mM EDTA and 2M NaCl) and keep them ready for the next step.

Note: 1X B&W buffer (5mM Tris-HCl pH=7.5, 0,5 mM EDTA and 1 M NaCl). Prepare a 2x stock and autoclave it.

Capture sample

Once the beads are ready, we use them to capture the biotinylated double-stranded cDNA.

1. Add 20µl of cDNA to the prepared beads. Mix and put on a rotator wheel at RT for 15 min to allow the capture of the ds-cDNA.
2. Using a magnet stand, wash 2 times with 200µl 1x-B&W-buffer and 1 time with 200µl EB.
3. Resuspend in 21 ul EB

End repair

Once the 3' terminal cDNA molecules have been captured, it is necessary to add a common sequencing adapter to the unbiotinylated end. For this, we follow the same procedure used in standard library constructions by Illumina, while making use of the fact that our samples are bound to the magnetic beads. The first step of this process is to produce blunt end molecules.

1. Mix the sample containing Dynabeads from the previous step with 2.5µL 10X End repair buffer and 1.25 End repair enzyme mix (NEBNext DNA Sample Prep Master Mix Set 1, NEB).
2. Incubate the tubes for 30 min at 20ºC.
3. Wash the beads twice with 200 µL 1X B&W buffer, once with 200 µL EB and resuspended in 21µL EB.

A - tailing

In order to produce common sticky ends for the ligation of the sequencing adapter, it is necessary to introduce a common 3' adenine overhang.

1. Mix the sample containing Dynabeads from the previous step with 2.5µL of dA tailing buffer (10X NEBuffer 2 from NEB, supplemented with 0.2mM dATP) and 1.5µL Klenow Fragment (3´→5´ exo–) (5U/µL, NEB).
2. Incubate the tubes for 30 min at 37ºC.
3. Transfer the tubes to a magnetic stand. Wash the beads twice with 200 µL 1X B&W buffer, once with 200 µL EB and resuspended in 8µL EB.

Ligation

The 3' A-overhang produced in the previous step is now used to ligate the sequencing adapter (compatible with the PE 2.0 from Illumina) having a 3' T-overhang. It was used a common P7se adapter and add the indexing at the PCR step. In that way we can use a dedicated read for the multiplexing and do not need to go or paired end.

1. Thaw the P7MPX_linker annealed adapter (2.5 µM) on ice.
2. Mix the sample containing Dynabeads from the previous step with 12.5µL 2X Quick Ligation buffer (NEB), 2µL P7MPX_linker double-stranded linker (2.5µM) and 2.5µL T4 DNA ligase (2000U/µL, NEB). If less than 10µg of starting material is used, the adapter concentration should be adapted accordingly to avoid adapter self-ligation.
3. Incubate the samples for 15 to 30 min at 20ºC. *Is using a normal ligase incubate 1-3h at 16ºC.*
4. Transfer the tubes to a magnetic stand and remove the supernatant.
5. Wash 4 times with 200 µL 1X B&W buffer and once with 200 µL EB. Resuspended in 50µL EB.

Enrichement PCR

To enrich for molecules that contain the correct combination of sequencing adapters and to obtain fragments that are not bound to beads, the samples are amplified by PCR.

1. Since an excess of input DNA inhibits PCR amplification, we use only part of the beads (usually ½) for the PCR amplification. The optimal proportion and cycle number should be tested for each setup individually.
2. Mix 24µL beads with DNA with 25µL 2X Phusion Master Mix with HF buffer (Finnzymes) and 0.5µL each of oligo PE1.0 and PE2_MPX (10µM, Illumina). Use a different PE2_MPX for each simple if we want to multiplex.
3. Incubate the sample in a thermocycler with the following program: 30 seconds at 98ºC, 18 cycles (10 seconds at 98ºC, 10 seconds at 65ºC and 10 seconds at 72ºC) and a final extension of 5 min at 72ºC.
4. Transfer the PCR product to a magnetic stand and recover the 50µL supernatant containing the PCR product.
5. The beads used for the PCR should be kept at 4ºC in case a re-amplification is needed.

6. Purify the eluted PCR product with 1.8X Ampure XP beads, elute in 10 ul EB. Concentration measured by Qubit (total of ≥ 150ng)

After that, the samples are analysed by Bioanalyzer following the manufacturer protoclo (buscar), to ensure the correct DNA fragmentation and library formation.

Size selection

We do not need a stringent size selection, but a homogeneous population will increase the number of reads.

It is possible to select for a certain bp range using Ampure XP beads. Adding for example 0.6x the volume catches sizes >500bp. The supernatant of this selection can then be used to add another 0.2x of beads for a final 0.8x selection. This should result in a ~200-500bp range.

- add to your sample 0.6x the volume of beads (e.g. 100µl sample + 60µl beads)
- pipet-mix 15 times, let stand 5min
- put on magnet stand, let stand 2min
- transfer supernatant to a new tube with 0.2x beads (e.g. 160µl supernatant + 20µl beads) (Note that the sample was in the supernatant!!)
- pipet-mix 15 times, let stand 5min
- put on magnet stand, let stand 2min
- take off supernatant (Note that the sample is now on the beads!!)
- add 200µl of 70% ethanol, take of supernatant
- add 200µl of 70% ethanol, take of supernatant
- shortly centrifuge down remaining ethanol and put on magnetic stand again
- pipet off remaining ethanol
- air dry 2-10min

- add desired amount of Elution buffer or water
- pipet-mix 15 times, let stand 2min
- put on magnet stand, let stand 1min
- transfer supernatant to new tube

Alternatively use E-Gel 2% SizeSelect (invitrogen), or a classical gel size selection

Confirm the sample in a 2% agarose gel after 40 cycle PCR or using a Agilent Bioanalyzer. Primer dimer (100-120 bp should not be pressent). Library size around 250-350 bp is optimal.

For the first time the method it is performed, cloning of the library and Sanger sequencing of some clones is recommended to confirm the correct construction of the library.

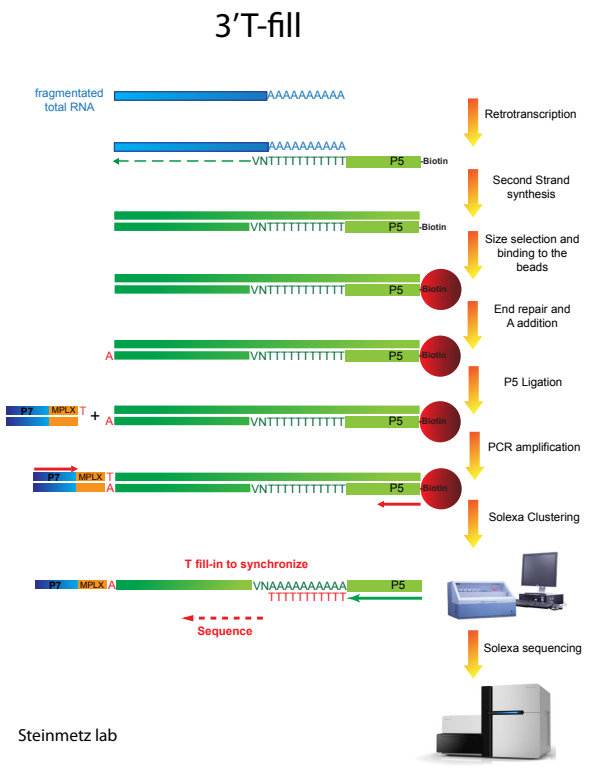

Figure 33. Overview of 3' T-fill amplification protocol.

RNA seq data analysis

The raw next generation sequencing reads to be first assessed for their quality with the FASTQC tool kit Bad quality reads (phred score < 20) were trimmed. The genome sequence of *S. cerevisiae* S288c (version R64) and its annotations were retrieved from SGD (Saccharomyces Genome Database, http://yeastgenome.org/) and used for all the analyses. Raw reads were aligned against the reference genome using BWA/ Bowtie2. We quantified the gene expression from the mapped reads using the HTSeq-count package (Anders, Pyl et al. 2015) in order to obtain counts of mapped reads per gene (in the 'intersection nonempty' mode). As the count process was dependent on sequencing depth, those samples with a small number of reads were removed, whereas those samples with a huge number of reads were down-sampled using the FastqSampler utility from the Shortread package (Morgan, Anders et al. 2009). The statistical environment R (version 3.1; (R Development Core Team (2015)), was used to performthe statistical analysis. Hierarchical clustering, boxplots, andMultidimensional Scaling (MDS) analyses were performed before and after normalization to measure the differences among samples. The edgeR package from R/ BioConductor (Robinson, McCarthy et al. 2010) was used to normalize and fit count data for the differential gene expression analysis. In order to avoid a bias in poorly expressed genes, those genes with less than five mapped reads per million in at least two samples were removed. An isoform-specific analysis was performed and an assignment was made to transcripts using GSNAP (version 2012–01–11) as previously described (Wilkening, Pelechano et al. 2013).

7. Bibliography

- Acar, M., J. T. Mettetal, et al. (2008). "Stochastic switching as a survival strategy in fluctuating environments." Nat Genet 40(4): 471-475.
- Airoldi, E. M., C. Huttenhower, et al. (2009). "Predicting cellular growth from gene expression signatures." PLoS Comput Biol 5(1): e1000257.
- Aldridge, B. B., M. Fernandez-Suarez, et al. (2012). "Asymmetry and aging of mycobacterial cells lead to variable growth and antibiotic susceptibility." Science 335(6064): 100-104.
- Altschuler, S. J. and L. F. Wu (2010). "Cellular heterogeneity: do differences make a difference?" Cell 141(4): 559-563.
- Anders, S., P. T. Pyl, et al. (2015). "HTSeq--a Python framework to work with high-throughput sequencing data." Bioinformatics 31(2): 166-169.
- Anderson, J. S. J. and R. Parker (1998). "The 3,Ä≤ to 5,Ä≤ degradation of yeast mRNAs is a general mechanism for mRNA turnover that requires the SKI2 DEVH box protein and 3,Ä≤ to 5,Ä≤ exonucleases of the exosome complex." The EMBO Journal 17(5): 1497-1506.
- Arkin, A., J. Ross, et al. (1998). "Stochastic kinetic analysis of developmental pathway bifurcation in phage lambda-infected Escherichia coli cells." Genetics 149(4): 1633-1648.
- Austin, D. W., M. S. Allen, et al. (2006). "Gene network shaping of inherent noise spectra." Nature 439(7076): 608-611.
- Avery, S. V. (2006). "Microbial cell individuality and the underlying sources of heterogeneity." Nat Rev Micro 4(8): 577-587.
- Balaban, N. Q., K. Gerdes, et al. (2013). "A problem of persistence: still more questions than answers?" Nat Rev Microbiol 11(8): 587-591.
- Balaban, N. Q., J. Merrin, et al. (2004). "Bacterial persistence as a phenotypic switch." Science 305(5690): 1622-1625.

- Beadle, G. W. and E. L. Tatum (1941). "Genetic Control of Biochemical Reactions in Neurospora." Proc Natl Acad Sci U S A 27(11): 499-506.
- Bertoli, C., J. M. Skotheim, et al. (2013). "Control of cell cycle transcription during G1 and S phases." Nat Rev Mol Cell Biol 14(8): 518-528.
- Bienaime, C., J. N. Barbotin, et al. (2003). "How to build an adapted and bioactive cell microenvironment? A chemical interaction study of the structure of Ca-alginate matrices and their repercussion on confined cells." J Biomed Mater Res A 67(2): 376-388.
- Boulineau, S., F. Tostevin, et al. (2013). "Single-cell dynamics reveals sustained growth during diauxic shifts." PLoS One 8(4): e61686.
- Brakhage, A. A. (2013). "Regulation of fungal secondary metabolism." Nat Rev Microbiol 11(1): 21-32.
- Brauer, M. J., C. Huttenhower, et al. (2008). "Coordination of growth rate, cell cycle, stress response, and metabolic activity in yeast." Mol Biol Cell 19(1): 352-367.
- Caballero-Córdoba, G. M. and V. C. Sgarbieri (2000). "Nutritional and toxicological evaluation of yeast (Saccharomyces cerevisiae) biomass and a yeast protein concentrate." Journal of the Science of Food and Agriculture 80(3): 341-351.
- Chang, H. H., M. Hemberg, et al. (2008). "Transcriptome-wide noise controls lineage choice in mammalian progenitor cells." Nature 453(7194): 544-547.
- Chavez, S., J. Garcia-Martinez, et al. (2016). "The importance of controlling mRNA turnover during cell proliferation." Curr Genet.
- Cogoni, C. and G. Macino (1999). "Gene silencing in Neurospora crassa requires a protein homologous to RNA-dependent RNA polymerase." Nature 399(6732): 166-169.
- Cohen, A. A., N. Geva-Zatorsky, et al. (2008). "Dynamic proteomics of -individual cancer cells in response to a drug." Science 322(5907): 1511-1516.
- Colman-Lerner, A., A. Gordon, et al. (2005). "Regulated cell-to-cell variation in a cell-fate decision system." Nature 437(7059): 699-706.
- Condit, C. M. (2002). "The Misunderstood Gene." Heredity 88(4): 330-330.
- Costanzo, M., J. L. Nishikawa, et al. (2004). "CDK activity antagonizes Whi5, an inhibitor of G1/S transcription in yeast." Cell 117(7): 899-913.

- Cross, F. R., M. Hoek, et al. (1994). "Role of Swi4 in cell cycle regulation of CLN2 expression." Mol Cell Biol 14(7): 4779-4787.
- Davey, H. M. and M. K. Winson (2003). "Using flow cytometry to quantify microbial heterogeneity." Curr Issues Mol Biol 5(1): 9-15.
- de Bekker, C., G. J. van Veluw, et al. (2011). "Heterogeneity of Aspergillus niger microcolonies in liquid shaken cultures." Appl Environ Microbiol 77(4): 1263-1267.
- de Bruin, R. A., W. H. McDonald, et al. (2004). "Cln3 activates G1-specific transcription via phosphorylation of the SBF bound repressor Whi5." Cell 117(7): 887-898.
- de la Cruz, A. F. and B. A. Edgar (2008). "Flow cytometric analysis of Drosophila cells." Methods Mol Biol 420: 373-389.
- Decker, C. J. and R. Parker (1993). "A turnover pathway for both stable and unstable mRNAs in yeast: evidence for a requirement for deadenylation." Genes Dev 7(8): 1632-1643.
- Delbruck, M. (1940). "Statistical Fluctuations in Autocatalytic Reactions." The Journal of Chemical Physics 8(1): 120-124.
- Delbruck, M. (1945). "The Burst Size Distribution in the Growth of Bacterial Viruses (Bacteriophages)." Journal of Bacteriology 50(2): 131-135.
- Derrigo, M., A. Cestelli, et al. (2000). "RNA-protein interactions in the control of stability and localization of messenger RNA (review)." Int J Mol Med 5(2): 111-123.
- Dirick, L., T. Bohm, et al. (1995). "Roles and regulation of Cln-Cdc28 kinases at the start of the cell cycle of Saccharomyces cerevisiae." EMBO J 14(19): 4803-4813.
- Eagle, H. and E. M. Levine (1967). "Growth Regulatory Effects of Cellular Interaction." Nature 213(5081): 1102-1106.
- Eldar, A. and M. B. Elowitz (2010). "Functional roles for noise in genetic circuits." Nature 467(7312): 167-173.
- Elowitz, M. B., A. J. Levine, et al. (2002). "Stochastic gene expression in a single cell." Science 297(5584): 1183-1186.
- Elsasser, W. M. (1984). "Outline of a theory of cellular heterogeneity." Proc Natl Acad Sci U S A 81(16): 5126-5129.

- Enver, T., M. Pera, et al. (2009). "Stem cell states, fates, and the rules of attraction." Cell Stem Cell 4(5): 387-397.
- Eser, P., C. Demel, et al. (2014). "Periodic mRNA synthesis and degradation co-operate during cell cycle gene expression." Mol Syst Biol 10: 717.
- Fernandez, L. A., E. W. Hatch, et al. (2005). "Validation of large particle flow cytometry for the analysis and sorting of intact pancreatic islets." Transplantation 80(6): 729-737.
- Ferrezuelo, F., N. Colomina, et al. (2010). "The transcriptional network activated by Cln3 cyclin at the G1-to-S transition of the yeast cell cycle." Genome Biol 11(6): R67.
- Flick, K., D. Chapman-Shimshoni, et al. (1998). "Regulation of cell size by glucose is exerted via repression of the CLN1 promoter." Mol Cell Biol 18(5): 2492-2501.
- Furusawa, C. and K. Kaneko (2008). "A generic mechanism for adaptive growth rate regulation." PLoS Comput Biol 4(1): e3.
- Gaillard, H., T. Garcia-Muse, et al. (2015). "Replication stress and cancer." Nat Rev Cancer 15(5): 276-289.
- Gañan-Calvo, A. M. (2004). "Perfectly monodisperse microbubbling by capillary flow focusing: an alternate physical description and universal scaling." Phys Rev E Stat Nonlin Soft Matter Phys 69(2 Pt 2): 027301.
- Gañan-Calvo, A. M. (1998). "Generation of Steady Liquid Microthreads and Micron-Sized Monodisperse Sprays in Gas Streams." Physical Review Letters 80(2): 285-288.
- Garcia-Martinez, J., L. Delgado-Ramos, et al. (2016). "The cellular growth rate controls overall mRNA turnover, and modulates either transcription or degradation rates of particular gene regulons." Nucleic Acids Res 44(8): 3643-3658.
- Gascoigne, K. E. and S. S. Taylor (2008). "Cancer Cells Display Profound Intra- and Interline Variation following Prolonged Exposure to Antimitotic Drugs." Cancer Cell 14(2): 111-122.
- Gomez-Herreros, F., L. de Miguel-Jimenez, et al. (2012). "TFIIS is required for the balanced expression of the genes encoding ribosomal components under transcriptional stress." Nucleic Acids Res 40(14): 6508-6519.

- Gupta, I., S. Clauder,ÄêM√ºnster, et al. (2014). "Alternative polyadenylation diversifies post,Äêtranscriptional regulation by selective RNA,Äìprotein interactions." Molecular Systems Biology 10(2): 719.
- Harris, S. D., J. L. Morrell, et al. (1994). "Identification and characterization of Aspergillus nidulans mutants defective in cytokinesis." Genetics 136(2): 517-532.
- Hartwell, L. H. (1974). "Saccharomyces cerevisiae cell cycle." Bacteriological Reviews 38(2): 164-198.
- Hartwell, L. H., J. Culotti, et al. (1970). "Genetic control of the cell-division cycle in yeast. I. Detection of mutants." Proc Natl Acad Sci U S A 66(2): 352-359.
- Heinemann, M., H. Meinberg, et al. (2005). "Method for quantitative determination of spatial polymer distribution in alginate beads using Raman spectroscopy." Appl Spectrosc 59(3): 280-285.
- Herskowitz, I. and D. Hagen (1980). "The lysis-lysogeny decision of phage lambda: explicit programming and responsiveness." Annu Rev Genet 14: 399-445.
- Holliday, R. (1964). "A mechanism for gene conversion in fungi." Genetics Research 5(02): 282-304.
- Hsu, C. L. and A. Stevens (1993). "Yeast cells lacking 5'-->3' exoribonuclease 1 contain mRNA species that are poly(A) deficient and partially lack the 5' cap structure." Mol Cell Biol 13(8): 4826-4835.
- Huang, S. (2009). "Non-genetic heterogeneity of cells in development: more than just noise." Development (Cambridge, England) 136(23): 3853-3862.
- Ibrahim, S. F. and G. van den Engh (2003). "High-speed cell sorting: fundamentals and recent advances." Curr Opin Biotechnol 14(1): 5-12.
- Inglese, J., R. L. Johnson, et al. (2007). "High-throughput screening assays for the identification of chemical probes." Nat Chem Biol 3(8): 466-479.
- Janssens, G. E., A. C. Meinema, et al. (2015). "Protein biogenesis machinery is a driver of replicative aging in yeast." Elife 4: e08527.
- Jazwinski, S. M. (1990). "Aging and senescence of the budding yeast Saccharomyces cerevisiae." Mol Microbiol 4(3): 337-343.

- Jo, M. C., W. Liu, et al. (2015). "High-throughput analysis of yeast replicative aging using a microfluidic system." Proc Natl Acad Sci U S A 112(30): 9364-9369.
- Johnston, G. C., J. R. Pringle, et al. (1977). "Coordination of growth with cell division in the yeast Saccharomyces cerevisiae." Exp Cell Res 105(1): 79-98.
- Jorgensen, P., J. L. Nishikawa, et al. (2002). "Systematic identification of pathways that couple cell growth and division in yeast." Science 297(5580): 395-400.
- Kailasapathy, K. (2002). "Microencapsulation of probiotic bacteria: technology and potential applications." Curr Issues Intest Microbiol 3(2): 39-48.
- Knuf, C. and J. Nielsen (2012). "Aspergilli: systems biology and industrial applications." Biotechnol J 7(9): 1147-1155.
- Kouzarides, T. (2007). "Chromatin modifications and their function." Cell 128(4): 693-705.
- Lee, C.-D. and B. P. Tu (2015). "Glucose-Regulated Phosphorylation of the PUF Protein Puf3 Regulates the Translational Fate of Its Bound mRNAs and Association with RNA Granules." Cell reports 11(10): 1638-1650.
- Lee, S. S., I. Avalos Vizcarra, et al. (2012). "Whole lifespan microscopic observation of budding yeast aging through a microfluidic dissection platform." Proc Natl Acad Sci U S A 109(13): 4916-4920.
- Lindstrom, D. L. and D. E. Gottschling (2009). "The mother enrichment program: a genetic system for facile replicative life span analysis in Saccharomyces cerevisiae." Genetics 183(2): 413-422, 411SI-413SI.
- Lipinski, K. A., L. J. Barber, et al. (2016). "Cancer Evolution and the Limits of Predictability in Precision Cancer Medicine." Trends Cancer 2(1): 49-63.
- Loewer, A. and G. Lahav (2011). "We're all individuals: causes and consequences of non-genetic heterogeneity in mammalian cells." Current opinion in genetics & development 21(6): 753-758.
- Longo, V. D., G. S. Shadel, et al. (2012). "Replicative and chronological aging in Saccharomyces cerevisiae." Cell Metab 16(1): 18-31.
- Mager, W. H. and R. J. Planta (1991). "Coordinate expression of ribosomal protein genes in yeast as a function of cellular growth rate." Mol Cell Biochem 104(1-2): 181-187.

- Martin-Banderas, L., M. Flores-Mosquera, et al. (2005). "Flow Focusing: a versatile technology to produce size-controlled and specific-morphology microparticles." Small 1(7): 688-692.
- Maruyama, R., E. Grevengoed, et al. (2011). "Genome-wide analysis reveals a major role in cell fate maintenance and an unexpected role in endoreduplication for the Drosophila FoxA gene Fork head." PLoS One 6(6): e20901.
- May, G. S. and T. H. Adams (1997). "The importance of fungi to man." Genome Res 7(11): 1041-1044.
- McAdams, H. H. and A. Arkin (1997). "Stochastic mechanisms in gene expression." Proc Natl Acad Sci U S A 94(3): 814-819.
- Miller, M. A. and W. M. Olivas (2011). "Roles of Puf proteins in mRNA degradation and translation." Wiley Interdiscip Rev RNA 2(4): 471-492.
- Miller, M. A., J. Russo, et al. (2014). "Carbon source-dependent alteration of Puf3p activity mediates rapid changes in the stabilities of mRNAs involved in mitochondrial function." Nucleic Acids Research 42(6): 3954-3970.
- Molenaar, D., R. van Berlo, et al. (2009). "Shifts in growth strategies reflect tradeoffs in cellular economics." Mol Syst Biol 5: 323.
- Morgan, M., S. Anders, et al. (2009). "ShortRead: a bioconductor package for input, quality assessment and exploration of high-throughput sequence data." Bioinformatics 25(19): 2607-2608.
- Morris, N. R. (1975). "Mitotic mutants of Aspergillus nidulans." Genet Res 26(3): 237-254.
- Mortimer, R. K. and J. R. Johnston (1959). "Life Span of Individual Yeast Cells." Nature 183(4677): 1751-1752.
- Muhlrad, D., C. J. Decker, et al. (1994). "Deadenylation of the unstable mRNA encoded by the yeast MFA2 gene leads to decapping followed by 5'-->3' digestion of the transcript." Genes Dev 8(7): 855-866.
- Muhlrad, D., C. J. Decker, et al. (1995). "Turnover mechanisms of the stable yeast PGK1 mRNA." Mol Cell Biol 15(4): 2145-2156.
- Newman, J. R., S. Ghaemmaghami, et al. (2006). "Single-cell proteomic analysis of S. cerevisiae reveals the architecture of biological noise." Nature 441(7095): 840-846.

- Nir, R., R. Lamed, et al. (1990). "Single-cell entrapment and microcolony development within uniform microspheres amenable to flow cytometry." Appl Environ Microbiol 56(9): 2870-2875.
- Novick, A. and M. Weiner (1957). "ENZYME INDUCTION AS AN ALL-OR-NONE PHENOMENON." Proceedings of the National Academy of Sciences of the United States of America 43(7): 553-566.
- Nurse, P. (1975). "Genetic control of cell size at cell division in yeast." Nature 256(5518): 547-551.
- O'Duibhir, E., P. Lijnzaad, et al. (2014). "Cell cycle population effects in perturbation studies." Mol Syst Biol 10: 732.
- Olivas, W. and R. Parker (2000). "The Puf3 protein is a transcript-specific regulator of mRNA degradation in yeast." EMBO J 19(23): 6602-6611.
- Orive, G. and J. L. Pedraz (2010). "Highlights and trends in cell encapsulation." Adv Exp Med Biol 670: 1-4.
- Overton, K. W., S. L. Spencer, et al. (2014). "Basal p21 controls population heterogeneity in cycling and quiescent cell cycle states." Proc Natl Acad Sci U S A 111(41): E4386-4393.
- Ozcengiz, G. and A. L. Demain (2013). "Recent advances in the biosynthesis of penicillins, cephalosporins and clavams and its regulation." Biotechnol Adv 31(2): 287-311.
- Pardee, A. B. (1974). "A Restriction Point for Control of Normal Animal Cell Proliferation." Proceedings of the National Academy of Sciences of the United States of America 71(4): 1286-1290.
- Parker, R. (2012). "RNA degradation in Saccharomyces cerevisae." Genetics 191(3): 671-702.
- Passos, J. F., G. Saretzki, et al. (2007). "Mitochondrial dysfunction accounts for the stochastic heterogeneity in telomere-dependent senescence." PLoS Biol 5(5): e110.
- Paulsson, J. (2004). "Summing up the noise in gene networks." Nature 427(6973): 415-418.
- Pelkmans, L. (2012). "Cell Biology. Using cell-to-cell variability--a new era in molecular biology." Science 336(6080): 425-426.
- Pereira, D. A. and J. A. Williams (2007). "Origin and evolution of high throughput screening." Br J Pharmacol 152(1): 53-61.

- Perez-Ortin, J. E., P. Alepuz, et al. (2013). "Eukaryotic mRNA decay: methodologies, pathways, and links to other stages of gene expression." J Mol Biol 425(20): 3750-3775.
- Perez-Ortin, J. E., L. de Miguel-Jimenez, et al. (2012). "Genome-wide studies of mRNA synthesis and degradation in eukaryotes." Biochim Biophys Acta 1819(6): 604-615.
- Pramila, T., W. Wu, et al. (2006). "The Forkhead transcription factor Hcm1 regulates chromosome segregation genes and fills the S-phase gap in the transcriptional circuitry of the cell cycle." Genes Dev 20(16): 2266-2278.
- Quenault, T., T. Lithgow, et al. (2011). "PUF proteins: repression, activation and mRNA localization." Trends in Cell Biology 21(2): 104-112.
- R Development Core Team (2015) R: A Language and Environment for Statistical Computing Vienna, Austria. The R Foundation for Statistical Computing, http://www.R-project.org/.
- Rabanel, J.-M., N. Bertrand, et al. (2006). Polysaccharide Hydrogels for the Preparation of Immunoisolated Cell Delivery Systems. Polysaccharides for Drug Delivery and Pharmaceutical Applications, American Chemical Society. 934: 305-339.
- Raj, A. and A. van Oudenaarden (2008). "Nature, nurture, or chance: stochastic gene expression and its consequences." Cell 135(2): 216-226.
- Ricicova, M., M. Hamidi, et al. (2013). "Dissecting genealogy and cell cycle as sources of cell-to-cell variability in MAPK signaling using high-throughput lineage tracking." Proceedings of the National Academy of Sciences of the United States of America 110(28): 11403-11408.
- Rinott, R., A. Jaimovich, et al. (2011). "Exploring transcription regulation through cell-to-cell variability." Proc Natl Acad Sci U S A 108(15): 6329-6334.
- Robert, L., G. Paul, et al. (2010). "Pre-dispositions and epigenetic inheritance in the Escherichia coli lactose operon bistable switch." Mol Syst Biol 6: 357.
- Robinson, M. D., D. J. McCarthy, et al. (2010). "edgeR: a Bioconductor package for differential expression analysis of digital gene expression data." Bioinformatics 26(1): 139-140.
- Rosenblatt, J. I., J. A. Hokanson, et al. (1997). "Theoretical basis for sampling statistics useful for detecting and isolating rare cells using flow cytometry and cell sorting." Cytometry 27(3): 233-238.

- Rubin, H. (1990). "The significance of biological heterogeneity." Cancer Metastasis Rev 9(1): 1-20.
- Saint-Georges, Y., M. Garcia, et al. (2008). "Yeast Mitochondrial Biogenesis: A Role for the PUF RNA-Binding Protein Puf3p in mRNA Localization." PLoS One 3(6): e2293.
- Sanchez-Romero, M. A. and J. Casadesus (2014). "Contribution of phenotypic heterogeneity to adaptive antibiotic resistance." Proc Natl Acad Sci U S A 111(1): 355-360.
- Schell, J. C., K. A. Olson, et al. (2014). "A role for the mitochondrial pyruvate carrier as a repressor of the Warburg effect and colon cancer cell growth." Mol Cell 56(3): 400-413.
- Schmoller, K. M., J. J. Turner, et al. (2015). "Dilution of the cell cycle inhibitor Whi5 controls budding-yeast cell size." Nature 526(7572): 268-272.
- Schroeder, T. (2008). "Imaging stem-cell-driven regeneration in mammals." Nature 453(7193): 345-351.
- Scott, M., C. W. Gunderson, et al. (2010). "Interdependence of cell growth and gene expression: origins and consequences." Science 330(6007): 1099-1102.
- Scott, M., S. Klumpp, et al. (2014). "Emergence of robust growth laws from optimal regulation of ribosome synthesis." Mol Syst Biol 10: 747.
- Seiler, S. and M. Plamann (2003). "The genetic basis of cellular morphogenesis in the filamentous fungus Neurospora crassa." Mol Biol Cell 14(11): 4352-4364.
- Sexton, A. C. and B. J. Howlett (2006). "Parallels in fungal pathogenesis on plant and animal hosts." Eukaryot Cell 5(12): 1941-1949.
- Shahrezaei, V. and S. Marguerat (2015). "Connecting growth with gene expression: of noise and numbers." Curr Opin Microbiol 25: 127-135.
- Sharma, S. V., D. Y. Lee, et al. (2010). "A chromatin-mediated reversible drug-tolerant state in cancer cell subpopulations." Cell 141(1): 69-80.
- Sigal, A., R. Milo, et al. (2006). "Variability and memory of protein levels in human cells." Nature 444(7119): 643-646.
- Simon, I., J. Barnett, et al. (2001). "Serial regulation of transcriptional regulators in the yeast cell cycle." Cell 106(6): 697-708.
- Skotheim, J. M., S. Di Talia, et al. (2008). "Positive feedback of G1 cyclins ensures coherent cell cycle entry." Nature 454(7202): 291-296.

- Slavov, N., E. M. Airoldi, et al. (2012). "A conserved cell growth cycle can account for the environmental stress responses of divergent eukaryotes." Mol Biol Cell 23(10): 1986-1997.
- Slavov, N. and D. Botstein (2011). "Coupling among growth rate response, metabolic cycle, and cell division cycle in yeast." Mol Biol Cell 22(12): 1997-2009.
- Smith, E. D., M. Tsuchiya, et al. (2008). "Quantitative evidence for conserved longevity pathways between divergent eukaryotic species." Genome Res 18(4): 564-570.
- Smith, J., J. Wright, et al. (2015). "A budding yeast's perspective on aging: the shape I'm in." Exp Biol Med (Maywood) 240(6): 701-710.
- Snijder, B. and L. Pelkmans (2011). "Origins of regulated cell-to-cell variability." Nat Rev Mol Cell Biol 12(2): 119-125.
- Snijder, B., R. Sacher, et al. (2009). "Population context determines cell-to-cell variability in endocytosis and virus infection." Nature 461(7263): 520-523.
- Spencer, S. L., S. Gaudet, et al. (2009). "Non-genetic origins of cell-to-cell variability in TRAIL-induced apoptosis." Nature 459(7245): 428-432.
- Spudich, J. L. and D. E. Koshland (1976). "Non-genetic individuality: chance in the single cell." Nature 262(5568): 467-471.
- St-Pierre, F. and D. Endy (2008). "Determination of cell fate selection during phage lambda infection." Proc Natl Acad Sci U S A 105(52): 20705-20710.
- Strohman, R. C. (1995). "Linear genetics, non-linear epigenetics: complementary approaches to understanding complex diseases." Integr Physiol Behav Sci 30(4): 273-282.
- Strohman, R. C. (1995). "Linear genetics, non-linear epigenetics: complementary approaches to understanding complex diseases." Integr Physiol Behav Sci 30(4): 273-282.
- Strohman, R. C. (1997). "The coming Kuhnian revolution in biology." Nat Biotechnol 15(3): 194-200.
- Sun, D. and S. V. Yi (2015). "Impacts of Chromatin States and Long-Range Genomic Segments on Aging and DNA Methylation." PLoS One 10(6): e0128517.

- Taniguchi, Y., P. J. Choi, et al. (2010). "Quantifying E. coli proteome and transcriptome with single-molecule sensitivity in single cells." Science 329(5991): 533-538.
- Tarunina, M., D. Hernandez, et al. (2014). "Directed Differentiation of Embryonic Stem Cells Using a Bead-Based Combinatorial Screening Method." PLoS One 9(9): e104301.
- Vander Heiden, M. G., L. C. Cantley, et al. (2009). "Understanding the Warburg effect: the metabolic requirements of cell proliferation." Science 324(5930): 1029-1033.
- Vlamakis, H., C. Aguilar, et al. (2008). "Control of cell fate by the formation of an architecturally complex bacterial community." Genes Dev 22(7): 945-953.
- Walser, M., R. M. Leibundgut, et al. (2008). "Isolation of monoclonal microcarriers colonized by fluorescent E. coli." Cytometry A 73(9): 788-798.
- Wan, K. H., C. Yu, et al. (2006). "High-throughput plasmid cDNA library screening." Nat Protoc 1(2): 624-632.
- Warner, J. R. (1999). "The economics of ribosome biosynthesis in yeast." Trends Biochem Sci 24(11): 437-440.
- Wijnen, H., A. Landman, et al. (2002). "The G(1) cyclin Cln3 promotes cell cycle entry via the transcription factor Swi6." Mol Cell Biol 22(12): 4402-4418.
- Wilkening, S., V. Pelechano, et al. (2013). "An efficient method for genome-wide polyadenylation site mapping and RNA quantification." Nucleic Acids Res 41(5): e65.
- Wu, C. Y., P. A. Rolfe, et al. (2010). "Control of transcription by cell size." PLoS Biol 8(11): e1000523.
- Yang, J., M. A. McCormick, et al. (2015). "Systematic analysis of asymmetric partitioning of yeast proteome between mother and daughter cells reveals "aging factors" and mechanism of lifespan asymmetry." Proc Natl Acad Sci U S A 112(38): 11977-11982.
- Yuan, T. L., G. Wulf, et al. (2011). "Cell-to-cell variability in PI3K protein level regulates PI3K-AKT pathway activity in cell populations." Curr Biol 21(3): 173-183.
- Zamore, P. D., J. R. Williamson, et al. (1997). "The Pumilio protein binds RNA through a conserved domain that defines a new class of RNA-binding proteins." RNA 3(12): 1421-1433.

- Zhang, J., C. Schneider, et al. (2002). "Genomic scale mutant hunt identifies cell size homeostasis genes in S. cerevisiae." Curr Biol 12(23): 1992-2001
- Zhang, Y., C. Luo, et al. (2012). "Single cell analysis of yeast replicative aging using a new generation of microfluidic device." PLoS One 7(11): e48275.
- Zugasti, O., N. Thakur, et al. (2016). "A quantitative genome-wide RNAi screen in C. elegans for antifungal innate immunity genes." BMC Biol 14(1): 35.